UNIVERSITY OF CAPE COAST

RADIOFREQUENCY EXPOSURE FROM GSM MOBILE PHONE HANDSETS IN GHANA: EXPOSURE ASSESSMENT AND MODELLING WITH EXPOSURE PARAMETERS

SAMUEL OSEI

2021

UNIVERSITY OF CAPE COAST

RADIOFREQUENCY EXPOSURE FROM GSM MOBILE PHONE HANDSETS IN GHANA: EXPOSURE ASSESSMENT AND MODELLING WITH EXPOSURE PARAMETERS

BY

SAMUEL OSEI

Thesis submitted to the Department of Physics of the School of Physical Sciences, College of Agriculture and Natural Sciences, University of Cape Coast, in partial fulfilment of the requirements for the award of Doctor of Philosophy degree in Physics

JULY 2021

DECLARATION

Candidate's Declaration

I hereby declare that this thesis is the result of my own original research and that no part of it has been presented for another degree in this university or elsewhere.

Candidate's Signature …….. Date ……

Name: Samuel Osei

Supervisors' Declaration

We hereby declare that the preparation and presentation of the thesis were supervised in accordance with the guidelines on supervision of thesis laid down by the University of Cape Coast.

Principal Supervisor's Signature …….. Date ……...

Name: Dr. Joseph Kwabena Amoako

Co-Supervisor's Signature ……..... Date ……...

Name: Prof. Frederick Sam

ABSTRACT

Ghana remains one of the countries in the world with high cellular communication subscription. The public is becoming more concerned about any potential Radiofrequency (RF) health hazards that may exist. However, very little studies have been conducted in Ghana on RF exposure from mobile phones. This work researched on the influencing factors that affect GSM mobile phone SAR. It concentrated on how distance of phone from the head, phone position, phone orientation and transmission channel affect the Specific Absorption Rate (SAR) of regulatory approved and unapproved Global System for Mobile Communication (GSM) mobile phones. Even though the approved phone recorded statistically significant higher SAR values relative to the unapproved phone, its SAR values were more regular and predictable compared to the unapproved phone. SAR values were below the ICNIRP and FCC basic restrictions with the highest SAR being 25 % of the limit. SAR values of high earn phones agreed with that of the unapproved phone but rather lower than the approved phone. The study shows that, moving the phone just 1 cm from the head reduces the 10 g SAR of the approved phone by 53 % whiles interestingly increasing that of the unapproved phone by 71 %. A one-phase exponential model and an exponential decay model were derived to predict SAR as a function of phone distance from head. A SAR calculator application has been developed, providing mobile phone users with an alternative, inexpensive, and easy way to estimate their RF exposure. The work adds to base line data for regulators and government agencies to inform policy. It also complements relevant scientific knowledge expanding the data frontiers on mobile phone RF exposure.

KEY WORDS

GSM mobile phone

Radiofrequency fields

Regulatory approved phone

Regulatory unapproved phone

SAR calculator application

Specific absorption rate

ACKNOWLEDGEMENTS

This research could not have been successful without the dedicated guidance, mentoring and support of my supervisors, Dr Joseph Kwabena Amoako and Dr Fredrick Sam. I am most grateful and appreciate them.

The head of Laboratory Operations, Peter Onyekwere, and Head of Standard and Technical Regulations Unit, Roland Yaw Kudozia, all of the National Communications, have been pillars in this work, guiding me through the practical aspect of the work and helping to shape the research. I am thankful for their willing support. I am indeed indebted to Dr Philip Deatenyah, head of non-ionizing radiation and to my colleagues of the Health Physics Centre at the Radiation Protection Institute for the technical support and contributions offered for the success of this work. I thank all staff of the Physics Department of the University of Cape Coast for their support. I am also grateful to the National Communications Authority and the Radiation Protection Institute for supporting and sponsoring this work.

I thank my beautiful wife, Lily, and my children, Gabriel, Michelle, Desmond and Henry for their unflinching support and love, bearing with a mostly occupied husband and father all these years. I love you all. There are many personalities who have impacted on this work both spiritually and physically. I appreciate them all.

DEDICATION

To my sweet mother, Mrs Juliana Maakua Asiedua Agyemang and my family.

TABLE OF CONTENTS

LIST OF TABLES

LIST OF FIGURES

LIST OF ABBREVIATIONS

1G	-	First Generation
2G	-	Second Generation
3G	-	Third Generation
4G	-	Fourth Generation
AC	-	Alternating Current
ADP	-	Policy for Accelerated Development
AI	-	Artificial Intelligence
AM	-	Amplitude Modulation
AMPS	-	Analog Mobile Phone System
ANSI	-	American National Standards Institute
APC	-	Automatic Power Control
APP	-	Approved Phone
ARPNSA	-	Australian Radiation Protection and Nuclear Safety Agency
BSC	-	Base Station Controller
BTS	-	Base Transceiver Station
CDMA	-	Code Division Multiple Access
CENELEC	-	Commission Européenne de Normalisation Électrique
CW	-	Continuous Wave
dB	-	Decibel
DECT	-	Digital Enhanced Cordless Telecommunications
DVB	-	Digital Video Broadcasting
EDGE	-	Enhanced Data Rates for GSM Evolution
ELF	-	Extremely Low Frequency

EM	-	Electromagnetic
EMF	-	Electromagnetic Field
eV	-	Electron Volts
FCC	-	Federal Communication Commission
FDMA	-	Frequency Division Multiple Access
FDTD	-	Finite Difference Time Domain
FEM	-	Finite Element Method
FIT	-	Finite Integration Technique
FM	-	Frequency modulation
Gbps	-	Giga bits per second
GHz	-	Giga Hertz
GPRS	-	General Packet Radio Service
GSM	-	Global System for Mobile Communication
HD – TV	-	High-Definition Television
HSCSD	-	High Speed Circuit-Switched Data
Hz	-	Hertz
IARC	-	International Agency for Research on Cancer
ICNIRP	-	International Commission on Non-Ionizing Radiation
IEC	-	International Electrochemical Commission
IEEE	-	Institute of Electrical and Electronics Engineers
IMEI	-	International mobile equipment identity
IMTS	-	Improved Mobile Telephone Service System
IP	-	Internet Protocol
IRPA	-	International Radiation Protection Association
ITU	-	International Telecommunication Union

JOSE	-	International Journal of Occupation and Ergonomic
kbps	-	Kilo Bits Per Second
kHz	-	Kilo Hertz
LCD	-	Liquid-crystal display
LCH	-	Left Ear - Cheek Position - High channel
LCL	-	Left Ear - Cheek Position - Low channel
LCM	-	Left Ear - Cheek Position - Middle channel
LED	-	Light emitting diodes
LTE	-	Long Term Evolution
LTH	-	Left Ear - Tilt Position - High channel
LTL	-	Left Ear - Tilt Position - Low channel
LTM	-	Left Ear - Tilt Position - Middle channel
Mbps	-	Mega Bits Per Second
MC-CDMA	-	MiltiCarrier CDMA
MHz	-	Mega Hertz
MIMO	-	Multiple In Multiple Out
MoM	-	Method of Moments
MP	-	Mobile Phone
MPE	-	Maximum permitted exposure
ms	-	Milli Seconds
MTA	-	Mobile Telephone system A
MVG	-	Microwave Vision Group (MVG)
mW	-	Milli Watts
NCA	-	National Communications Authority

NCRP	-	National Council on Radiation Protection and Measurement
NIR	-	Non-Ionizing Radiation
OFDM	-	Orthogonal Frequency Division Multiplexing
PIFA	-	Plane Inverted F Antenna
PM	-	Phase Modulation
PML	-	Perfectly Matched Layer
PSTN	-	Public Switch Telephone Network
RCH	-	Right Ear - Cheek Position - High channel
RCL	-	Right Ear - Cheek Position - Low channel
RCM	-	Right Ear - Cheek Position - Middle channel
RF	-	Radiofrequency
RSS	-	Root Sum Square
RTH	-	Right Ear - Tilt Position - High channel
RTL	-	Right Ear - Tilt Position - Low channel
RTM	-	Right Ear - Tilt Position - Middle channel
SA	-	Specific Energy Absorption
SACCH	-	Slow Associated Control Channel
SAM	-	Specific Anthropomorphic Mannequin
SAR	-	Specific Absorption Rate
SMS	-	Short Messaging Services
S/N	-	Serial Number
TACS	-	Total Access Communication Systems
TDMA	-	Time Division Multiple Access
TV	-	Television

UAP	-	Unapproved Phone
UHF	-	Ultra-High Frequency
UMTS	-	Universal Mobile Telecommunication System
UTMS	-	Universal Mobile Telecommunication
UV	-	Ultraviolet
VC	-	Video channel
VHF	-	Very high frequency
VNA	-	Vector network analyser
WCDMA	-	Wideband Code Division Multiple Access
WiMAX	-	Worldwide Interoperability for Microwave Access
wwww	-	World Wide Wireless Web

CHAPTER ONE

INTRODUCTION

Background to the Study

Mobile telecommunication is a rapidly evolving technology that uses radiofrequency energy or radiation for mobile communication. Communication by mobile phones is through its base stations which have immobile antennas. Radiofrequency (RF) electromagnetic radiation falls under the non-ionizing radiation (NIR) in the electromagnetic spectrum. Non-ioinzing electromagnetic radiation has energy only enough to cause excitation but cannot produce charges when it encounters matter. However, biological effects caused by NIR are known. The International Commission on Non-Ionizing Radiation Protection (ICNIRP) defines NIR to encompass the long wavelength (> 100 nm) and low photon energy (<12.4 eV) portion of the electromagnetic spectrum, ranging from 1 Hz to 3 x10^{15} Hz. Radiofrequency ranges from 300 Hz to 300 GHz (ICNIRP, 2009). It lies between static frequency and infra-red in the non-ionizing region of the electromagnetic spectrum. RF is used in telecommunications, radar, satellite links, mobile phones, microwave ovens, TV and radio transmitters. It is also used in radio communications, visual display units, and television sets (ICNIRP, 2009).

The Federal Communications Commission (FCC, 1999) indicates that, electromagnetic radiation can be defined as waves of electric and magnetic energy moving together (i.e., radiating) through space. The magnetic and electric fields propagate orthogonal to each other. These waves are generated by the movement of electrical charges. They also specify that, electromagnetic field refers to the

electric and magnetic environment existing at some location due to a radiating source such as an antenna (FCC, 1997a; FCC, 1997b; FCC, 2001). Electric fields are produced with the presence of electric charge, and magnetic fields result of movement of electric charge and current (ICNIRP, 2009).

The elementary properties of electromagnetic fields (EMF) include its wavelength and field polarization, and associated exposure circumstances of the near-field or far-field regions. It is mostly near-fields conditions situations which result in high electromagnetic field exposure in an occupational environment. Various physical parameters can be used to assess EMF exposure. These parameters could be body internal dosimetric quantities which are thermal related such as Specific Energy Absorption Rate (SAR). Or related to nerve excitation as in internal electric field $\boldsymbol{E}_{in}$ and induced currents $\boldsymbol{J}$. Also, they could be body external quantities like the power density ($\boldsymbol{S}$), contact and induced limbs current ($\boldsymbol{I}$), magnetic field ($\boldsymbol{H}$), electric field strengths ($\boldsymbol{E}$), magnetic flux density ($\boldsymbol{B}$) and high frequency heating at the body surface. (International Journal of Occupation and Ergonomics, 2009).

In 2011, the International Agency for Research on Cancer (IARC) reclassified radiofrequency electromagnetic fields on the carcinogenic scale, moving it to Group 2B (possibly carcinogenic to humans), a category used when a causal association is considered credible, but when chance, bias or confounding cannot be ruled out with reasonable confidence (International Agency for Research on Cancer, 2011).

In the RF range, by far, the most applications which emit EMF are in the frequency range above 100 kHz up to some GHz. Multiple sources of RF radiation exit that contribute to an individual's exposure. In particular, RF transmitter technologies used in close vicinity to the human body like mobile phone, have become the key source of RF exposure for the general population and workers. However, distance of the body from the source is one of the main determinants of levels of RF radiation exposure. It is assisted by other factors like transmission power and duty factor. For the brain tissues in particular, the use of mobile phone handset at the ear has become the core source of RF radiation exposure. The aftermath of the first generations of mobile phones has focused on limiting RF power of the handsets including Digital Enhanced Cordless Telecommunications (DECT) phones. Global System for Mobile Communication (GSM) phones, which operate within networks of different technologies, as well as other portable wireless devices, like tablets and laptop computers, increased the complexity of the user's exposure and changed the exposed body region. Due to the various sources used near to the human body, it has become unavoidable to consider several sources of exposures for risk assessment (European Commission, 2015).

Mobile or cellular phones are now an integral part of modern telecommunications. It has become an inevitable part of our daily activities. In many countries, including Ghana, over 50 % the population use mobile phones and the usage keeps growing rapidly. For some countries, cellular telecommunications are the only phone available or reliable form of

communication. With these large numbers of the population relying on mobile communications, it is important we study, assess, appreciate and monitor any likely occupational and public health impact.

Statement of the Problem

The use of mobile phone handsets has increased dramatically in recent years in Ghana. In 1995, the Government of Ghana passed the 5-year Telecommunications Policy for Accelerated Development, dabbed 'ADP 2000'. This reform was basically aimed at introducing rapid expansion in the provision of telecommunications services and achieving substantial improvement in the quality of services and efficiency in the telecoms sector. Recent figures from the National Communications Authority (NCA) shows that, Ghana with a population of around 30.8 million (Ghana Statistical Service, 2021), has about 41 million mobile voice subscribers, and 31.3 million mobile data subscribers in Ghana. The data also shows 2.5 million 4G and 28.6 million 2G/3G subscribers (NCA, 2020).

This rapid growth of the mobile telecommunication industry in Ghana has created a booming market for mobile phone handsets leading to the influx into the country of all kinds of mobile phone handsets with very little consideration for RF exposure from the handset. With the use of these handsets everywhere in Ghana, and increasing frequency and duration of use, there are serious public and worker concerns about any potential health implications associated with exposure to electromagnetic fields from mobile phone handsets. Some users in Ghana have complained about some heating effects, headaches and fatigue (Osei, Amoako, Fletcher, 2015; Azah, Amoako, Fletcher, 2013; Amoako, Fletcher, Darko, 2009;

Deatanyah et al., 2012). These heightened possible health effects about RF exposures have led to public agitations and even legal tussles about the siting of mobile telecommunication base stations.

Despite all these concerns, very little is known about exposures from mobile phone handsets to users in Ghana. No scientific research has been published on the influencing factors that influence the levels of RF exposure from these mobile phone handsets used in Ghana.

Given the large number of mobile phone users in Ghana, it is relevant that we investigate, comprehend and monitor any possible public and occupational health implications from these mobile phone handsets (World Health Organisation, 2014).

Purpose of the Study

This research seeks to assess the levels of RF SAR from GSM mobile phone handsets used by the public in Ghana. And to investigate how distance of mobile phone from the head, phone positioning, phone orientation, and operating frequency affect the RF SAR of GSM mobile phones used in Ghana. The study also sets out to develop a mathematical or statistical model to estimate SAR of GSM mobile phone handset as a function of distance of phone from the head.

Research Objectives

The fundamental objective of this study is to measure SAR from GSM mobile phone handsets used in Ghana and determine if levels comply with the basic SAR restriction of ICNIRP and the limits of Federal Communications Commission (FCC). This would be achieved through the following specific objectives:

- Experimentally determine how distance of GSM mobile phone handset from the head, phone positioning (left or right ear), phone orientation (cheek or tilt), and operating frequency (low, middle or high) affects the SAR.
- To measure the RF SAR from GSM mobile phones used in Ghana with focus on regulatory approved phones and unapproved phones.
- Compare the levels of RF SAR from GSM mobile phone handsets to levels set by national and international standards like those set by ICNIRP.
- Develop a mathematical model to estimate SAR as a function of distance of phone from the head.

Significance of the Study

The largest retrospective case-control study to date on adults, Interphone, coordinated by the International Agency for Research on Cancer (IARC, 2013), was designed to determine if use of mobile phones is associated in any way to head and neck cancers in adults. Data from people with usage history of over 10 years in 13 countries found no increased risk of glioma or meningioma. However, they reported some hints of an increased risk of glioma for those who reported the highest 10% of collective hours of mobile phone usage. It is however important to emphasise that there was no consistency in the trend of risk increasing with mobile phone duration usage. A casual explanation could not be arrived at due to errors and biases restraining the strength of their conclusions. Based largely on this result, IARC has reclassified radiofrequency electromagnetic fields as

possibly carcinogenic to humans (Group 2B). This category is used when a causal association is considered credible, but when chance, bias or confounding cannot be ruled out with reasonable confidence (IARC, 2011). Christopher Wild, Director of IARC in his comment on the RF re-classification emphasized the need for research into possible long-term effects and at the same time taking steps to reduce exposure (IARC, 2011). Reducing exposure from mobile phones requires an understanding of how the influencing factors impact on the SAR. This work is in line with this research call.

Mobile phone technology in Ghana, has become a critical part of our personal and national economy, and an essential tool in the daily lives of Ghanaians. Even though Ghana has one of the highest figures in terms of subscribers of mobile telephony, the numbers keep growing daily. There is public and workers concerns on the potential health risks that may exist, yet very little is known about the levels of exposure and the factors that influence the levels of RF exposure from mobile phone handsets in Ghana. Some research has been done on mobile phone handsets and base stations, FM and TV stations (Osei, Amoako, Fletcher, 2015; Azah, Amoako, Fletcher, 2013; Amoako, Fletcher, Darko, 2009; Deatanyah et al., 2012). The World Health Organization (WHO, 2013) indicates that, typical RF field levels from mobile phones are over a 1000 greater than levels from telecommunication base stations. However, there is very little studies on RF exposure from mobile phones used in Ghana.

The research intends to fill in the knowledge gap about the nature of SAR levels of mobile phones used in Ghana and their influencing factors. To reduce

and control RF exposure form mobile phone handsets in Ghana, it is important that we know the extent of RF SAR exposure and understand the parameters that influence it. This research will add to base line data on the levels of RF exposure form mobile phone handsets in Ghana. Regulatory bodies, occupational health and safety professionals will be provided information needed for the exposure assessment of the general public and workers. Results from the research shall provide the relevant data to establish the health risk due to RF exposure form mobile phone handsets in Ghana. The results will also help to address what appears to be a lack of RF guidelines on mobile phones usage in Ghana. It shall serve as the basis for any needed regulations on mobile phone handsets, its use and exposure reduction technical requirements for service providers. The SAR calculator application will provide an easy-to-use and less expensive alternative method for assessing RF exposure from mobile phone handsets.

Delimitations

The work focuses on the assessment of levels of RF SAR levels from GSM mobile phone handsets used in Ghana, investigates how distance affects its SAR and develop a mathematical model to estimate SAR of GSM mobile phone handset considering distance of phone from head when in use.

The work does not consider mobile phones which are not GSM, nor does it consider phones that do not have block form.

Limitations

The research is limited to two GSM mobile phones. Also, the number of distance points is small (four points) and has wide intervals, hence reducing the

accuracy of predictive model developed. SAR measurement at smaller intervals provides a better description of the SAR behaviour within the near field of the antenna. This also applies to the use of just one phone in each category of regulatory approved phones and unapproved phones. Other factors like source geometry, anatomical domain, type of phone and type of antenna that impact on the SAR of a mobile phone were not considered. Due to limited time, laboratory availability and equipment breakdown, the predictive model was developed to have a reliability range of 0.0 cm to 3.0 cm and not beyond. The model is also limited to only GSM phones with brick structure.

Organisation of the Study

This research work has been arranged in an organised manner. Chapter one has introductory notes on radiofrequency fields in general, the extent of mobile phone usage in Ghana is also touched on. The objectives and the significance of the work are also discussed after the specific problem this work intends to solve is revealed. Chapter two reviewed scholarly work in the area and discussed the theories guiding the thesis. Chapter three elaborates the equipment and procedures used in data collection. The chapter also explains how the data was analysed. In chapter four, data obtained from the study is presented in tables and figures. The data is also assessed and analysis. It also discusses the significance of the results obtained and their implications in relation to other relevant published works and existing scientific knowledge. Chapter five summarizes the work, draws conclusions regarding the significance of the study

results and makes recommendations to mobile phone users, regulators, organizations and for further study based on the results of this study.

Chapter Summary

This chapter contains the introductory aspects of the thesis. It commences with a background description which provides some brief theoretical basics, presents the problem the study indents to solve, and enumerate some rational for the work. It also outlines the objectives of the research, declare the delimitations and limitations, and presents how the thesis is structured.

CHAPTER TWO

LITERATURE REVIEW

Introduction

This chapter explains some relevant terms and quantities applied in the work. It also reviews the key concepts and theories around which the study is built, and declare the conceptual basis and theoretical framework of the study. The chapter also provides a review of similar work done by other researchers.

The use of technologies applying electromagnetic (EM) fields has increased enormously in the resent times. These applications involve technologies using EM radiations covering all parts of the electromagnetic spectrum. This increase in usage, has also led to a rapid expansion of technologies using radiofrequency (RF) fields such as radio and TV transmitters, telecommunications links and satellite communication, mobile phones and their supporting base stations as well as wireless computer networking (Health Protection Agency, 2008). As its uses grows, so does the level of exposure, and this happening at a time where there is keen public and worker concerns about the possible safety and health risks associated with this EM radiations, in particular with low levels of exposures over a long period of time (Vorst, Rosen & Jetuka, 2009).

In Ghana, mobile phone telephony and mobile phone use has witnessed a tremendous rise, with the number of voice subscribers doubling the population. This has led to growing concerns from workers and the public about the potential adverse health effects (Osei, Amoako & Fletcher, 2015; Azah, Amoako & Fletcher, 2013; Amoako, Fletcher & Darko, 2009; Deatanyah et al., 2012;

Deatanyah, Abavare, Menyah & Amoako, 2018; Deatanyah, Amoako, Abavare & Menyeh, 2018; Azah, Amoako & Sam, 2019).

Many organizations, both government and nongovernment, have established RF safety standards or guidelines for exposure. Organizations like the International Commission on Non-Ionizing Radiation Protection (ICNIRP) under the World Health Organization (WHO), the National Council on Radiation Protection and Measurement (NCRP), the International Radiation Protection Association (IRPA), , the Institute of Electrical and Electronic Engineers (IEEE), and Federal Communications Commission (FCC) exist and are charged with formulating and recommending exposure guidelines aimed at protecting workers and the general public from the harmful effects of both ionizing and non-ionizing radiations.

Relevant Terms and Quantities

It is important to take a discuss some key terms and quantities that will be useful as we progress through this work.

Electric field

Michael Faraday first described an electric field as a "field of force". Later, James Clerk Maxwell defined it as the space around an electrified object where the electric force act (Fleisch, 2008). It is realised that, the similar parameters that run through most definitions shows that fields and forces are closely related. So, we can define electric field as the electrical force per unit charge (Fleisch, 2008) or the force exerted on a tiny positive test charge placed at a point (Giancoli, 2009). Then we can write the electric field $\vec{E}$ as in Equation 1.

$$\vec{E} = \frac{\vec{F}_e}{q_0} \quad (1)$$

Magnetic field

The concept of electric field can be applied in this instance. Remember that an electric charge only experiences a magnetic force when they are in motion. Then my applying Lorentz definition of magnetic force, we can write the magnetic field $\vec{B}$ as in Equations 2 and 3.

$$\vec{F}_B = q\vec{v} \times \vec{B} \quad (2)$$

and of course, the magnitude of $\vec{B}$ as

$$\left|\vec{B}\right| = \frac{|\vec{F}_B|}{q|\vec{v}|sin\theta} \quad (3)$$

where q is the particles, $\vec{v}$ is the velocity of the charge particle, θ is the angle between $\vec{v}$ and $\vec{B}$, whiles $\vec{F}_B$ is the magnetic force (Fleisch, 2008; Giancoli, 2009). The quantities and its units used in this work are presented in Appendix B.

Electromagnetic fields

In reference to the discussions on a "field", we can describe an electromagnetic field as the existence of EM energy, in other words, the presence of electric and magnetic environment at a specific place (FCC, 1999).

Electromagnetic fields are something we cannot run away form. Television (TV) and radio signals we receive, the use of mobile phones, electrical gadgets and the wiring in our home, and many more are some of the sources of EM fields. It is employed in the medical sector for both diagnosis and treatment purposes. It is used in medical imaging, and also for electrocardiography,

electroencephalography, and electrophysiological assessments. The fields are all around us, even they are in our bodies that give movement to our muscles, they enable brains to function and also make our hearts beat. It is also applied in treatment in the form of therapeutic interventions for cancer, pain control, bone growth, soft tissue repair, electrophysiological stimulation, and others. Electromagnetic field even though it has many useful applications, it can also cause injure and can cause death through or kill us through deep electrical burns and shock, and lightning strikes (Fruse, Christensen & Duney, 2009).

As already stated, EM fields are in used in a wide range of devices used in the medical sector. We can look forward to further applications like assisting the deaf to hear and the blind to see, and also helping the paralysed to walk. There are a whole lot of possibilities in the field of bioelectromagnetics.

EM waves / radiation

A good way of considering EM waves is in terms of its field, radiation and energy. Electromagnetic radiation are waves of electric and magnetic energy propagating together through space. The movement of electrical charges generate these electromagnetic waves (FCC, 1997).

Electromagnetic waves are generated by antennas of a mobile communication base station, a TV station or a radio station and propagates into space. These waves are then intercepted by our mobile phone device and our TV or radio antennas (FCC, 1999).

In Figure 1, the charging and discharging spark creates an EM wave which then moves in particular direction indicate ***Z***. It is observed that, the wave has

both magnetic field ***B*** and electric field components ***E***, orthogonal to each other, and moving together in the one specific ***Z***. We shall discuss antennas further later in this chapter.

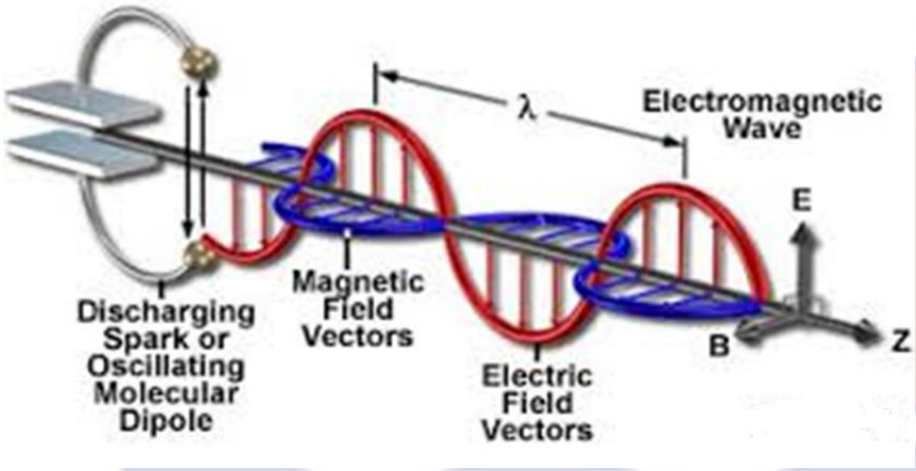

Figure 1: Propagation of Electromagnetic Wave (Molecular Expressions Microscopy Primer, 2016).

Electromagnetic spectrum

This is an arrangement of all the electromagnetic radiation to frequency or wavelength. Figure 2 shows the electromagnetic spectrum. The spectrum comprises of all the various forms of electromagnetic energy from extremely low frequency (ELF), very low frequencies, all the way to X-rays and gamma rays, which have the highest frequencies. Radio waves, microwaves, infrared radiation, visible light, and ultraviolet (UV) radiation falls midway.

The spectrum is broadly group into ionizing and non-ionizing radiation (NIR) as demonstrated in Figure 2. Ionising in the sense that, their energies are not sufficient to ionize matter, but the ionising radiations can ionize because they carry energy enough to do that. Non-ionizing radiation cover the long wavelength

(> 100 nm), low photon energy (<10 eV) portion of the electromagnetic spectrum, from 1 Hz to 3 x10^{15} Hz (Ng, 2003; ICNIRP, 2020). The NIR region transcend into the ionizing section within the UVA part of the spectrum. RF radiation are non-ionizing.

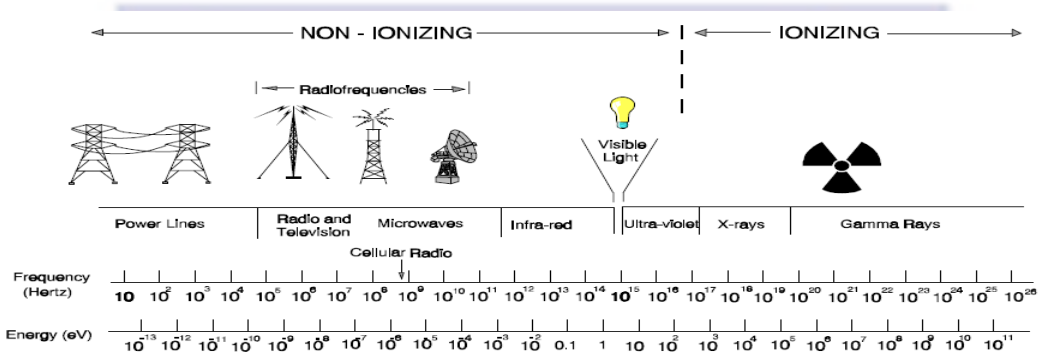

Figure 2: Electromagnetic Spectrum (FCC, 1997).

Radiofrequency (RF) Radiation

RF radiation are part of the electromagnetic spectrum from 300 Hz to 300 GHz. They are between static frequency and infra-red in the non-ionizing region. It includes radio waves, micro waves and part of infra-red radiation.

RF parameters

We shall now put RF in perspective and discuss some of its parameters. These parameters include frequency range, source parameters, and antenna field regions.

Frequency range

The RF range of 300Hz to 300GHz can further be put into sections according to their applications. They can be classified as follows:

Frequency range from 300Hz to 300MHz

Shortwave broadcasting, very high frequency (VHF) radio, frequency modulation (FM), analogue amplitude modulation (AM) and maritime navigation are all applications of this range. It also includes amateur radio communication, mobile broad communication, fixed services and television broadcasting.

In this range, procedures for measurement differ with respect to service type and frequency. The electric and magnetic fields may be measured in cases of services with frequency lower than 300MHz. Measurement of induced and contact currents may be essential in cases of high-power transmission (Industry Canada, 2005).

Frequency range from 300MHz to 3GHz

This is where ultra-high frequency (UHF) television, fixed land line, personal computer systems (PCS), satellite systems, and digital radio broadcasting are located.

Measurement is done in the far field due to the associated small antenna dimensions and wavelength. Measuring only the electric field $|\boldsymbol{E}|^2$ is necessary as it can be used to estimate the power density (Industry Canada, 2005). The magnetic field, $\boldsymbol{H}$, and the electric field, E are related by a constant characteristic impedance of 377Ω in the far field region.

Source parameters

The level of exposure to RF from broadcast antennas are determined by the design properties of the antenna, emitted power, mounted antenna height,

distance from antenna and type of station. (Industry Canada, 2005). Some source parameters are also discussed in the subsequent sections.

Antenna field region

Antenna regions are key concepts in understanding exposure as EM field in different antenna regions have different characteristics. The area surrounding the antenna is divided into field regions, generally far-field and near-field regions (ITU, 2008). Figure 3 depicts these regions.

In the Far-field (Fraunhofer) region the antenna where the angular field distribution is fundamentally not dependent of the distance from the antenna. In this region, the field has mainly plane-wave in character.

The near-field region exists in proximity to an antenna. In this region, fields (electric and magnetic) differ greatly form one area to the other and do not have a substantially plane-wave character. This region has additional divisions called reactive near field, reactive-radiative near field, and radiating near field.

The reactive near field is closest to the antenna and retains most of the stored energy. It is the area immediately surrounding the antenna. It usually extends about one wavelength from the antenna.

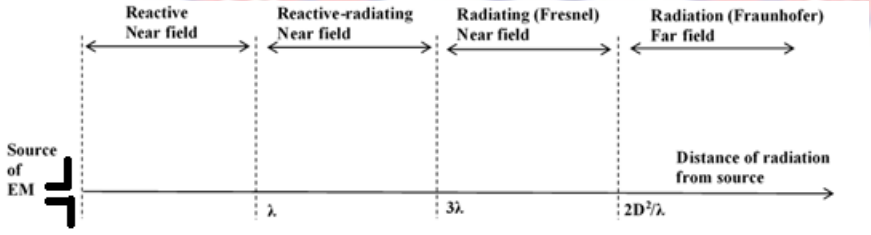

Figure 3: Field Zones around an RF Radiating Source (ITU, 2008).

At the boundary to the reactive near-field region to the radiating near field exist a transition region called the reactive-radiative near field region where the radiating field begins to be significant. This field is known to extend some few wavelengths form the antenna.

Fresnel zone or better known as the radiating near field sometimes exist between the reactive-radiative near field and the radiating far field if maximum dimensions of the antenna is large compared to the wavelength of the EM wave. Here, the radiation field dominates. But even though the radiation is not propagating as a plane wave, the electric and magnetic components of the field can be considered locally normal each other; moreover. This implies the ratio E:H can also be assumed constant and almost equal to the intrinsic impedance of free space, Z_0.

There is a constant radiated power density whiles the angular field distribution is independent on the separation distance. In this region, the electric and magnetic fields are transvers to each other and propagates s a plane wave. The inner boundary of the radiating far-field region is defined by the larger between 3λ and $2D/\lambda$. This means the limit is $2D2/\lambda$ if the maximum dimension D of the antenna is large compared with the wavelength λ (ITU, 2008; 2012).

Modulation

When transmitting human voice or talk directly as electromagnetic waves, there is the problem of interference resulting, and an almost impossibility. Since the human voice has low frequencies which spans from 20Hz to 300Hz, these waves have huge wavelengths, this will require antennas of thousands of meters

in length to provide any significant transmission of these frequencies. In other to overcome these challenges of transmitting voice, the process of modulation is used.

This challenge is solved by varying (modulating) a property of the RF wave like frequency, phase or amplitude to transmit the information. This enables the propagation the low frequency information (voice) with a higher frequency (EM) carrier. These modulated EM waves can have different forms with the most fundamental been a continuous wave (CW) or and un-modulated carrier in which the wave oscillates at a single frequency as shown in equation 4

$$V = V_p \sin(\omega t + \emptyset) \quad (4)$$

Where V = instantaneous value

V_p = peak value

ω = angular velocity = $2\pi f$ and f is frequency

$\emptyset$ = phase angle

Varying the phase angle $\emptyset$, results in phase modulation (PM). If the amplitude term, V_p, is the parameter varied, it is called amplitude modulation (AM). If the frequency is varied, it is frequency modulation (FM).

Variability of the source

Variability of the antenna pattern, and the its transmitted power is key to measurements as it poses a serious challenge in measurements because it makes it difficult to predict the precise condition of the antenna or source at any particular time (ITU, 2008). Antennas used in telecommunications are mostly variable and

hence the need to look at the issue of antenna variability. Below are some variable parameters of the antenna or source.

Power variability

ITU maintains that, maximum radiated power of the transmitter must be considered when assessing exposure (ITU, 2008). Automatic Power control (APC) or channel use variability are systems used in telecommunication to control power output. In the case of APC, it compensates for adverse propagation conditions such connectivity by adjusting the output power.

Dynamic channel allocation where the channels are turned on or off as needed and variation in channel occupancy, where the amount of data transmitted over a channel varies (however, even if no data is transmitted, the channel carrier remains) are two classes of the channel variability. There is a projected small effect of the modulation of the signal by this Channel occupancy variation.

Antenna variability

Antennas used in telecommunication systems employ active antennas that can dynamically vary their radiation pattern (ITU, 2008). How much radiation is concentrated in in a particular direction relative to other directions is determined by the directional pattern of the antenna. A pattern taken in the same plane as the *E* is known as the *E*-plane pattern whiles the one taken in the plane orthogonal to the *E*-plane is known as the *H*-plane pattern (Industry Canada, 2005).

Electromagnetic waves are radiated into space via antennas. The radiation pattern generated by the source is the spatial distribution of the EM fields with respect to the source and it determines the spatial distribution of the radiated

energy (Industry Canada, 2005). The ICNIRP points out that, angular field distributions relate to the distance from the source and alter immensely in the near-field. However, this is not so in the far-field as the angular field pattern does not change significantly with distance. Presence of reflecting objects in this field invalidates this far field assumption (ICNIRP, 2009).

Intermittent sources

Certain sources used in telecommunications are intermittent. Such sources emit RF energy only if they need to transmit some information, but may operate in a regular manner, transmitting data at regular intervals or to a defined schedule.

Polarization

Polarization is the orientation of an electric field vector and/or the magnetic field vector in the plane orthogonal to the direction of propagation is called polarization. The polarization may be constant in a particular direction or can be rotating. These are called linear polarization and elliptical polarization respectively (Industry Canada, 2005). The ICNIRP asserts that, if the electric field vector is always oriented in a given direction, the wave is linearly polarized and if the electric field vector rotates around the direction of propagation, maintaining a constant magnitude, the wave is circularly polarized (ICNIRP, 2009). When the extremity of the electric field vector traces an ellipse, the wave is elliptically polarized. The rotation of the electric field vector occurs in one of two directions, either clockwise or counter-clockwise.

Health Canada (2009) maintains that, it is difficult to predict the orientation of the electric field in the near field region, as the transmitting antenna

cannot be considered as a point source in this region. In the far field region, the antenna becomes a point source, the electric and magnetic components of the field become orthogonal to the direction of propagation and their polarization characteristics do not vary with distance (Health Canada, 2009).

Maxwell's Equations

The theoretical prediction of electromagnetic waves was the work of the Scottish physicist, James Clerk Maxwell who unified in one theory, all the phenomena of electricity and magnetism. Even though the development of electromagnetic theory began with Oersted, Ampere whiles Faraday introduced the idea of field, it was generally not applied until Maxwell was able to show that all the electric and magnetic phenomena, we experience can be described in only four equations, named Maxwell's equations (Giancoli, 2009) as written in integral form in Equations 5 – 8. The feat led to the introduction of new areas in the field of communication, which include TV, cell phones, Bluetooth and Wi-Fi, simple things like remote-control devices.

Maxwell's equations are said to be even more fundamental equations of electromagnetism (relative to universal law of gravitation and Newton's laws of motion) since they are consistent with the theory of relativity whiles Newton's three laws of motion are not. In fact, Maxwell's four equations are considered one of the greatest accomplishments of the human intellect (Giancoli, 2009).

$$\oint \vec{E} \cdot d\vec{A} = \frac{Q}{\epsilon_0} \quad (5)$$

$$\oint \vec{B} \cdot d\vec{A} = 0 \quad (6)$$

$$\oint \vec{E} \cdot d\vec{l} = -\frac{\partial \Phi_B}{\partial t} \quad (7)$$

$$\oint \vec{B} \cdot d\vec{l} = \mu_0 I + \mu_0 \epsilon_0 \frac{d\Phi_E}{dt} \quad (8)$$

Where $\vec{E}$ = electric field strength in V/m^2

$\vec{B}$ = magnetic field in T

$d\vec{A}$ = an incremental of the surface area in m^2

$d\vec{l}$ = an incremental segment of path

Q = net charge enclosed by the surface in C

I = enclosed electric current in A

ϵ_0 = electric permittivity of free space

μ_0 = magnetic permeability of free space

Φ_E = electric flux

Φ_B = magnetic flux

(Giancoli, 2009)

These equations are in their simplest form where it is in space. In subsequent subtitles, their behaviour and how they modify when present in a material will be discussed. Maxwell is not the sole originator of these equations, but it was he who put these equations together and identified their importance in predicting the existence of electromagnetic waves (Young & Freeman, 1996). Maxwell developed the idea of displacement current as an adjustment to Ampere's law.

The first two equations of Maxwell, Equations 5 and 6, involve the integral of the electric and magnetic fields over an enclosed surface and these are

the same as Gauss's law for electric and magnetic fields. Equation 7 is the Faraday's law whiles Equation 8 is the Ampere's law as modified by Maxwell. Let us discuss them in further detail.

Gauss's law for electric fields

Integral form of Gauss's law for electric fields

Equation 5 is the integral form of Gauss's law for electric field. It states that the integral of the electric field over any closed surface is directly proportional to the net charge Q enclosed within the surface (Young & Freeman, 1996). In other words, an electric charge produces an electric field, and the flux of the field passing through any closed surface is proportional to the total charge enclosed with that surface (Fleisch, 2008). The left-hand side of Equation 2 describes an electric flux (which is number of electric lines) passing through a closed surface whiles the right-hand side of the equation talks about the amount of electric charge contained in that surface as a ratio of the permittivity of free space (Fleisch, 2008). It is a general form of Coulomb's law that relates electric field to its sources, electric charges (Giancoli, 2009). Let's remember that the integral form of Gauss's law for electric field relates the electric field over a surface to the charge enclosed by that surface (Fleisch, 2008).

This integral form is useful specifically in two ways. The electric flux through a surface enclosing a charge can be determined when the electric charge distribution is known. It can also be used to find total electric flux through an enclosed surface if the electric charge enclosed by the surface is given (Fleisch, 2008).

Differential form of Gauss's law for electric fields

The differential form of Gauss's law for electric field is generally written as

$$\vec{\nabla} \cdot \vec{E} = \frac{\rho}{\varepsilon_0} \qquad (9)$$

ρ = the charge density in C/m^3

ε_0 = electric permittivity of free space

The right-hand side of the Equation 9 is the ratio of the electric charge density and the electric permittivity and the left-hand side of the equation is the mathematical description of the tendency of the electric field to say "flow" away form a particular location (Fleisch, 2008). It is called the divergence of the electric field. The equation implies that, the electric field produced by electric charges diverges from positive charges and converges upon negative charges. That is to say, the divergence is zero only at places where there is no charge (Fleisch, 2008). Meaning there is always divergence when a charge is present. But negative charges at a point produces negative divergence which "flow" towards that particular point whiles a positive charge produces the vice versa. It is important to state that, whiles the differential form of Gauss's law for electric fields talks about the divergence of the electric field and the charge density at individual points in space, the integral form of deals with the integral of the normal component of the electric field over a surface (Fleisch, 2008).

Gauss's law for magnetic fields

Gauss's law for magnetic fields and its associated Gauss's law for electric fields although are similar in structure, they are quite different in content form Gauss's law for electric fields. The basic difference is the opposite electric

charges, to be specific negative and positive charges, can be separated from each other, but this does not occur in the case of magnetic poles, south and north poles (Fleisch, 2008). This lack of isolated magnetic poles in nature impacts profoundly on the behaviour of the magnetic flux and its associated divergence for its field (Fleisch, 2008).

This differential form is used to determine the volume charge density at a location where the spatial variation of the vector field is known at that location (Fleisch, 2008). It can also be used to find the divergence of the electric field when the charge density.

Integral form of Gauss's law for magnetic field

The second Maxwell's equation, Equation 6 is Gauss's law for magnetic fields. This law is the analogous relation for magnetic fields. Its states that, the surface integral of the magnetic field $\boldsymbol{B}$ over any closed surface is at all times zero (Young & Freeman, 1996). In other words, it says that the total magnetic flux passing through any closed surface of any shape must always be zero (Fleisch, 2008). It is important to note that this statement does not imply zero magnetic lines penetrate the surface, but rather say for every negative or inward magnetic flux, there should be a positive outward magnetic flux to cancel it out (Fleisch, 2008). This means among other things that, there are no mono or isolated magnetic poles in nature unlike as in the case of electric fields. Another implication is the fact that magnetic field lines are continuous and have no beginning or end (Giancoli, 2009).

With this knowledge that total magnetic flux through a closed surface is zero, it allows you to solve complex problems involving surfaces, especially when integration can be used to determine the flux through one portion of the surface (Fleisch, 2008).

Differential form of Gauss's law for magnetic fields

Because of the continuous nature of the magnetic field lines, the differential form of Gauss's law for magnetic fields is simple. It is

$$\vec{\nabla} \cdot \vec{B} = 0 \qquad (10)$$

The left side of the equation describes the divergence of the magnetic field. In simple language, this law states that the divergence of the magnetic field at any point is always zero. This again is as a result of the fact that we cannot isolate magnetic monopoles.

The fact that the divergence of the magnetic field is zero enables you to determine if a particular vector field could be a magnetic field and also permit you to solve problems involving the spatial change of the component of the magnetic field (Fleisch, 2008).

Faraday's law

After the discoveries that electric current produces a magnetic field and a magnetic field exerts a force on an electric current, Scientist started investigating if the vice versa is true, that is, if a magnetic field can produce and electric current. It was the American Joseph Henry and the Englishman Michael Faraday who independently established this narrative. Even though it was Henry who made the first discovery, it was Faraday who first published it and went further to

investigate in more detail (Giancoli, 2009). He discovered that an electric current can be induced in an electric circuit by a changing magnetic flux. Put in general terms, we can say a changing magnetic field produces. Let us note that, this electric field differs from the electric field produced by an electric charge (Fleisch, 2008). In other words, a changing magnetic field induces an electromotive force (emf). Note that the name emf may be deceptive as it is not a force, it is the potential difference between the terminal of an electric source when no current flows to an external circuit (Giancoli, 2009). Young & Freeman (1996) defines Faraday's law as the induced emf in a closed loop equals the negative of the time rate of change of the magnetic flux through the loop.

Integral form of Faraday's law

Equation 7, is the integral form of Faraday's law. It states that a changing magnetic field induces an emf. In much detail the equation says a changing magnetic flux through a surface induces an emf in any boundary path of that surface, and a changing magnetic field induces a circulating electric field. The left-hand side of the equation is the emf.

The negative sign has deep implications. In simple terms, it means the emf induced opposes the change in the magnetic flux and by so doing tends to maintain the existing flux. And we call this the ***Lenz's law*** after Heinrich Lenz, a German physicist, who discovered it. It states that the current produced by an induced emf moves in a direction so that the magnetic field created by that current opposes the original change in flux (Giancoli, 2009). In other words, an induced emf is always in a direction that opposes the original change in flux that caused it

(Giancoli, 2009). Let's remember that the changing magnetic flux induces an electric field no matter if there exist conducting path in with the current will flow. Lenz law is to indicate the direction of the flow of the induced electric fields.

The integral form of Faraday's law, Equation 7, is useful to determine the induced emf when information on the changing magnetic flux is known and also find the rate of change of the magnetic field magnitude or direction or the area bounded by the path if the induced emf in a specific path (Fleisch, 2008).

Differential form of Faraday's law

The differential form can be written as;

$$\vec{\nabla} \times \vec{E} = -\frac{\partial \vec{B}}{\partial t} \quad (11)$$

where $\frac{\partial \vec{B}}{\partial t}$ is the time rate of change of the magnetic field (Fleisch, 2008). The key idea espoused by this equation is that, a circulating electric field is produced by a magnetic field that changes with time. The left side of Equation 11 is the mathematical description of the tendency of the electric field lines to circulate around a point, called the curl of the electric field (Fleisch, 2008). This form of Faraday's law is very useful in deriving the electromagnetic wave equation (Fleisch, 2008).

Ampere – Maxwell law

It had always been known that the only sources of magnetic fields were particular iron ores and magnetised materials until the French physicist Andre-Marie Ampere stated quantifying the relation between magnetic fields and electric currents after Hans Christian Oersted had been able to deflect a compass needle

when he passed electric current close to it (Fleisch, 2008). At that time, Ampere's law only related a steady electrical current to a circulating magnetic field as shown in Equation 12 (Fleisch, 2008).

$$\oint \vec{B} \cdot d\vec{l} = \mu_0 I \quad (12)$$

It only applied to static conditions that involves steady current. Maxwell added an additional term, which is the changing electric flux, that made the equation applicable to time-dependent situations (Fleisch, 2008). Again, by adding the additional time dependent term, it enabled Maxwell to recognise the electromagnetic nature of light and helped him to come up with a detail electromagnetic theory that we all-benefit form today (Giancoli, 2009).

Ampere – Maxwell's law states that a magnetic field is produced by an electric current or also by a changing electric field (Giancoli, 2009).

Integral form of Ampere – Maxwell law

Equation 8 is Ampere-Maxwell law in integral form. The right-hand side describe the two sources of the magnetic field. These are the steady conduction current (the first term) and the changing electrical flux represented by the second term. The left-hand side of the equation is the mathematical expression of the circulation of the magnetic field (Fleisch, 2008). The main impulse of this law is that, an electric current or a changing electric flux through a surface produces a circulating magnetic field around any path that bounds the surface (Fleisch, 2008). It is good to mention that; the magnetic field would be produced whether a path exits or not (Fleisch, 2008).

Differential form of Ampere – Maxwell law

Generally, the differential form of Ampere – Maxwell law can be written as in equation 13 where $\vec{J}$ is the electric current density in A/m^2 (Fleisch, 2008)..

$$\vec{\nabla} \times \vec{B} = \mu_0 \left(\vec{J} + \varepsilon_0 \frac{\partial \vec{E}}{\partial t} \right) \quad (13)$$

The left side of the equation expresses the tendency of the magnetic field lines to circulate around a point called the curl of the magnetic field. The central message of this differential form can be put in this way; a circulating magnetic field is produced by an electric field that changes with time and by an electric current (Fleisch, 2008).

Maxwell defined the second term of Equation 13, which is $\mu_0 \varepsilon_0 \frac{\partial \vec{E}}{\partial t}$, as been equivalent to an electric current (has units of A/m^2 same as the electric current density) and he called ***displacement current*** (Giancoli, 2009) because he initially thought to be the physical displacement of electrical particles caused by elastic deformation of magnetic vortices and others (Fleisch, 2008). Note that an ordinary current is known as conduction current (Giancoli, 2009). In all these, let us not lose focus of the key concept of this term, which is, a changing electric field produces a changing magnetic field even when charges are absent and no physical current flows (Fleisch, 2008). The Faraday and Ampere–Maxwell's equations enable the prediction of electric and magnetic fields in the biological body.

From Maxwell's equations to the EM wave equation

The main achievement of Maxwell was his ability to derive from these four laws a comprehensive theory of electromagnetism (Fleisch, 2008). A changing magnetic field is produced by a changing electric field and this changing magnetic field will in turn produce a changing electric field and the process continues (Giancoli, 2009). Maxwell derived that, the end product of these interacting fields is an ***electromagnetic wave*** of electric and magnetic fields that propagate through space (Giancoli, 2009).

Starting with Faraday's law in differential form, and taking the curl of both sides

$$\vec{\nabla} \times \vec{E} = -\frac{\partial \vec{B}}{\partial t}$$

$$\vec{\nabla} \times (\vec{\nabla} \times \vec{E}) = \vec{\nabla} \times \left(-\frac{\partial \vec{B}}{\partial t}\right) \quad (14)$$

$$\vec{\nabla} \times \left(\vec{\nabla} \times \vec{E}\right) = -\frac{\partial(\vec{\nabla} \times \vec{B})}{\partial t} \quad (15)$$

Using the identity that the curl of the curl of a vector field is equal to the gradient of the divergence of the field minus the Laplacian of the field, we can write

$$\vec{\nabla}\left(\vec{\nabla} \cdot \vec{E}\right) - \nabla^2 \vec{E} = -\frac{\partial(\vec{\nabla} \times \vec{B})}{\partial t} \quad (16)$$

Remember that the Cartesian means;

$$\nabla^2 \vec{E} = \frac{\partial^2 E_x}{\partial x^2} + \frac{\partial^2 E_y}{\partial y^2} + \frac{\partial^2 E_z}{\partial z^2} \quad (17)$$

From Ampere – Maxwell's law, Equation 13, we know that;

$$\vec{\nabla} \times \vec{B} = \mu_0 \left(\vec{J} + \varepsilon_0 \frac{\partial \vec{E}}{\partial t}\right)$$

Then Equation 16 will become;

$$\vec{\nabla}\left(\vec{\nabla}\cdot\vec{E}\right)-\nabla^2\vec{E}=-\frac{\partial[\mu_0(\vec{J}+\varepsilon_0(\partial\vec{E}/\partial t)]}{\partial t} \quad (18)$$

We now need to substituted Gauss law for electric fields which is Equation 9

$$\vec{\nabla}\cdot\vec{E}=\frac{\rho}{\varepsilon_0}$$

We will then have

$$\vec{\nabla}\frac{\rho}{\varepsilon_0}-\nabla^2\vec{E}=-\mu_0\frac{\partial\vec{J}}{\partial t}-\mu_0\varepsilon_0\frac{\partial^2\vec{E}}{\partial t}$$

Grouping terms of $\vec{E}$, we

$$\nabla^2\vec{E}-\mu_0\varepsilon_0\frac{\partial^2\vec{E}}{\partial t}=\mu_0\frac{\partial\vec{J}}{\partial t}+\vec{\nabla}\frac{\rho}{\varepsilon_0}$$

In the situation of current free and no charge ($\vec{J}=0$ and $\rho=0$), we then arrive at

$$\nabla^2\vec{E}=\mu_0\varepsilon_0\frac{\partial^2\vec{E}}{\partial t^2} \quad (19)$$

Similarly, taking the curl of both sides of Ampere-Maxwell's law and applying identities result in

$$\nabla^2\vec{B}=\mu_0\varepsilon_0\frac{\partial^2\vec{B}}{\partial t^2} \quad (20)$$

Both Equations 19 and 20 are ***linear*** (the space and time derivatives of the wave function shows the first power and not with cross terms), ***second-order***, ***homogenous*** (no forcing or source terms present because all terms involve the wave function and its derivatives), and ***partial*** (the wave function as multiple variables which is space and time) differential wave equation that describes the electric field, as in Equation 19. and magnetic field, as in Equation 20, respectively traveling from one point to another. They are EM wave equations.

These two equations are consistent with the general wave equation for a plane wave travelling in the x direction

$$\vec{\nabla}^2\vec{A} = \frac{1}{v^2}\frac{\partial^2\vec{A}}{\partial t^2} \quad (21)$$

which can also be written as

$$\frac{\partial^2\vec{A}}{\partial x^2} = \frac{1}{v^2}\frac{\partial^2\vec{A}}{\partial t^2} \quad (22)$$

Then we can write the speed of the electromagnetic wave as

$$v = \frac{1}{\sqrt{\mu_0\varepsilon_0}} \quad (23)$$

Substituting the values of $\mu_0 = 4\pi \times 10^{-7}$ mkg/C^2 and ε_0= 8.8541878×10^{-2} C^{2}s^2/kgm^3, we have

$$v = c = 2.99792458 \times 10^{16} \text{ ms}^{-1}$$

where c the special symbol for the speed of light in vacuum. This value that Maxwell calculated, agreed excellently with the measured value of the speed of light and caused Maxwell to make this comment – "light is an electromagnetic disturbance propagated through the field according to electromagnetic laws" (Fleisch, 2008). It can also be derived that

$$v = \frac{E}{B} \quad (24)$$

That is, $\vec{v}$ is in the direction of $\vec{E} \times \vec{B}$ and

$$\frac{\partial B}{\partial x} = -\mu_0\varepsilon_0\frac{\partial E}{\partial t} \quad (25)$$

Energy, momentum and pressure of EM waves

After deriving the wave equation of EM waves, and calculating the speed in vacuum, let's turn our attention to the energy and momentum of EM waves.

EM waves just like in the case of moving electric and magnetic fields have energy associated with them and carry this energy from one place to another as they travel from one point to another. The ***energy density*** stored in the $\vec{E}$ and $\vec{B}$ are Equations 26 and 27 respectively (Giancoli, 2009; Young & Freeman, 1996),

$$u_E = \frac{1}{2}\varepsilon_0 E^2 \quad (26)$$

$$u_B = \frac{1}{2}\frac{B^2}{\mu_0} \quad (27)$$

Total energy is given u carried by the wave will be given by

$$u = \frac{1}{2}\varepsilon_0 E^2 + \frac{1}{2}\frac{B^2}{\mu_0}$$

Since $c = 1/\sqrt{\mu_0\varepsilon_0}$ and $B = E/c$, then we can simplify the total energy of the wave, Equation 27, to various forms as

$$u = \varepsilon_0 E^2 \quad (28)$$

$$u = \frac{B^2}{\mu_0} \quad (29)$$

$$u = \sqrt{\frac{\varepsilon_0}{\mu_0}EB} \quad (30)$$

The energy that the EM wave transport per unit time, or in other words the energy flow rate (Power), known as the ***Poynting Vector*** is represented by the symbol $\vec{S}$ with units of W/m^2. It was introduced by the British physicist John Poynting.

$$\vec{S} = \frac{1}{\mu_0}\left(\vec{E} \times \vec{B}\right) \quad (31)$$

Equation 31 states that, the direction of $\vec{S}$ is in the same direction as $\vec{v}$, that is perpendicular to $\vec{E}$ and $\vec{B}$. Also

$$S = \varepsilon_0 c E^2 \quad (32)$$

$$\bar{S} = \frac{E_0 B_0}{2\mu_0} = \frac{E_{rms}\, B_{rms}}{\mu_0} \quad (33)$$

$\bar{S}$ is the average value, E_0 is the maximum value of E and $E_{rms} = \sqrt{\overline{E^2}}$, the others apply appropriately (Giancoli, 2009; Young & Freeman, 1996).

It is proper to argue that if EM waves do have energy, then they must possess linear momentum which has the symbol *p* which has ***momentum density***

$$\frac{dp}{dV} = \frac{EB}{\mu_0 c^2} = \frac{S}{c^2} \quad (34)$$

Take note that the momentum is not related to the mass of a moving particle in this case but it is the property of the field. We can go ahead and state the momentum flow rate per unit area as

$$\frac{dp}{Adt} = \frac{S}{c} = \frac{EB}{\mu_0 c} \quad (35)$$

Just like moving objects, when EM waves strikes a surface there will be momentum transfer and the momentum will also exert a force *F=dp/dt*. The ***radiation pressure*** predicted by Maxwell can be defined as the force per unit area exerted by the EM waves

$$P_{rad} = \frac{\bar{S}}{c} \quad \text{(radiation fully absorbed)} \quad (36)$$

$$P_{rad} = \frac{2\bar{S}}{c} \quad \text{(radiation fully reflected)} \quad (37)$$

Propagation of EM waves in tissue

The equation governing the propagation of electromagnetic waves in tissues can be derived from Maxwell's equations as Equation 38, where μ_r and ε_r are the relative magnetic permeability and relative electric permittivity, k_0 is the

free space wave number in per meters, and ω is he angular frequency in Hz with j representing the complex term $\sqrt{-1}$.

$$\nabla \times \frac{1}{\mu_r}(\nabla \times E) - k_0^2\left(\varepsilon_r - \frac{j\sigma}{\omega\varepsilon_0}\right)E = 0 \quad (38)$$

Analysis of EM waves involve applying boundary scattering conditions on the other ends of the domain evaluated giving us equation 39.

$$n \times (\nabla \times E) - jkn \times (E \times n) = -n\big(E_0 \times jk(n-k)\big)exp(-jk.r) \quad (39)$$

The r is the radial distance of separation between the source and the human tissue.

Production of EM waves

Maxwell was able to show that the changing magnetic field producing an electric field which is itself also changing and producing a changing magnetic field. All these result in the creation of electromagnetic waves that propagate through space. When an antenna made up two conducting rods is connected to the terminals of a direct current DC power source as described in Figure 4, current flows through the rods and electric field lines are produced as indicated with the red lines in Figure 4(a). A magnetic field will be also produced near the antenna which encircles the antenna indicated in blue in Figure 4(a). Magnetic field is orthogonal to the electric field. Hence, the magnetic field lines going into the page are indicated by cross in the small circle whiles the magnetic field lines coming out of the page is indicated by a dot in the small circle according to the right-hand rule. In this static case, the field lines extent indefinitely into the surrounding. Electric and magnetic fields store energy and hence can't be transported to far

positions at infinity speeds. So even though the fields are produced close to the antenna, they take a lot of time to reach far positions (Giancoli, 2009; Young & Freeman, 1996).

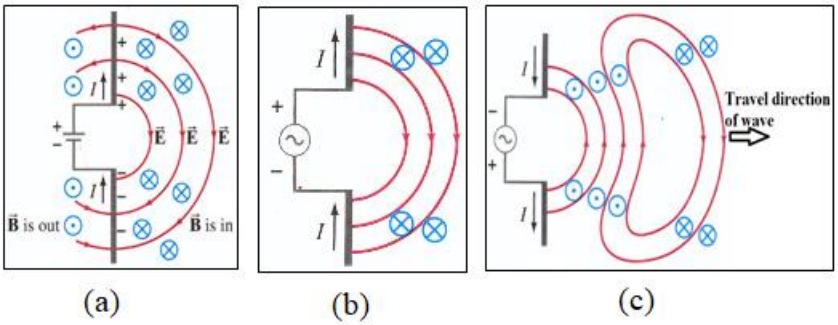

Figure 4: Production of EM Waves by an Antenna *(*Giancoli, 2009; Young & Freeman, 1996).

If the antenna is connected to an alternating current (AC) source, the two rods will constantly be interchanging polarity. When in the first instance as in Figure 4(b), the top rod is positive, the magnetic field on the right is directed into the page whiles the electric field is clockwise. But when the polarity of the rods' reverses, the new magnetic field is directed opposite as the new electric field is now clockwise. The old electric field lines then fold up to connect forming loops and proceed traveling outward as indicated in Figure 4(c). The combination of continually changing electric field producing a changing magnetic field which in turn produces a changing electric field make these old fields self-sustaining and does not depend the antenna again but proceed infinitely into space as EM waves.

The wave intensity of the wave is inversely proportional to the square of the separation. Is important to note that the field strength varies from maximum to

zero and to minimum in one direction, meaning they are in phase. At far points the waves become flat and are known as plane waves.

Interaction of RF with matter

There are three important parameters to consider when considering interactions of ***B*** and ***E*** with matter. These interactions are very complicated making it difficult to follow each charge, hence the usefulness of three parameters to explain the interactions at the macroscopic level. These parameters are:

- permittivity (ε, with units of Fm^{-1})
- conductivity (σ, with units of Sm^{-1})
- permeability (μ, has units of Hm^{-1})

Permittivity or dielectric constant accounts for the alignment and induced polarization of electric dipoles and characterizes the interaction between the electric field and the bound charges in the material. It also explains the quantity of partial alignment and induced polarization of permanent electric dipoles that will be produced for a specific ***E*** applied. Conductivity determines conduction current produced, which in turn explains the amount of conduction current density created for an applied ***E***. Permeability defines the quantity of partial alignment of permanent magnetic dipoles produced and it also determines if there will be any alignment when a ***B*** is applied (Fruse, Christensen & Duney, 2009).

Because in most cases, the interaction on the microscopic level is almost impossible to account for, the interaction can be followed at the macroscopically in terms of three effects of fields on the charges in the material

- induced dipole polarization

- alignment of already existing electric dipoles
- movement of free charges

Free movement of free charges apply to conductors whiles dielectrics are affected by the first two conditions (Fruse, Christensen & Duney, 2009).

Interaction of RF with lossy material (biological tissue)

Biological tissue is a lossy material. A material is lossy if conductivity, σ, is not equal to zero. Power will be deposited in the lossy material as a wave passes through it, thus causing losses to the propagating wave. The material also heats as a result of the power deposited.

Effects of RF on humans

Radiofrequency is known to cause some biological effects but not health effects. They are basically of two forms, namely thermal and non-thermal effects.

Thermal effects

In the presence of EM fields, there is polarization of molecules in the material (millions of times per second) owing to the oscillation of the electromagnetic field. The molecules re-orient themselves continuously in response to the external field. This rapid polarization and orientation and re-orientations creates molecular friction which translates into thermal energy and hence increasing the temperature of the material.

It is important to mention that most biological tissues contain high percentage of water, and because of the polarization nature of water molecules,

makes it more "dielectrically lossy" than any other molecule found in materials containing water. As a result, they heat the fastest and most efficiently.

The committee on man and radiation emphasis that, known RF health hazards only occur at levels that cause heating, and the effect is a function of the body's ability to regulate heat and damage to tissues occur when the RF heating exceeds the body's cooling mechanism intensity. Hence tissues like the eye which has which as no blood supply is venerable and high exposure can lead to cataract. The good news is that, such high RF intensities are highly unlikely and limited to work place where control is maximum (Bansal, 2002).

Studies involving animals and human volunteers have found that adverse health effects are observed only when the heating produced by RF exposure raises tissue or body temperature by more than about 1 ºC. Induced heating of this magnitude may provoke various physiological and thermoregulatory responses, including a decreased ability to perform certain tasks. The development of the foetus may also be affected by induced heating, and birth defects could occur if the foetus' temperature were raised by 2-3 ºC for a number of hours. Induced heating can also affect male fertility (The Expert Group on Health Effects of EM Fields, 2005).

Non-thermal effects

According to ICNIRP (2020), the only established and substantiated adverse health non-thermal effects caused by RF fields are:

- changes in the permeability of cell membranes

- nerve stimulation

RF and cancer

In a press release on 31 May, 2011, the WHO/International Agency for Research on Cancer (IARC) classified radiofrequency electromagnetic fields as possibly carcinogenic to humans (Group 2B), based on an increased risk for glioma, a malignant type of brain cancer, associated with wireless phone use (IARC, 2011). Group 2B category is used for agents for which there is limited evidence of carcinogenicity in humans and less than sufficient evidence of carcinogenicity in experimental animals. It may also be used when there is inadequate evidence of carcinogenicity in humans but there is sufficient evidence of carcinogenicity in experimental animals. In some instances, an agent for which there is inadequate evidence of carcinogenicity in humans and less than sufficient evidence of carcinogenicity in experimental animals together with supporting evidence from mechanistic and other relevant data may be placed in this group. An agent may be classified in this category solely on the basis of strong evidence from mechanistic and other relevant data.

Recently, the U.S. National Toxicology and the Ramazzini Institute studies into carcinogenic potential of long-term exposure to RF fields associated with mobile phones produced results that have key limitations and inconsistencies (ICNIRP, 2020; ICNIRP, 1998). In fact, various research work in this area produced results which are either inconsistent or have replication issues (Agarwal, Singh, Hanada & Kesari, 2011; BC centre for Disease Control, 2016).

The Physics of Mobile Phones (MP)

It is appropriate to detail some applicable terms, and give a fair idea of the operation of a mobile phone. Let us now explore some fundamental elements of wireless telecommunication

Basically, telecommunication involves a transducer, which converts information to electrical signal and vice versa, and transmitter or receiver which transmits the signal or receives the signal for a transducer to convert to information to be displayed or listened to. This is demonstrated in Figure 5.

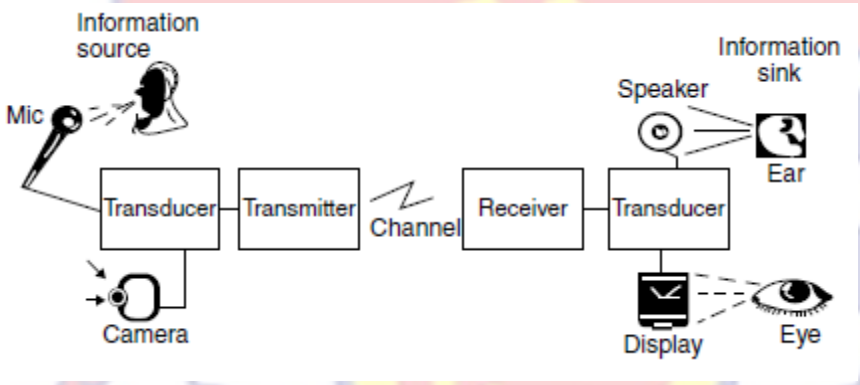

Figure 5: Fundamental Elements of Telecommunication (Das, 2010).

In a wireless telecommunication system, the signal is transmitted via electromagnetic wave and does not need a material medium. An oscillating electric charge that is accelerating, produces EM waves whose frequency is the same as the frequency of oscillation of the electric charge (Das, 2010).

Now, let us discuss some to the terms on telecommunication we might come across as we move on.

Signal

A signal can be described as the amplitude of varying event. The signal can be digital or analog. Fourier theory can be used to decompose a signal to create pure tones also known as cosine and sine waves at various frequencies. A signal can be discrete or continuous with respect to time based on its repetitive nature (Das, 2010).

Sampling

An analog signal can be converted to digital one and vice versa by the use of a converter. The process of converting an analog (continuous) signal to a digital (discrete) one is what we call sampling. But a sample is the set of values or value at a point in space or time (Das, 2010).

Fourier Transforms (FT)

Baron Jean Baptise Fourier demonstrated that all waveforms can be generated or represented by summing sine waves. Even though there may be some dc (direct current) terms in it, any real-world signal can be broken down or produced by a combining sine waves. FT is applied in antenna theory, radio wave propagation modelling, as well as in a host of other ways including stochastic modelling (Das, 2010).

Most importantly, FT enables us to relate events in the time domain to events in the frequency domain, hence enabling us to convert a continuous aperiodic signal, form the time domain to the frequency domain whiles the Fourier series enable the transformation of periodic signals (Das, 2010).

We can write this time domain Fourier transformation to a frequency domain and the vice versa is defined in Equations 40 and 41 respectively (Das, 2010).

$$S(\omega) = \int_{-\bowtie}^{\bowtie} s(t)\left[e^{-j2\pi ft}\right]dt \quad (40)$$

$$s(t) = \int_{-\bowtie}^{\bowtie} s(\omega)\left[e^{-j2\pi ft}\right]df \quad (41)$$

Where $S(\omega)$ = frequency signal

$s(t)$ = time signal

j = $\sqrt{-1}$

f = frequency

t = time

ω = $2\pi f$

System

The process of describing the relationship that exist between input and output is called a system. A system can be linear or non-linear (Das, 2010).

Statistical methods

The imperfections that might arise that can cause the received signal be different from the one transmitted is either deterministic (linear or non-linear) in form or nondeterministic (noise, fading, additions). The nondeterministic nature can be modelled as a random process (Das, 2010).

Bandwidth (bw) of a signal

The range of frequencies which a signal occupies is called the bandwidth of the signal. It is the part where the main power of the signal is concentrated. It is

mostly stated in terms of the difference between the lowest and highest (Das, 2010).

Channel capacity

The capacity of the channel determines the highest rate of communication through that channel without an error (Das, 2010).

Concept of the Antenna

The antenna is a metallic conductor and can be in the form a small wire, a metallic strip or a rod. It is one of the most important components in the mobile phone. Basically, an antenna is a transducer that converts electrical energy into EM waves. The antenna can also do the vice versa. Again, the working of how an antenna produces EM waves was discussed under Maxwell's equations. It is good to mention that an antenna requires a minimum length of at least $\lambda/4$ (where λ is the wavelength of the EM wave) to effectively receive or transmit the wave (Das, 2010).

The transmitted waves are transformed back to electrical signals when they reach the receiving antenna as waves try to penetrate the receiving antennas. Because the EM waves consist of electric and magnetic fields perpendicular to each other, the magnetic component by virtue of Maxwell's third equation generates a surface electric current in the receiving antenna but due to the principle of skin depth, this current will decrease and terminate as it travels into the body of the antenna. In another vein, the electric field will generate a potential difference as a result of Maxwell's fourth equation. Hence the EM wave has been transformed into electrical signal again (Das, 2010).

Antenna parameters

The operation of the antenna is affected by some essential factors. Let us take a look at some of them.

Radiation pattern

The pictographic illustration of the radiation fields or power fields along various directions in space is referred to as radiation pattern.

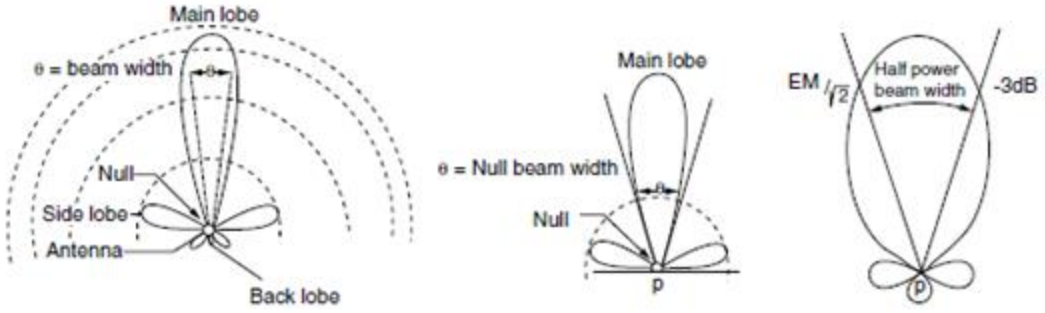

Figure 6: Radiation Patterns (Das, 2010).

Generally, a radiation field pattern resembles a conical lobe with angular width as represented in Figure 6. Note that at point p, the beam is reduced to zero.

Directivity and gain

The measure of concentration of radiated power of an antenna, in a specific direction (θ,Φ), is called the directivity $D(\theta,\Phi)$ of the antenna. Gain is the product of the directivity and the efficiency of the antenna.

Antenna efficiency

Efficiency of an antenna, or better put, the radiation efficiency is the ratio of the power radiated to the total power input.

Resonant frequency

This frequency, or sometimes called electrical resonance, is depended on the electrical length of an antenna. The ratio of physical length of an antenna to its velocity factor is the electrical length. This is as a result of the parasitic features causing the antenna length to the slightly longer than its physical length. Because of some properties of the antenna like the impedance and radiation pattern, the antenna resonant frequency will be close to the centre frequency as antennas are produced for a specific frequency but effective for a range of frequencies around the resonant frequency (ITU, 200; 8Das, 2010).

Impedance

Impedance is usually encountered as the arriving EM wave propagates through the antenna. The impedance of an antenna is dependent on the electrical length at the wavelength in use (ITU, 2008).

Polarization

The orientation of the electric field vector with reference to the ground is what we refer to as polarization of the EM wave. In relation to an antenna, its polarization is electric field orientation of the EM wave in reference to the surface of the earth. Polarization can be elliptical, circular, horizontal or vertical (Das, 2010; ITU 2008).

Mobile phone antennas

Currently, most mobile phones have their antennas either within the top part of the phone, or extending out of the top, all of different types and form (Das, 2010). But the primary antenna is mostly at the bottom of the phone. Let us discuss a few of them.

Helical antenna

This is made up of a conducting wire, coiled to form a helix structure (as shown in Figure 7), which is mounted on a ground plane, and emits radiation (polarised circularly) when the circumference of the helix structure is at least one wavelength long. Helical antennas are directional in nature with the radiation strongest along the axis of the helix structure. The antenna also provides high broadband frequency and gain properties (Das, 2010).

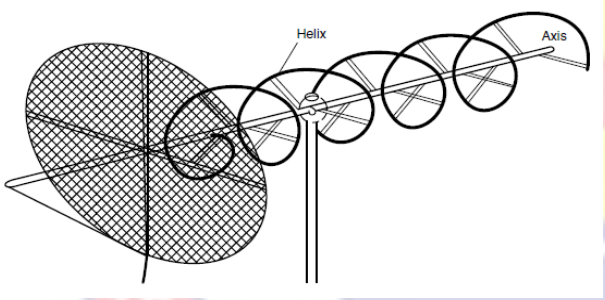

Figure 7: Helical Antenna (Das, 2010).

In the normal mode, helical antennas tend to be ineffective radiators and hence are mostly employed for mobile communications where the reduced phone size is crucial. The axial mode tends to be mostly used in space communications where the polarization of the signal may change, in that case, orientation of receiver and sender are not easily controllable, but not popular in mobile phones because of the size (Das, 2010).

Microstrip patch antennas

This type of antenna is popular in mobile communications because of their various advantageous features including low production cost, smaller size, robustness, and its structure which are simple. It is made up of a metal strip on a dielectric substrate which is covered by a plane on the reverse side as depicted in Figure 8. In effect the antenna is a resonant cavity that leak radiation along their edges (Das, 2010).

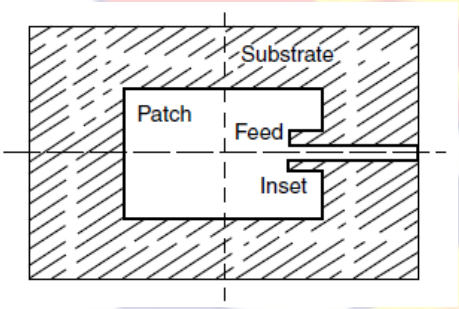

Figure 8: Microstrip Antenna (Das, 2010).

In today's world, because of the demand for multi-band antennas, the microstrip antenna easily provides for that purpose as it fabricated by photographic processes easily and can also be integrated with other microwave gadgets without difficulty.

Plane inverted F antennas (PIFA)

These types were employed in mobile phones for a long period. Currents oscillate in the inverted L section when functioning and possesses low resonant element profile. Figure 9 shows the form of the antenna (Das, 2010).

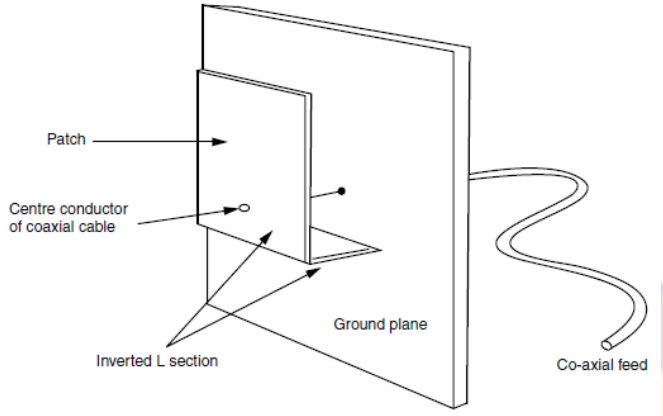

Figure 9: Planer Inverted F Antenna (Das, 2010).

Whip antenna

This is usually used in 2-way handheld cell phones and attached to vehicles but flexible. The structure is single-element and usually short. Their length directly determines their operating wavelength. It is sometimes called a half-dipole.

Subscriber identity module (SIM)

An important component of a mobile phone is the detachable GSM card called the SIM in short. It contains some basic information of the subscriber including the phonebook enabling the subscriber to retain his information even when handsets are switched (Das, 2010).

Cellular Mobile Communication

The Bells laboratory introduced the concept of cells as a solution to the challenge of providing mobility to users of phones, eliminating frequency interference, and at the same time maintaining connection with other users. This

concept divides an area into a number of hexagonal cells as shown in Figure 10(a).

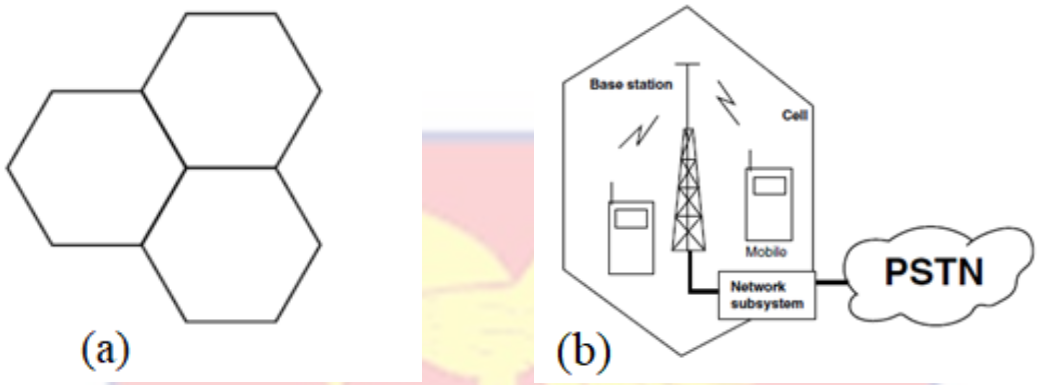

Figure 10: Planer Inverted F Antenna (Das, 2010).

The cells are circular in reality because the antennas transmit equally in all directions. Figure 10(b) shows a typical cell, with its infrastructure comprising of a base station with radio transceiver and controller, that receive, sent and manage signal to or from mobile phone users in the cell. The radio transceiver in one cell is connected to other transceivers in other cells, and at the same time, also connected to all users in other cells and different networks through the public switch telephone network (PSTN), or it also through data networks and mobile. The base station does the routing and switching for one user in one cell to call another user in another cell or land phone. This enables all mobile phone users achieve mobility and have connectivity globally (Das, 2010).

Frequency reuse

This concept enable the Cellular communication makes use of the concept of frequency reuse where the same frequencies used in one cell, is also used in

distant cells without interference. This enable a larger number of customers to be hooked up (Das, 2010).

Making a call

All mobile phones in a cell must be listening to the base station always, so as to receive the information on power, system, location or synchronization. This is done by the base station using a broadcast channel. Transmission information to the mobile phone handset is also done using a different channel (Das, 2010).

In dialling a number to start a conversation, the phone request for channel from the base station which and it is allocated a free channel for the communication. The mobile phone releases this channel when the call ends (Das, 2010).

Handover

In mobile phone mobility, handover is a vital issue. It is this concept that enables a user moving from one cell into another to retain connection. Basically, it is the process of tearing down an existing connection and replacing it with a new connection to the cell the user handed over to. This happens due to the stronger signal strength that exist in the cell the user is moving into and also as the quality of the radio signal between the mobile phone and the former cell degrades (Das, 2010).

Handover is determined by the network controller, but its success depends on two items namely:

- the proper release of channels used by the phone when the handover is complete

- the radio resource allocated in the target cell

Power control in mobile communication

To ensure just only sufficient power is transmitted in other to maintain an acceptable link between the base transceiver station (BTS) and the mobile phone, ensure interference is minimal, and also ensure transmitted power is at its optimal, the Global System for Mobile Communication (GSM) system uses power control mechanism. An operator decides to use power control algorithm or not. In fact, the algorithm is manufacture specific which runs on the base station controller (BSC). If the BTS sends a command to the MP to change its power, this is done by the MP in 2 dB steps per every 60 ms until it reaches its maximum or minimum power class limit. The network conveying messages over the slow associated control channel (SACCH) controls the power transmitted by the MP which ranges from 0 to 15 (0 is -43 dB, 15 is -13 dB or 20 mW) (Das, 2010).

Fading

Fading is the variation in the channel condition because of fluctuations in strength of the signal at the receiver end (Das, 2010).

Multipath effect

This effect causes time delay in signals received, and amplitude and phase fluctuations, also known as fading. Because of obstacles in the environment, transmitted signals are reflected by these obstacles causing the signals to arrive at the receiving end from different directions along multiple paths. This is what is

called multipath effect. The arriving signals out of phase, can destructively cancel part of the signal for brief time periods (Das, 2010).

Transmission Features

Mobile phones are classified into three groups according to their transmitted output power capacity. Table 1 (Das, 2010) shows the three-power grouping and the classifications. The values are maximum permitted levels even though not used all the time since in most times, the power is reduced due to instructions received from the base station. The reduction or increase is always in steps of 2 dB. The change in output power (power control) is only ensure sufficient or optimal required to maintain acceptable call quality is used. This reduces interference and save battery power.

Table 1: Power Classifications of Mobile Phones

Power class of MP	Nominal maximum output power GSM		
	GSM	PSC-1900	DCS-1800
1	43 dBm (20 W)	30 dBm (1 W)	30 dBm (1 W)
2	39 dBm (8 W)	24 dBm (0.25 W)	24 dBm (0.25 W)
3	37 dBm (5 W)	33 dBm (2 W)	33 dBm (2 W)
4	33 dBm (2 W)	-	-
5	29 dBm (0.8 W)	-	-

(Source: Das,2010)

Mobile Phone Handsets

A mobile phone handset provides wireless communication by the use of elevated antennas and high-powered transceivers. Fundamentally, it is an

equipment the user needs to send or receive a signal, whether data or voice, to or from another user through the base station and network systems.

It consists of various modules that support its operations. These can be grouped under:

- *application*, which support the various user applications as speaker, digital to analog and vice versa convertors, microphones, liquid-crystal display (LCD), video camera, etc.
- *power*, that takes care of the providing power to the various subsystems.
- *modem*, that ensures reception and transmission of signal over the channel that is usually is made up of RF unit, the protocol processing unit and the modulation or demodulation unit.

There would be in addition to the hardware modules, one or so microprocessors modules that control the whole system and the various applications and protocol software. Figure 11 gives a graphical representation of building blocks of a typical mobile phone handset. Even though the baseband, the protocol processing, the RF and modulation units may differ because of the cellular mobile system standard used by the handset, whether Universal Mobile Telecommunication (UTMS) or GSM, the operational block of mobile phone handsets are similar (Das, 2010).

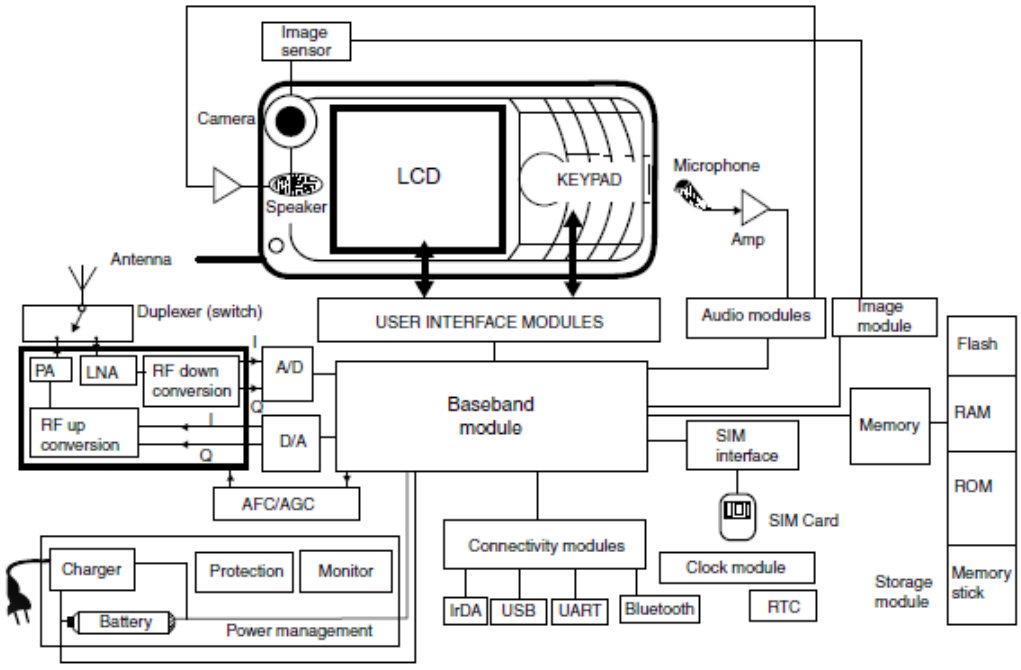

Figure 11: Mobile Phone Handset internal Bock Diagram (Das, 2010).

Evolutions of standards and technologies

Mobile phones have undergone a number of evolutions. In fact, there are generations of them. The first fully automated mobile phone system was introduced in 1956, in Sweden, by Mobile Telephone system A (MTA), but developed by Ericson. Later in 1971. This phone weighed a whole 40 kg which reduced the acceptability. APR network in Finland launched a successful commercial mobile phone network which is referred to as the 0th generation) (Das, 2010).

First generation (1G)

The Improved Mobile Telephone Service System (IMTS) introduced by Bell System in 1960s was the foundation for the first generation of mobile

communication systems. It is basically an analog system which uses Frequency Division Multiple Access (FDMA) in the frequency bands of 800 to 900 MHz. It provides mostly voice services (ICNIRP, 2009). The challenges with this system include poor voice quality, unreliable handovers, poor security and low traffic. The Analog Mobile Phone System (AMPS) and the Total Access Communication Systems (TACS) are examples (Das, 2010; Jain, Jain, Kurup, Gawade, 2014).

Second generation (2G)

Most of the principles in 1G also applied to 2G and both have comparable cell structure, but 2G has advanced features and also digital. Usually, 2G refers to the development of digital Global System for Mobile Communication (GSM) which uses the 935 to 960 MHz for uplink and 890 to 915 MHz frequency for downlink communications. It also applies the 19800 MHz bands too. A band is divided into 124 carrier frequencies with a bandwidth of around 200 kHz, and 9.6Kbit/s data rate for encoded conversation. By using Time Division Multiple Access (TDMA), each carrier frequency has a further division into eight 577 µs long time slots, and each slot represent a communication channel. Hence this will produce a total of 992 (8 multiply 124) channels for simultaneous communication. In effect, each user is "on" for 0.58 ms (4.615/8), and comes back in a period of 217 Hz with the other 7/8 time for other users. The system carry voice but has some limited data services (Das, 2010; Jain et al, 2014).

Second generation plus (2.5G)

The demand for higher data rates let to the development of 2.5G on the platform of the General Packet Radio Service (GPRS). It supported data speed of

up to 171.2 kbit/s and also packet based. Other examples include High Speed Circuit-Switched Data (HSCSD) and Enhanced Data Rates for GSM Evolution, EDGE, (Das, 2010).

Third generation (3G)

This system supports higher data transmission rates as well as higher capacity. It provides some features such as videoconferencing, multimedia, Web-browsing, navigation maps, paging and many more. It uses Wideband Code Division Multiple Access (WCDMA) as it efficiently uses the spectrum because of technique of Code Division Multiple Access (CDMA) which allows all base stations to use the same frequency but with a frequency reuse factor of one. The Universal Mobile Telecommunication System (UMTS) is an example of the 3G system (ICNIRP, 2009).

Fourth generation (4G)

This is a fully international protocol (IP) integrated system. This system should provide data speeds of 100Mbit/s to 1 Gbit/s. It offers multimedia messaging services, wireless broadband access, streaming services anywhere and anytime, mobile high-definition television (HD - TV) content, Digital Video Broadcasting (DVB), video charting, and many more including interactive services like video conferencing with=- more than two sites at the same time. It employs GSMer antennas uses MultiCarrier CDMA (MC-CDMA) and Orthogonal Frequency Division Multiplexing (OFDM) technologies. It is interesting to note that, currently, 4G is evolving through 3G Long Term Evolution (LTE), largely (Das, 2010; ICNIRP, 2009).

Fifth generation (5G)

This system should impact immensely on human activities positively as it comes with artificial intelligence (AI) and whole advance features in addition to what we have already as well as exciting data rate speeds. Table 2 summarises the five generations according to their various parameter to clearly bring out the differences and similarities.

Table 2: Comparing the various Generations of Mobile Phones

Item	Generation of Mobile Phone				
	1G	2G	3G	4G	5G
Definition	Analog	Digital narrow band circuit data, packet data	Digital broadband, packet data	Digital broadband, pocket all IP very high	Digital
Services	Voice only	Voice, short sms, fax, higher data capacity	High quality voice, multimedia. TV streaming, video conferencing, data, email, browsing, navigation	Multimedia, TV streaming, video conferencing, HD TV, DVB, wearable devices	Dynamic information, access, mobile TV wearable devices with IA
Technology	AMPS, IMTS, TACS	GSM, GPRS, EDGE	UMTS, HSDPA	LTE, WiMAX	wwww
Multiplexing	FDMA	TDMA, CDMA	W-CDMA	OFDM, MC-CDMA, MIMO	CDMA
Core network	PSTN	PSTN, packet network	Packet network	Internet	Internet
Bandwidth	2 kbps	64 kbps	2 Mbps	Gbps	> 1 Gbps

(Source: Shukla et al., 2013; Das, 2010; Chakraborty, 2013; Kumar et al., 2013)

Smell can be transmitted to a user. Currently, the Huawei company of China is known to have developed the 5G system and deployed them in some countries, mainly in Europe (Shukla, Khare, Garg & Sharma, 2013; Das, 2010; Chakraborty, 2013; ICNIRP, 2009; Kumar, Suman, & Renu, 2013.).

Specific Absorption Rate (SAR)

The widely accepted dosimetry quantity for RF is the specific absorption rate (SAR). It is used to estimate the time rate of energy absorption per unit tissue mass and is specified in units of joules per kilogram per second, or watts per kilogram. Especially in the case of devices that are used in close proximity to the body, like the mobile phone handset, SAR is the recommended dosimetry quantity (IEC, 2010; IEEE-1528, 2013; ICNIRP, 2020). Mathematically, it is defined as the time derivative of the incremental energy, δW, absorbed by or dissipated in an incremental mass, δm, contained in a volume element, δV, of a given tissue density ρ (ICNIRP, 2020), and expressed mathematically in Equation 42.

$$\text{SAR} = \frac{\delta}{\delta t}\left(\frac{\delta W}{\delta m}\right) = \frac{\delta}{\delta t}\left(\frac{\delta W}{\rho \delta V}\right) \quad (42)$$

Cember and Johnson (2009) describes SAR is a measure of the absorbed RF energy in the body per time and mass unit (W/kg). It is related to the internal electric field strength (Ayinmode & Faria, 2013). We can evaluate SAR from Equation 43, since electric or dielectric properties of biological tissues are represented as lossy, with relative magnetic permeability, μ_r is one and hence making biological tissues transparent magnetic fields (ICNIRP, 2020).

$$\text{SAR} = \frac{\sigma|E|^2}{\rho} = c\frac{dT}{dt} \quad (43)$$

Where σ is the specific conductivity, E is the root mean square (rms) value of the internal electric field generated in tissue, c is the heat capacity of the tissue, and dT/dt is the internal time derivative of the temperature (at t = 0) in the tissue in °C/s. ‘‘Specific energy absorption’’ (SA), which is the SAR integrated over time and thus the total absorbed energy SA (J/kg), is the corresponding unit for dose.

Exposure restriction values referred to as “basic restrictions” relate physical quantities to RF induced adverse health effects (ICNIRP, 2020). Basic limits for human exposure to RF are expressed as the specific absorption rate (SAR), specific energy absorption (SA), induced electric field strength and Current Density (ICNIRP, 1998; ITU, 2003).

Recently, ICNIRP (2020) has introduced absorbed power density and absorbed energy density as additional basic restrictions. Measuring these quantities inside the body is not in practice easy, so reference levels are derived which are quantities that are easily measurable. Some reference quantities are incident electric field strength, incident magnetic field strength and incident power density, and incident energy density (ICNIRP, 1998; ICNIRP, 2020).

SAR can be measured, even though not easily, and can also be evaluated. In this work, the two options are explored guided by international standards including the recommendations in IEC and IEEE standards.

ICNIRP basic restriction for local head SAR is 2 W/kg for the general public and 10 W/kg for the worker averaged over 10 g cubical region of mass

represented by SAR_{10g}. This limit is used by most European countries. The United State has one of the stringent head SAR limit of 1.6 W/kg for general public averaged over 1 g of mass and represented as SAR_{1g}. Ghana has adopted and uses the ICNIRP basic SAR restrictions for regulatory purposes. The ICNIRP basic restriction uses 6 minutes time averaging whiles the US uses 30 minutes averaging. The basic restrictions are presented in Appendix A.

Factors affecting SAR levels of the Mobile Phone

During the mobile phone handset's operation, a number of factors can influence its SAR, the key ones been time spent and output power (strength) of the RF signal of the phone, with the later been dominating (Hillert et al., 2006; Endreich et al., 2007).

Factors affecting the output RF power of the phone can be grouped as:

- Behavioural
- Environmental
- Engineering / technical

Generally, some of the factors can be listed under the Table 3, which is categorized under *Demographic and Personal* factors of the user, *Call parameters*, and *Physical properties* of the mobile phone handset. Some of these factors were investigated in this research.

Table 3: Some Factors that affect SAR

Call Characteristics	Phone Characteristics	Demographic and Personal factors
Length of call	Phone position	Employed
Service provider	Phone model	Socioeconomic status
Signal strength	2G, 3G, 4G	Age
Movement	Antenna type	Height
Time of day	Technology (GSM, CDMA)	Gender
Location	Phone type (bar, flip)	Weight

(Source: Endreich et al., 2007)

Finite Difference Time Domain (FDTD) Method

FDTD has been the most ordinary and simplified numerical method of solving applications in electromagnetism. This computational method, developed by Yee, provides a simple way to solve the partial differential equations of Maxwell's equations. Using the central difference approximations, the method discretises time and spatial domains into what we call Yee cells, which enables ***E*** and ***B*** fields to be evaluated at already selected points or some artificial boundary conditions. This artificial boundary conditions truncate the simulation. The recently developed perfectly matched layer (PML) can be used. Models on the effect of EM on the mobile phone hand set can be denoted by a current (Mouradi, Desai, Erdemir & Agarwal, 2011). The FDTD method then quantifies the amount of energy density within a layer which is the SAR.

Apart from its durability and ease of comprehension, the FDTD method enables determination in just one evaluation, the response in a specific frequency band by applying a pulse aggravation, this cannot be achieved by the Finite Element Method (FEM) or the Finite Integration Technique (FIT) frequency domain or the Method of Moments (MoM). FDTD possess vast capabilities in modelling, analysis and design of any radiation interacting with any material (Aly & Piket-May, 2014). It also allows for better modelling of the human body and mobile phone handset (ITU, 2012). FDTD is a tool deployed in this study.

Some Related Works

Musiige, Laulagent, and Anton (2012) presented a new methodology for emulating power consumption by the modem of LTE. They also suggested a method for assessing emitted SAR and RF strength in transmitting LTE signals. They emulated head SAR with polynomial interpolation models using FDTD simulations. They identified factors such as distance between head and phone, inclination between cheek and phone, transmitting device, and carrier frequency as high-level factors influencing the induced head SAR. However, they confirmed their expectations as their SAR values decreased linearly with distance. Their measured SAR and stimulated SAR differed by 0.7 %. They deployed the IEC 62209-1 and IEEE 1528 protocols. Musiige et al. also recorded a head SAR of 10.5 W/kg for the frequency 1500 MHz. However, their precisions of SAR emulation can only be guaranteed if the measurement uncertainties or simulation system uncertainties are less than or equal to the precisions of the mathematical estimate.

In a study by Bread, Kainz, Onishi and Iyama (2006) which compared computed mobile phone induced SAR in the specific anthropomorphic mannequin (SAM) phantom to that of anatomically correct models of the human head also employing the IEC 62209-1 and IEEE 1528 standards. Different institutions used different FDTD software and positioned the head models and MP as required by the protocol. There was a higher head SAR compared to the pinna SAR. The adult (larger) head recorded statistically significant higher peak SAR in all two cases of 10 g and 1 g SAR when compared results for children (smaller) head. This occurred for all configurations of phone position and frequency. They assigned reporting (exclusion or inclusion of pinna) and procedural issues which include modelling of EM source and inconsistent positioning of the MP as reasons to for already reported discrepancies of SAR underestimating and overestimating SAR in adults and children. They noted that simulation in the near-field SAR is basically a function of the RF current density distribution on the source, the geometrical separation of the MP from the head, and the source geometry. A 1 mm or 2 mm change in the case of a small separation distance can alter the SAR significantly. Their SAM data produced higher SAR compared to anatomically correct head models confirming the conservative nature of SAM results which indicate compliance with international standards. However, Bread et al could not explain slightly higher SAR of the anatomically correct head model as compared to SAM model.

Krstić, Zigar, Petković & Sokolović (2011) calculated absorbed EM energy in human head from mobile phones. They used the Finite integration technique

(FIT) to compute head 10 g and 1 g SAR for a flip and block mobile phones at an operating frequency of 900 MHz, a power of 0.5 W and impedance of 50 Ω. Significant difference was gotten from their results. Their obtained graph of 10 g SAR as function of distance of phone to the ear showed a sharp drop from 0 mm to around 20 mm then increases up to around 30 mm before gradually reducing over the distances for block MP. A comparison of their FIT method as supposed to the more efficient FDTD would have provided us a bases for validation.

In the work of Sole, Musu, Boi, Giusto & Popescu (2013), they proposed a system for designing and implementing and Radiofrequency identification (RFID) based sensor network safety management at the workplace. They simulated 1 g SAR at 869 MHz at a three different power values. Higher power resulted in increased SAR. They reported that the limit of 1.6 W/kg can be reached at the lower power of 0.6 W when the RFID reader system is 10 cm from the RF source. Their graph of 1 g SAR as a function of distance resulted in a decreasing curve that could be described by an exponential decay or inverse power relation.

Khan and Kaur (2019) presented electric and SAR analysis in multi-layered skin tissue to 5G mobile communication RF. They considered 28 GHz, 38 GHz and 60 GHz. In their numerical scheme, they showed that the EM energy from 5G is absorbed in the epidermis of the skin which can be interpreted as the penetration of 5G signals as superficial.

In another research by Khan and Ahmad (2015), they investigated the reduction in SAR at different frequencies for patch antenna at 1.8 GHz and 2.45 GHz frequencies. The maximum SAR for 10 g at 1.8 GHz was 0.55 W/kg and an

average value of 0.0013 W/kg. They did not consider different positioning of the phone in their competition.

Morega, Marinescu and Morega (2015) in their conference paper compared SAR results from measurements and numerical simulations by finite element method at an operating frequency of 1747.4 MHz. They indicated that, the energy absorbed by the human tissue from RF is dependent on four main factors. The anatomical domain, which includes the shape characteristics of the body, the electrical properties of the biological body, and the relative position of body in reference to the RF source. The second factor is the characteristics of the radiation source. This defines the frequency band, power, waveform of signal, type of antenna and the relative positioning of the phone. The ratification procedure is the third factor providing the standard and guidelines to compare the results with. The last factor is the physical aspect which determines the dosimetric quantities and the method of measurement or analytical estimation and even the techniques for averaging. They obtained and average 10 g and 1 g SAR of 0.580 W/kg and 1.023 W/kg respectively at cheek position and 0.404 W/kg and 0.693 W/kg respectively at tilt position. They also produced a non-linear relation of SAR and distance from 0 mm to 30 mm which can be modelled by an exponential decay relation. Their graph of SAR against distance showed cheek position producing relative higher SAR as compared to tilt position.

Mahfouz, Gati, Lautru, and Wiart (2012) investigated cumulative body exposure to simultaneous exposure to multi transmitters from mobile phones. They evaluated SAR using finite difference time domain (FDTD) for all varied

possible simultaneous transmission from multi and uni-antennas from the phone. They considered transmissions in the GSM, UTMTS, and WiFi systems at the same time. Instead of head model, they applied a liquid tissue, to simulate which made it easier to compare the different configurations. In all, the evaluated local SAR was always below the ICNIRP limit of 2 W/kg in 10 g of tissue, even though the maximum sum of SAR values from two different antennas evaluated was always lower than the maximum sum when evaluated separately. Even though their methodology is consistent with best practices, a validation of the values with actual SAR measurements would have provided a more representative picture. Nonetheless, the work estimated real life situations.

A number of researches have been undertaken to investigate the factors that influence the RF power output from mobile phone handsets as in Erdreich et al. (2007); Lena et al. (2006); and Lönn, Forssén, Ahlbom &. Feychting (2004). Study area (urban or rural) was the most influencing factor, whereas movement of user, location (indoors or outdoors) played lesser roles. Power output is directly proportional to SAR.

Subaar, Amoako, Owusu, Fletcher, & Suurbaar (2017), Wessapan, Srisawatdhisukul, Phadungsak, & Rattanadecho (2012), Aly & Piket-May (2014), Nguyen, Brown, Chang, Krycia, & Mirotznik, Habash, Bansal Krewski, Alhafid (2007), Wessapan, Srisawatdhisukul, Phadungsak, & Rattanadecho (2011); Sallomi (2012), Khalatbari, Sardari, Mirzaee & Sadafi (2006), and Spiegel (1984) estimated SAR in the human body by deploying either or both Maxwell's

equations and Pennes' bio-heat equation (Penne, 1948) through the use of FDTD or FED numerical approach.

Hillert et al. (2006) investigated three factors that influence the output power of mobile phones. By using three proxy parameters, they investigated the power distributions during calls. They used local switch logging information of calls made by a cohort of mobile phone users.

Lonn et al. (2004) also studied the output power of a mobile phone in relation to different geographical areas. They employed epidemiologic approach and used call records from a mobile communication operator. In the study of Kelsh et al. (2011), they researched the exposure during mobile phone use, by using epidemiologic studies in which they relied on software modified mobile phones to collect power control settings and a System Network Analyzer (SYNEHA) to measure the RF power output of the mobile phones in real life situations. The work investigated mobile phone power output as a relation of environmental conditions, the design of the handset, and the phone technology. In Erdreich et al. (2007), they deployed software modified phones and used the log information to investigate the relation between the engineering and behavioural factors in relation to how they affect the RF power output of GSM phones.

In a study by Mahfouz et al (2012), using various configurations, they evaluated SAR using the frequency division time domain approach of all possible simultaneous transmission from a mobile phone.

In this research, SAR is the measure of interest. The design employed in this research is in line with best practices, as it follows international protocols.

The SAR measurement is in line with the IEC 62209-1 (2016) international standard. This standard is a widely accepted and used protocol which recommends procedure for measuring SAR in the human head from wireless communication devices used close to the body like mobile phones.

Ghana's Situation

The study focuses on selected GSM mobile phone handsets used in Ghana. Ghana is a country in the west Africa sub region of Africa. It has a population of around 31 million people (Ghana Statistical Service, 2021). The ITU revels that, Ghana is one of the countries with a relatively high mobile cellular subscription. Ghana has surpassed Africa, Europe and the United States in subscribers per inhabitants (ITU, 2020). Figure 12 demonstrates this fact showing the trend over the years in perspective.

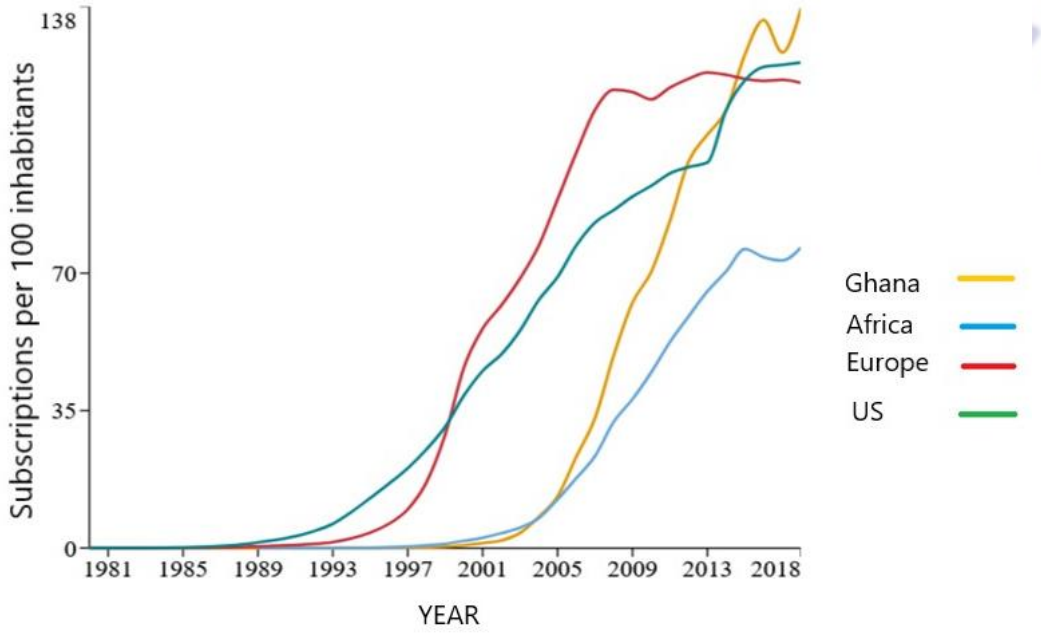

Figure 12: Mobile Cellular Subscription per 100 Inhabitants (ITU, 2020).

In Ghana, people start using internet as early as from age 12 with 96.79 % of the population covered by mobile cellular network, as indicted from data from ITU (2020). This gives us an idea of the exposed age groups in Ghana.

Data from the national regulator, NCA, indicates Ghana has over 41 million voice subscribers and around 25 million data subscribers. These figures approximately give an estimate of the number of mobile phones handsets in use currently in Ghana. Within the West Africa sub region, Ghana has the highest mobile penetration with mobile adoption at 50 % which exceeds the regional average of 44.8% (Omondi, 2020). This translates to the fact that; a huge portion of the population uses mobile phone handsets. In 2015, the government scrapped the customs duty on mobile phones making them more affordable. With the quest to feed the local demand of mobile phone handsets, it is not surprising that most of these handsets imported into the country have not been approved by the regulator but in use. Some others brought in by notable brand names generally submits for testing and approval before been sold in the Ghanaian market.

Based on my market survey, there are over roughly 200 brands of GSM mobile phone handsets currently in the Ghanaian market. This translates to around 1,000 different GSM mobile phone handsets. As at 2021, the NCA has approved 302 types of GSM mobile phones made up of 26 different brands (NCA, 2022).

Mathematical Relation of SAR and Distance

It is important to have an idea about the nature of the theoretical relation between SAR and distance. Equation 43 in Chapter 2 states that

$$\text{SAR} = \frac{\sigma|E|^2}{\rho} \qquad (43)$$

E is the electric field strength in tissue of density ρ. Coulombs law of charges requires that, the electric force F is related to the charge Q and a test charge q at a distance r by Equation 44 where ε is the electric property of the medium permittivity. The same force is related to the electric field strength by Equation 45. Putting Equation 44 and 45 into the SAR Equation 43 produces Equation 46.

$$F = \frac{1}{4\pi\varepsilon}\frac{Qq}{r^2} \tag{44}$$

$$E = \frac{F}{q} \tag{45}$$

$$SAR = \frac{1}{16\pi^2\varepsilon^2\rho}\frac{Q^2}{r^4} \tag{46}$$

Since we are dealing with antennas and hence electric current in this circumstance, we substitute the charge Q with current and time (It) in Equation 46 resulting in Equation 47.

$$SAR = \frac{1}{16\pi^2\varepsilon^2\rho}\frac{I^2t^2}{r^4} \tag{47}$$

In the experiment conducted to measure SAR in this research, all the variables in Equation 47 were held constant except the distance r. From Equation 47, we can state that the relationship between SAR and distance is an inverse to the fourth power relation. We can write Equation 47 by putting all the other factor as a single constant m as in Equation 48 where m is given by Equation 49.

$$SAR = m\frac{1}{r^4} \tag{48}$$

$$m = \frac{I^2t^2}{16\pi^2\varepsilon^2\rho} \tag{49}$$

Chapter Summary

The chapter opens with a broad perspective of the theoretical and physical concepts underpinning the research. This includes electromagnetism and Maxwell's equations. It then narrows down to the mobile phone, discussing its physical properties like antennas and supporting systems of the generations of mobile phones. The chapter closes by discussing some applied concepts and gave a critique of some related research work done elsewhere.

CHAPTER THREE

RESEARCH METHODS

Introduction

It is important to state that, in evaluation of exposure of RF radiation to the human head, the recommended initial step is the determination of the induced electric field as described by Wessapa et al. (2012). In line with this fact, this work measures SAR of the head from a mobile handset and determines the factors that affect this SAR.

In this chapter, materials, methods and analytical tools used for the research work are described. The chapter also describes how data was derived and analysed.

Sampling Procedures

The stratified method of sampling was employed in selecting the two GSM mobile phone handsets used in this study. This method satisfies the design of the study to investigate some call parameters of GSM mobile phones. The stratified method is a form of probability sampling which enables determining a basis for forming opinions and making conclusions about the population of interest. This approach provides a more accurate representation of the population as the diversity of each group is represented in the sample selected. Mobile phones used in Ghana were categorised into two subgroups:

- The first subgroup had GSM mobile phone brands names that have been tested by the regulator, NCA, and passed for use in the country.

- The other subgroup is made of GSM mobile phone brand names which has not been tested by NCA but are in use in Ghana

For the purpose of this research, one mobile phone handset was then selected from each of these two groups to be used in the experimentation. All measurement results were included in the analysis without sampling.

Data Collection Instruments

SAR is a measure of the time rate of RF energy absorbed by the body. In earnest, a SAR value tells us the maximum RF energy absorbed by a unit mass of tissue over a given time.

The SAR measurements were done in the NCA Type Approval Laboratories. They have the SAR laboratory where the SAR measurements were done, an RF signalling laboratory, and an EMF laboratory. The ComoSAR SAR measuring system used for this study was manufactured by Microwave Vision Group (MVG) of France. The group is made up of four leading industry players namely SATIMO, ORBIT/FR, AEMI AND RAINFORD EMC who are well known for their credentials.

The SAR measuring system generally has three main components, these are the SAR bench, the remote computer on which the SATIMO software runs, and instrumentation. The ComoSAR bench is enclosed in a Faraday cage which is designed to prevent interference from fields from the environment. In the cage, there is also the base station antenna connected to the Base station emulator. The SAR measuring system is made up of a ComoSAR twin bench which holds the robot, phantoms in which the SAR liquids are poured into, handset positioning

systems, probe holder with security sensor and a video positioning system (VPS). The bench is shown in Figure 13 and has a product number of SAR_4316_01, a project code of PAR21585 and originates from France. The Faraday cage of dimensions 400 cm by 300 cm by 302 cm. The other components include the robot controller, the multimeter, the network emulator, the voltmeter, the vector network analyser, the power meter, the signal generator, validation dipoles, SAR liquids and the computer which controls the process.

The role of each of these components of the SAR measuring system used this research are described below.

ComoSAR Bench

The ComoSAR bench is as shown in Figure 13. It is a standard COMOSAR twin bench with complete turn-key system. The bench has the video positioning system which is designed to ensure the exact positioning of the phantoms, the Device Under Test (DUT) and the probes. This bench is developed such that, it is used for device certification as all measurements are made in full compliance with international standards. Below, the components of the bench and their role are discussed. All these components are designed to ensure the exactness in positioning the probe for measurements.

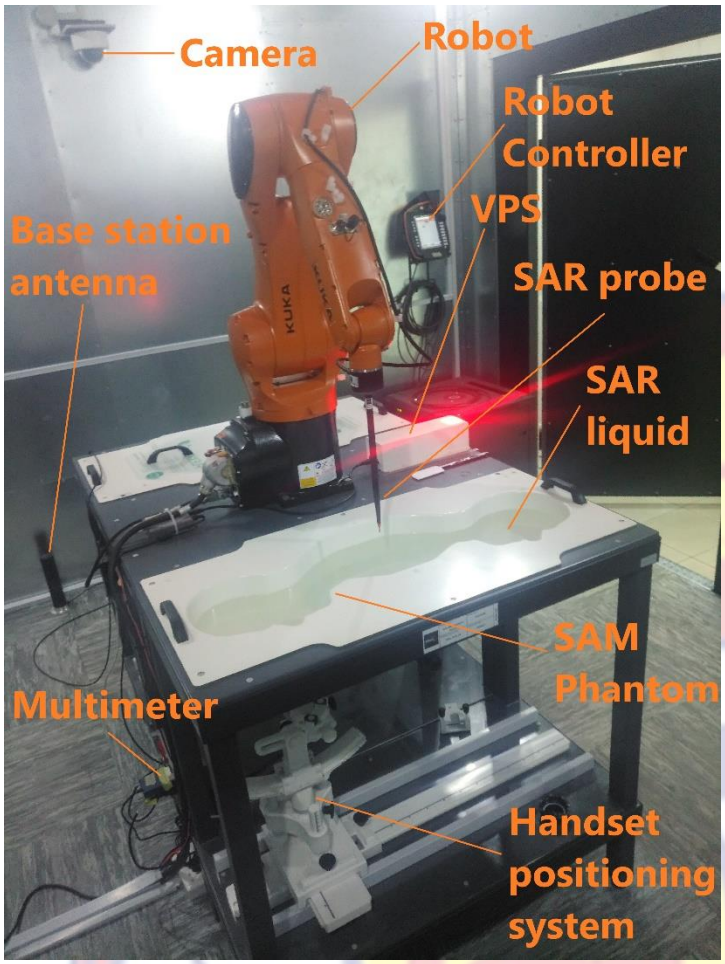

Figure 13: ComoSAR Bench and its components made up of Robot, Probe, Phantoms, Multimeter, Handset Positioning System and Robot Controller.

Robot

This a six-axis robot which comprises of a mechanical arm with a probe holder in which the measuring probe is fixed and used for the measurement. The robot uses the video position system to establish a reference point in the phantom to ensure the measurement points are exact to a specific area in the phantom for a test whiles the mobile phone held below the phantom operates at its maximum power. The robot comes with a controller device.

Phantoms

There are two phantoms on either side of the bench. One is a head phantom for head measurements whiles the other is a flat phantom for amplified performance check and body measurements, as well as to enable the measurement of exposure from different areas as a result of the asymmetric location of the phone antennas. The head phantom has two replicated sides for the right and left side of the head obviously to enable the measurements for the left and right ear. For the purpose of this research, the head phantom was used.

The phantom is a Specific Anthropomorphic Mannequin (SAM) based on the recommendations of the IEEE 1523-200X or CENELEC 50361 standards. The SAM Phantom is integrated with the wooden bench and has a thickness of 2 mm $\pm$ 0.2 mm made from polyurethane shell. The phantom comes with a cover to reduce evaporation of the SAR liquids when not in use and also a tap to drain liquids. It is required to fill with 20 L of SAR liquids or 15 mm depth. The phantom has compressed ears to account for persons with smaller ears. Its reference points are marked near its mouth purposely for mobile phone measurements and also marked at centre of the flat side.

Tissue Simulation Liquids

There are SAR liquids that emulate human tissues which is poured in the phantom for SAR measurements. No singular SAR liquid can correctly stimulate human tissues over the stretch of frequencies. Hence, different liquids are used for different frequencies. These homogenous liquids are produced according to frequency bands which ranges from 300 MHz to 6 GHz. The SAR liquid used in

this work were produced in reference to IEC standards and has a tolerance from related standard target values of ± 10 % and ± 5 %.

Multimeter

The multimeter measures and control the amount of current that the robot uses and also the voltage that each dipole returns and sends this information to the computer system.

Handset positioning system

This device plays an important role as correct positioning of the DUT is required because of the effect of distance to SAR. The system is indicated in Figure 13. Its function is to hold and position phone handsets below the phantom for SAR measurements. The system which is fixed on rails, enables a handset positioning resolution better than 1 mm and has a scaled curved rail to allow the quick switch from cheek position to tilt positions when making measurements. The rails have precision of less than one degree. It is devoid of metallic parts. All these properties increase accuracy and precision of the measurements. It is made of extremely stable material Polyethylene Terephthalate (PETP) which provides lower permittivity, all aimed at reducing its influence on the results of measurements. The design of the system ensures easy reproducible positioning of the handset, easy handing, and allows proper positioning of measuring dipoles as recommended by Commission Européenne de Normalisation Électrique (CENELEC), International Electrotechnical Commission (IEC), Institute of Electrical and Electronics Engineers (IEEE) and American National Standards Institute (ANSI).

Video position system

This system has a very important function as it ensures that measuring probes position exactly, allowing a small difference of ± 0.1 mm. It is composed of LED, mirror, mechanical parts and a camera. The software measures the exact location of the probe when the robot positions the probe just above the mirror. This enables good accuracy of the probe and also ensures its safety. It serves as reference point where the robot calibrates before taking the measurement points in the phantom.

SAR probes

The probe measures the internal electric field distribution in the phantom due to EM fields produced by the phone. They are electric field detectors used for SAR measurement because they enable the measurement of fields in air or liquid according to standards such as IEEE 1528, IEC 62209-1 and IEC 62209-2, EN 50383 and EN 50361 as well us FCC OET Bulleting (Ed. 97-01) supplement C. They are made up of loops linked to special Schottky diodes which has low detection thresholds, or orthogonal dipoles and available with a frequency range of 30 MHz to 6 GHz. Measurements can be made without embedded battery or amplification as the probes are developed with materials of high permittivity which minimises disturbances of the E-field.

The SSE5 and SSE2 probes used for the research had 5 mm or 2 mm as the tip diameter and a dynamic range from 0.01 Wkg^{-1} to 100 Wkg^{-1}. The probe's linearity and spherical isotropy were both greater than 0.25 dB whiles the axial isotropy is greater than 0.50 dB.

Interpolation and extrapolation scheme of the probe

Small dipole sensing elements of the probe measure the local SAR inside the phantom. In doing so, and to minimize errors, the probe tip must not touch the surface of the phantom. However, the maximum local SAR occurs at the surface. Hence, the system uses an extrapolation algorithm which is premised on fourth-order-least-square polynomial fit of the data measured to determine this maximum value, extrapolating 1 mm from the phantom surface.

Very fine resolution in three-dimensional scanned data array give the required accurate highest SAR averaged over 1 g and 10 g. This is achieved with the system employing interpolation to provide an array of sufficient resolution. Because of its quick time response and higher sensitivity, the electric field probe is the suitable sensor for measuring SAR.

Other Instrumentation and Materials

Outside the Faraday cage, there are several devices that play a role in the SAR measurement. There is the base station simulator or network emulator which performs the function of base station to which the mobile handset DUT connects to during the measurement. It enables the choice of communication technology, power and other call factors such as side of the head used for the call, the orientation of the phone, and the operating frequency.

The signal generator as the name indicates, produces the RF waves or signal needed in the communication.

Validation dipoles play an important role in the calibration process before measurement is done. They are used with the Vector Network Analyser

equipment to conduct Liquid property measurement which ensure the SAR liquid been used for the measurement has the required dielectric properties before measurements are done.

The Vector network analyser (VNA) as discussed earlier, is used to conduct the liquid property measurement as one of the key calibration processes before measurements. It is an Anristu MS2025B model. The Power Amplifier has the role of working with the network emulator to amplify the power of the communication signal.

All these components are connected to the computer on which the OPENSAR software is installed as indicated in Figure 14. Using the software, all the various components can be controlled and operated.

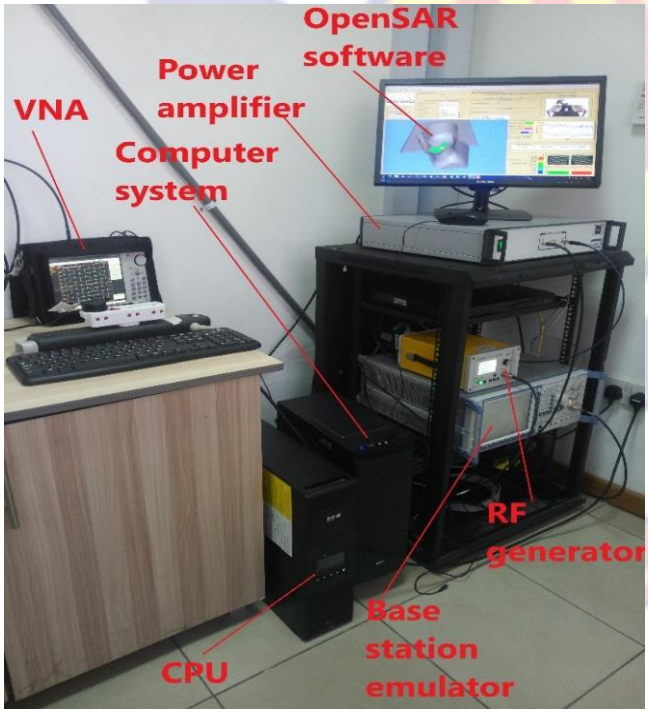

Figure 14: Other components connected to the Computer System made up of Base Station Emulator, RF generator, a Computer System with the controlling OpenSAR software, the VNA and Power Amplifier.

Mobile Phones Used

Two GSM mobile phones were used in this research. One GSM mobile phone was chosen at random from a group of mobile phones (MPs) that have been tested and approved for sale in Ghana by the NCA's Type Approval laboratory.

The second GSM phone, bought in the open market, is not in the list of phones approved by NCA. It is inexpensive and affordable to many categories of Ghanaians. Table 4 describes the two MPs used in the research and their characteristics such as the video channel (VC), the product serial number (S/N) and the international mobile equipment identity (IMEI) which are unique identifier for the mobile phone based on the number of subscriber identity modules (SIM) allowed by the phone.

Table 4: GSM Mobile Phones used in the research and their features such as the International Mobile Equipment Identifier (IMEI)

Item	Phone A	Phone B
Name of phone	Tecno Camon 15 Air	X-inova
Model	Techno CD6	G16
Android version	10	7.0
Video channel	601410	-
Serial number	IZN1	-
IMEI	353782110015845 353378211005852	353855111838090 353855111838108
Regulatory approval	Approved	Unapproved
Manufacturer Head SAR (W/kg)	0.802	0.80

(Source: Research work)

Data Collection Procedures

Measurements were done during the day, between the times of 8 am to 5 pm, and spanning the three months of October to December 2020. All measurements were conducted by the researcher under the supervision of the NCA type approval laboratory Manager.

All the various components or devices of the SAR system were manually powered individually. This includes the robot, the power amplifier, the VPS, the signal generator, the VNA, the multimeter, and the computer to which the various devices were connected and the OpenSAR software was launched. Using the robot controller, which uses SATIMO software, communication between the robot and the computer is established.

Three pre-measurement processes were done before measurements were made. These processes are; liquid property measurement, noise evaluation, and dipole system evaluation.

Liquid property measurement

This is done using the VNA, a thermometer, the liquid measurement kit, a jack, andOSLKF50 probe, distilled water and an RF cable to connect the probe to the VNA. The setup is as shown in Figure 15 without the computer system which has already been shown in Figure 15.

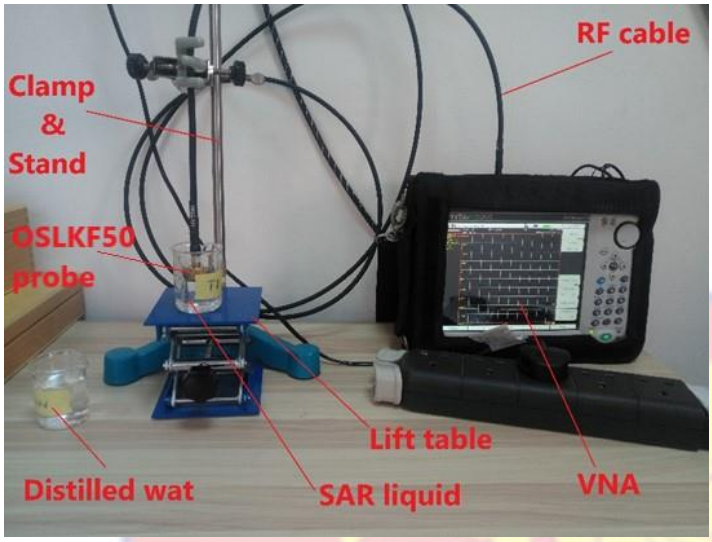

Figure 15: SAR Liquid Property measuring setup.

The purpose of the measurement was to ensure that the dielectric properties of the SAR liquid to be used for the measurement was still within the approved standards. The steps in this process were as follows.

The correct SAR liquid to correlate the frequency band for which the measurement is been done was selected and poured onto the phantom to a height of 15 mm at the head side and 13 mm for the flat side by help of a measuring dip stick. The OSLKF50 probe and the VNA were connected via the RF cable as shown Figure 15. Then the probe was then calibrated with air using the calibrating tool and the OpenSAR software. The temperature of the SAR liquid and a distilled water were taken using the thermometer. The water temperature was entered into the software. The probe was calibrated with distilled water by bringing the probe in touch the surface of the distilled water. The process was repeated but this time with the SAR liquid fetched from the phantom.

The software then generates a report in which figures in green indicate a pass in the range of ±5% or ±10% of the standard, whiles red figures indicate those parameters of the SAR liquid do not conform with standards.

Noise Evaluation

This is basically the background check. The evaluation was done to ensure the ambient RF noise was within the standard of been less than 12 $mWkg^{-1}$. The following steps were followed.

The measuring SAR probe to is connected to robot and record its serial number recorded. The robot was referenced on the OpenSAR software, the serial number was confirmed, and the correct parameters selected on the software. A report was printed after the evaluation which include the Noise level evaluation. This was incorporated in the SAR measurement results.

Dipole System Evaluation

This was the final evaluation which was done before the actual test was conducted. It was used to determine if the probe is measuring correctly. In essence, if a specific amount of RF power is delivered and emitted by the SAR measuring dipole, the probe is expected to measure a SAR value that falls in the calibration range. It also ensures that the test results meet standards. It involves the power meter, the validation dipole of the appropriate frequency, the signal generator, the coupler, the power amplifier and RF cable. Figure 16 shows the dipole been positioned under the phantom. The frequency corresponding spacer is to create a space between the dipole and the phantom.

Using the OpenSAR, the system prints the Dipole test SAR value results taking into consideration losses in the coupler, the connectors and the RF cables. This was compared to calibration values.

Figure 16: Positioning of Dipole Antenna in the Handset Positioning System for Dipole System Evaluation.

Mobile Phone SAR Measurement

It was only after the liquid property test, the noise evaluation test, and the dipole evaluation, that the actual SAR DUT measurement can be done. These tests form part of the quality assurance (QA) and quality control (QC) measures of the system. The measurement was conducted in line with the recommendations of IEC 62209-2 (2010), IEC 62209-1 (2016), IEC 62704-1 (2017), IEEE 1528 (2013), IEEE (2013). The following process were used.

The mobile phone was fully charged at each measurement. Robot referencing was conducted to ensure the robot measures at exact measurement

points withing the phantom. The Universal Subscriber Identity Module (USIM) was inserted in the MP and connected to the base station simulator. The MP was then positioned with the horizontal line crossing the centre of the earpiece and the vertical centre line of the body of the phone in a plane parallel to the sagittal plane of the phantom.

The phone was tested both in the check and tilt position as indicated in Figure 17. The figure also indicates the front and top views of the phone positions. Measurement parameters were then confirmed on the menu of the OpenSAR software. This involve choosing the side of the head for the measurement, choosing tilt or cheek orientation, and choosing operating frequency. Zoom scan was selected and measurement started. Each measurement takes 25 mins. The robot, using the SAR probe then automatically takes several SAR measurements in the phantom within 25 minutes. The system generates and prints a measurement report in Microsoft Word format.

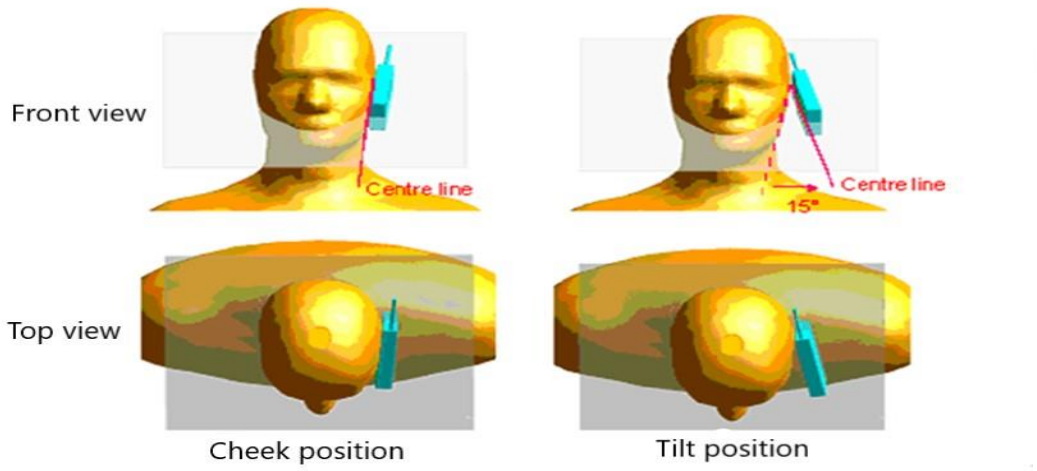

Figure 17: SAR measurement Phone Orientation Positions, showing Cheek and Tilt Phone Positions (Credits: OpenSAR software SAR measurement report).

It is important to emphasise that, the correct positioning of the MP below the phantom is key to ensure accurate results. Figure 18 shows the researcher positioning a phone in the handset positioning system under the bench below the head phantom, before measurement is made.

For the purpose of the research, some parameters were held constant through the experiment. The parameters held constant are, network technology (GSM), frequency of transmission (1800 MHz), standard for measurement (IEC 62209-1, 2016), temperature (18 ºC – 25 ºC), transmission power (phone maximum), and time (25 mins). These parameters were held constant to ensure these parameters do not influence the SAR values of the factors been investigated.

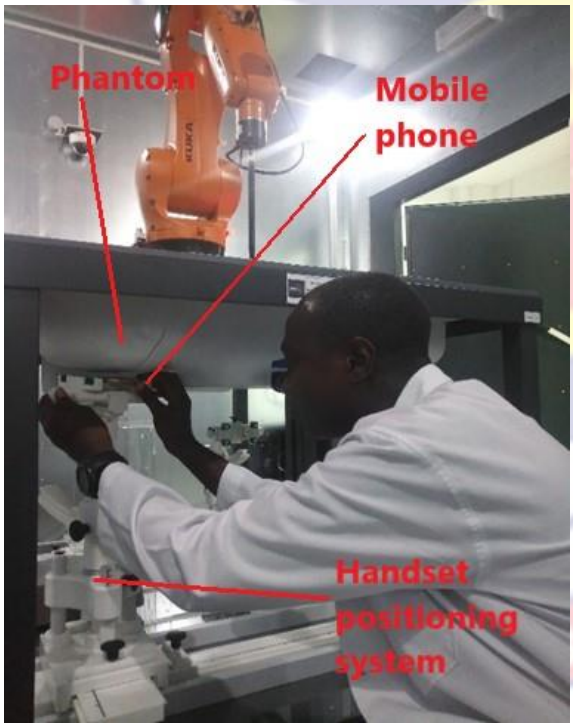

Figure 18: Positioning the Phone in the Handset Positioning System below the Phantom for SAR measurement.

Call Parameters Investigated

The following phone call parameters (call parameters) of interest were investigated to find how they affect the head SAR by keeping other factors constant whiles the particular parameter of interest is altered. These are distance of phone from ear (1.0 cm. 2.0 cm, 3.0 cm), phone positioning (side of head used), phone orientation (cheek or tilt position) and operating Frequency (high, middle, low)

The SAR system occasionally goes offline and has to be restored. This took some of the laboratory time. After three months of taking measurements, the robot froze whiles conducting measurements, and had to be dismantled and sent back to manufacturers outside the country. The measured SAR data of the approved and unapproved phone are provided in Appendix C and Appendix D respectively.

Data Processing and Analysis

The values of Peak SAR, 10 g SAR, and 1 g SAR, all of units of Watts per kilograms (W/kg), were recorded for every distance position (units in cm) were recorded in the SAR report generated by the OpenSAR software. These SAR values in the report produced, were crosschecked against the data logged as notepad files during measurement and stored in folders in the OpenSAR system as a way of limiting data entry errors.

SAR was measured at four different distances, 0.0 cm (at skin surface), 1.0 cm. 2.0 cm and 3.0 cm from the head. The reference positioning (how the phone has been positioned) of the phone has three letter components. The first letter

represents the side of the ear, the left (L) ear or right (R) ear. The second letter is the tilt (T) or cheek (C) position, whiles the third letter represent the frequency band of transmission. The frequency band is either low(L), middle (M) or high (H) band. So, an LCL reference position code of the phone means, the phone is on the left ear, at cheek position, and transmitting in the low frequency band. Table 5 further describes these coded reference phone positions. All these codes have been explained in Appendix E.

As a control to the research, the average SAR measurement results of the approved and unapproved phone were compared to that of high-end phones (HEP). High-end phones are phones of highest quality, from trusted manufacturers, have passed all necessary vigorous international and national regulatory requirements, and are expected to behave as model phones. SAR measurement data of high-end phones from the NCA laboratory were used. The NCA measures SAR in line with IEC 62209-1 (2016).

Table 5: Coding of Reference Positioning of Phones

Side of Ear	Position of Phone	Band	Frequency	Channel
Right (R)	Cheek (C)	Low (L)	1710.199951	512
Left (L)	Tilt (T)	Middle (M)	1747.400000	698
		High (H)	1784.599976	884

(Source: Research work)

The data was analysed with the help of Microsoft Office Excel and R-Programming Language. These analytical tools are very efficient, widely used and

well recognised. The results are described as graphs, statistical quantities, absolute numbers, tables and statements in the next chapter, chapter four.

Derived Distance-SAR Mathematical Model

Predictive models to estimate SAR in the head when phone is at distances 0.0 cm to 3.0 cm were derived from the data collected using RStudio programming, GraphPad Prism and Microsoft Excel analytical tools.

The derived relationship between SAR in the head (SAR_{Head}) and distance of the phone from the head (d_{head}) is a one phase exponential relation for the approved phone and an exponential decay relation for the unapproved phone, generalized in Equations 50 and 51 respectively. The constant Y_0 is the intercept, whiles K is the rate constant, and P_l is the plateau of the SAR.

$$SAR_{Head} = (Y_0 - P_l)\, e^{-Kd_{head}} + P_l \quad (50)$$

$$SAR_{Head} = Y_0\, e^{-Kd_{head}} \quad (51)$$

The implications of the two equations are wide and varied and is well discussed in Chapter 4. The exponential decay models relating SAR and distance for each of the 12 different reference phone positions for the approved phone and unapproved phone and for all the three depended quantities were derived. These predictive models (Appendix F and G) were then programmed as an application using MATLAB programming called SAR calculator, of which one can estimate the 10 g head SAR by inputting parameters like the phone been approved or unapproved, choosing right or left ear, tilt or cheek phone orientation, high, middle or low frequency channel, and distance of phone from head. The programming codes for the MATLAB programming are presented in Appendix I.

Validation of distance-SAR mathematical models

In validating the derived relations of Equations 50 and 51, different independent set of data from different phones assessed by the NCA SAR laboratory were used. These NCA SAR data were inputted into the relations and the calculated SAR agreed well with the NCA data SAR. This quality assurance was done to ascertain the validity of the relations derived.

Measurement Uncertainty Evaluation

The measured SAR values will only be properly reported when they include their uncertainty analysis. The uncertainty estimation used here is guided by IEC 62209-1 (2016).

Both Type A and Type B evaluations of standard uncertainty were used. The student's-t factor was used as the coverage factor k since the degrees of freedom are less than 30. The standard uncertainty u_i for the Type B evaluation is derived from the upper and lower limits, a_+ and a_- respectively depended on the probability distribution function that defines the half-length of the interval set by limits of the influencing quantity a, where a is given by Equation 52.

$$a = (a_+ - a_-)/2 \qquad (52)$$

Hence, with k as the coverage factor, we can write:

- Normal distribution - $\boldsymbol{u_i = a/\sqrt{k}}$
- Triangular distribution - $\boldsymbol{u_i = a/\sqrt{6}}$
- Asymmetric / U-shaped distribution - $\boldsymbol{u_i = a/\sqrt{2}}$
- Rectangular distribution - $\boldsymbol{u_i = a/\sqrt{3}}$

To achieve the 95% confidence level, the student's-t factor was approximated as the coverage factor k as the degrees of freedom are less than 30. Hence, the coverage factor k_p for small sample populations is then evaluated using Equation 53 where the subscript p is the approximate confidence level.

$$k_p = t_p(v_{eff}) \quad (53)$$

Equation 54 was used to estimate the uncertainty due to isotropy, u_{iso}, where the fields incidence angles around an imaginary sphere enclosing the probe tip is accounted for by the weighing factor, w_i.

$$u_{iso} = \sqrt{(1 - w_i)(axial\ isotropy)^2 + w_i(hemispheri\ cal\ isotropy)^2} \quad (54)$$

A rectangular probability distribution was assumed for the probe linearity uncertainty and the continuous wave (CW) percentage linearity tolerance SAR_{lt}, was determined using Equation 55. The CW signal SAR measured at the ith power level, P_i, is $SAR(P_i)_{CW_i}$ associated with the percentage probe linearity.

$$SAR_{lt} = \left(MAX_{SAR(P_i)_{CW_i}=0.12\ W/kg}^{SAR(P_i)_{CW_i}=100\ W/kg} \left(100 \times \left| \frac{SAR(P_i)_{CW_i}}{P_i} - 1 \right| \right) \right) \quad (55)$$

The percentage relative uncertainty u_{ru}, using the probe detection limit, is then evaluated using Equation 56.

$$u_{ru} = 100 \times \left| 1 - {}^{detection\ limit}/_{0.4\ W/kg} \right| \quad (56)$$

The percentage uncertainty associated with the modulation of the signal was determined using Equation 57, where $SAR(P_i)_{mod\ x_i}$ is the measured SAR with the modulated signal at an average power and $SAR(P_i)_{CW_i}$ in this instance is the measured SAR with a continuous wave at the same average power.

$$SAR_{um} = MAX_{i=(x,y,z)}(MAX_{P_i=P_0}^{P_0+20\ dB}\left(100 \times \left|\frac{SAR(P_i)_{mod\ x_i}}{SAR(P_i)_{CW_i}} - 1\right|\right) \quad (57)$$

Equation 58 is an estimate for the percentage boundary effect uncertainty, SAR_{ube}, which is based on exponential and linear extrapolations, where d_{be} is the length in mm between the closest zoom-scan measurement point and the surface, d_{step} is the distance in mm between second and first measurement locations closest to the surface of the phantom when we assume a negligible boundary effect at the second point, and δ is the least penetration depth in mm of the head tissue equivalent liquid.

$$SAR_{ube} = \delta SAR_{be}\frac{(d_{be}+ d_{step})^2\,(e^{-d_{be}/(\delta/2)})}{\delta d_{step}} \quad (58)$$

Using the first-order error approximation, the percentage scanning system uncertainty is evaluated by Equation 59, where d_{ss} is the highest position uncertainty between the actual position considering the reference point described by the manufacturer and the evaluated position.

$$SAR_{ss} = \frac{d_{ss}}{\delta/_2} \times 100 \quad (59)$$

The phantom uncertainty SAR_{pu}, expressed as a percentage in Equation 60 was determined in which d is the highest tolerance of the shape phantom and thickness of the shell and a in this case is the separation between the position of the equivalent filament current density of the source.

$$SAR_{pu} = 100 \times \left(\frac{(a+d)^2}{a^2} - 1\right) \quad (60)$$

The uncertainty associated with probe positioner in relation with the phantom shell was evaluated with Equation 59 where d_{ss} is replaced by d_{ph},

which is the uncertainty used for evaluating the distance between the phantom shell and the tip of the probe.

Equations 61 was used to estimate the percentage uncertainty associated with the device holder SAR_{dhu}. $SAR_{w/\ holder}$ is the SAR when device is in holder and $SAR_{w/o\ holder}$ is the SAR when without a holder.

$$SAR_{dhu} = \left(\frac{SAR_{w/\ holder} - SAR_{w/o\ holder}}{SAR_{w/o\ holder}}\right) \times 100 \quad (61)$$

The temperature range of 25 ˚C to 18 ˚C is recommended for SAR measurements. So (a ± 2) in ˚C allowance is recommended for measuring dielectric properties. The liquid temperature uncertainty, SAR_{lt_ε} , was also derived as a percentage using Equation 62, where $\varepsilon_T T_{high}$ is the temperature (T_{high}) relative permittivity. The temperature T_{high} is the maximum temperature at which the dielectric properties were measured, and vice versa for T_{low}. The uncertainty for the liquid conductivity was also evaluated with Equation 62 by replacing ε_r with relative conductivity, σ_r.

$$SAR_{lt\_\varepsilon} = \left|\frac{\varepsilon_r(T_{high}) - \varepsilon_r(T_{low})}{\varepsilon_r(T_{high}) + \varepsilon_r(T_{low})} \times \frac{2\ ℃}{T_{high} - T_{low}}\right| \quad (62)$$

$SAR_{compensated}$, which is the uncertainty of the SAR drift (measured) of the GSM mobile phone was accounted by using Equation 63. $SAR_{measured}$ is the measured SAR.

$$SAR_{compensated} = SAR_{measured}\left(1 + \frac{|drift|}{100\ \%}\right) \quad (63)$$

The OpenSAR software evaluates and present an uncertainty analysis as part of the report it prints. The summary of the uncertainty analysis is summarised in Appendix H as an uncertainty budget for the SAR measurements made with an

expanded uncertainty of 20.32 % and 20.06 % for 1 g SAR and 10 g SAR respectively and a confidence interval of 95 %.

Chapter Summary

The chapter starts by presenting some methods applied by researchers in measurement and evaluation of SAR. The chapter then takes a dive into the study area, describing the sampling technique employed, evaluating the equipment used and explaining the data collection procedures.

Some limitations in the methodology include the small number of GSM phones whose SAR was measured and limiting the distances to only 4 different distances.

CHAPTER FOUR

RESULTS AND DISCUSSION

Introduction

This chapter presents and examine in detail the outcomes of the measurements. Generally, four quantities were presented, 10 g SAR, 1 g SAR and Peak SAR according to distance and phone position. The results are provided in relation to the type of mobile phone. The chapter begins by providing the results at each of the four different distances that SAR was measured, then carefully examines these results, analysing the trends, similarities, differences and implications of the results. The chapter concludes by presenting derived distance-SAR predictive models of the two phones from which a phone SAR calculator application has been designed. The chapter then ends with a summary of main results.

The results of the measurements are presented starting with the Regulator Approved GSM Phone, followed by the Regulator Unapproved GSM Phone. Then, a comparison is made of the two phones and other related results whiles ending by comparing the results of the two GSM phones to that of a high-end phone (HEP) of high standard which has passed all the necessary international and national requirements. The HEP is used as the control for the experiment.

Figures 19 to 22 provides the levels and trends of the 10g SAR, 1 g SAR and Peak SAR for each distance (0.0 cm, 1.0 cm, 2.0 cm, and 3.0 cm) from the phantom head for the 12 different reference position the phone was placed for the approved phone. Their corresponding figures for the unapproved phone are

provided in Figures 32 to 35. The trends of the reduction of SAR levels with increase in distance are presented in Figures 23 to 28 for the approved phone and Figures 36 to 41 for the unapproved phone. Figures 29 to 31 compares trend behaviour of each of the measured quantities across the four distances for the approved phone whiles Figures 42 to 44 also does same for the unapproved phone.

The SAR values of the two phones are compared at each distance point in Figures 45 to 48 which brings out the differences and similarities. The average and maximum SAR measurements are given in Figures 49 and 50. That of the left ear are then compared to that of the right ear in Figures 51 to 53. The SAR levels of the two phones are then juxtaposed to that of High Earn Phone (HEP) at 0.0 cm of phone from the phantom head in Figures 54 to 56. Table 6 provides a glance of the percentage SAR reductions as distance increases. The summary of the SAR measurement results is given in Table 7, whiles a statistical summary of the measured SAR values is also presented in Table 8.

Results of Regulator Approved GSM Phone

This section puts the approved GSM phone in perspective. It describes the results of the SAR measurement quantities of 10 g SAR, 1 g SAR and Peak SAR of the approved phone.

Nature of approved phone SAR values at individual distances

Figures 19, 20, 21, and 22 provides the SAR levels and trends at 0.0 cm (when the phone is touches the phantom head), 1.0 cm, 2.0 cm and 3.0 cm from the phantom head respectively at each reference position of the phone.

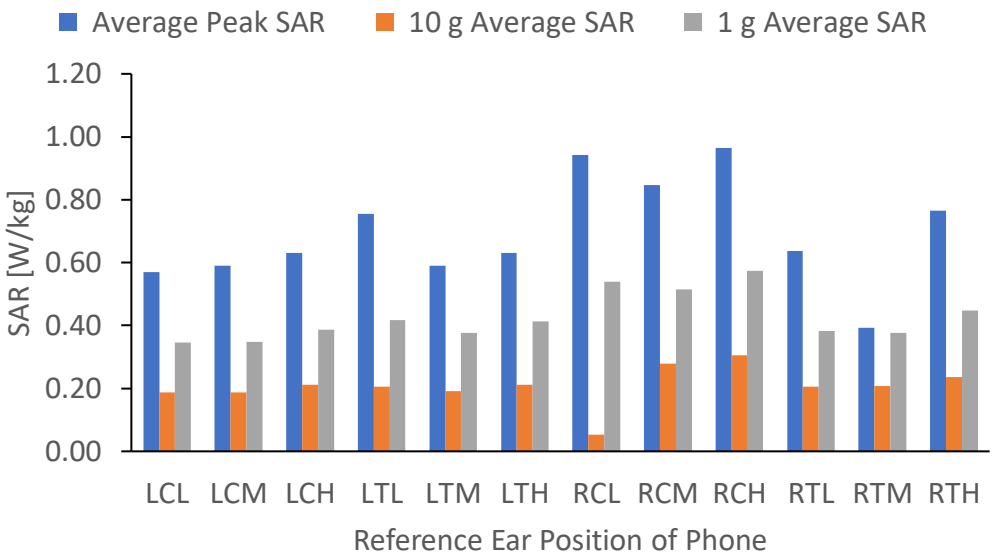

Figure 19: SAR levels of Approved Phone at 0.0 cm from Phantom Head at different Reference Ear Positions.

At 0.0 cm (Figure 19), where the phone touches the phantom head, recorded generally the highest SAR values compared to the 1.0 cm, 2.0 cm, and 3.0 cm. This is expected as SAR has an inverse power relation with distance as demonstrated with Equation 48 of Chapter 3 where SAR decreases as inverse power with increasing distance. It is also consistent with the results of Musiige et al. (2012), Krstić, et al. (2011), and Morega et al. (2015) in terms of the nature of the relation between SAR and distance. For the approved phone, it is observed in Figure 19 that, the right-cheek (RC) reference positions have relatively higher SAR levels for all three quantities of average 10 g SAR, average 1 g SAR and average peak SAR. At 0.0 cm, the highest 10 g SAR and 1 g SAR were 0.5067 ± 0.0106 W/m2 and 0.9942 ± 0.1994 W/m^2 respectively which occurred at the right-cheek-high (RCH) frequency band reference position. The minimum value for 10 g occurred at right-cheek-low (RCL) band reference position. There

appeared to be a similar SAR level trend for the three quantities across the reference positions as seen in Figure 19. The similarity of SAR trends is expected for the 10 g and 1 g but not for the peak SAR.

The trend similarities of 10 g, 1 g and peak SAR levels over the reference phone positions continues at 1.0 cm for the approved phone with the highest levels occurring still on the right ear for the approved phone, specifically at the right-tilt-high (RTH) reference position, as seen in Figure 20.

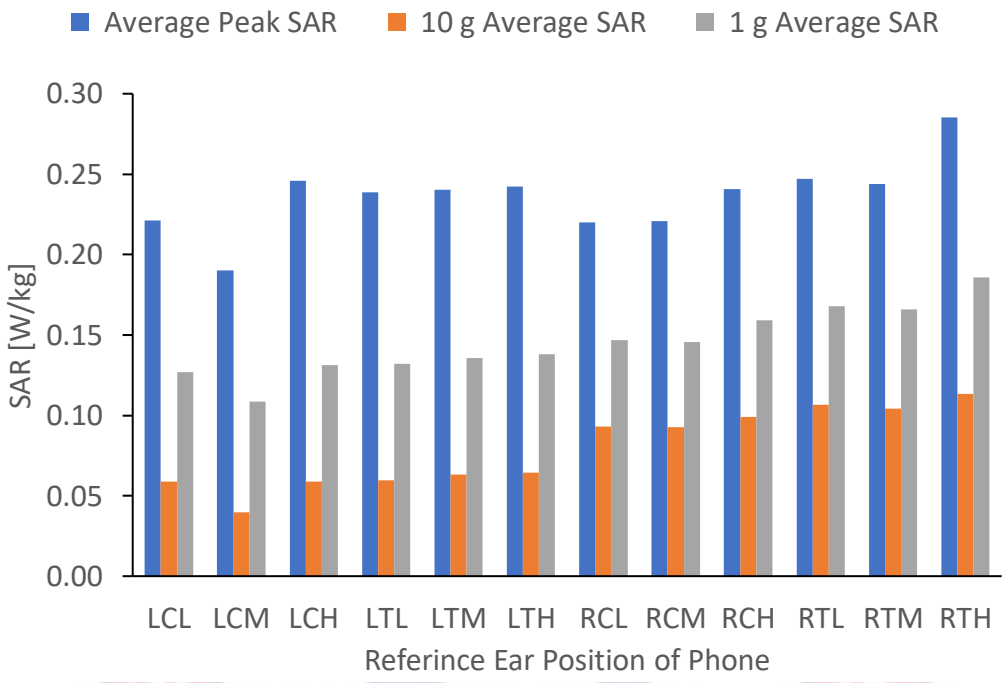

Figure 20: SAR levels of Approved Phone at 1.0 cm from Phantom Head at different Reference Ear Positions.

Figure 21 depicts the nature of average SAR quantities at 2.0 cm from the phantom head. The SAR levels drops at left-tilt positions and rise but rises on the right ear. As seen in Figure 22, the 3.0 cm SAR levels of the approved phone are generally lower than that of 2.0 cm. The SAR levels are lower at left-tilt positions.

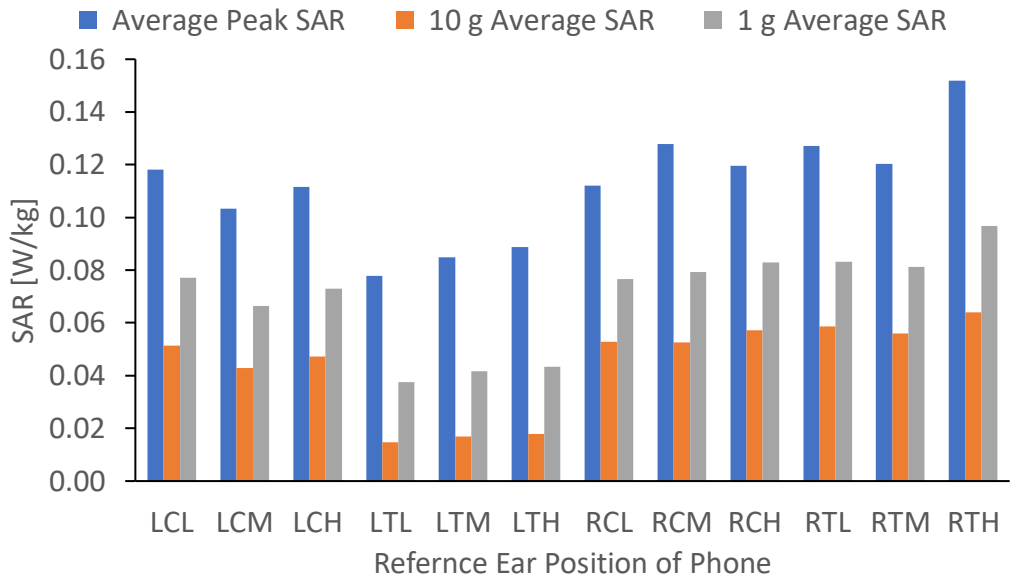

Figure 21: SAR levels of Approved Phone at 2.0 cm from Phantom Head at different Reference Ear Positions.

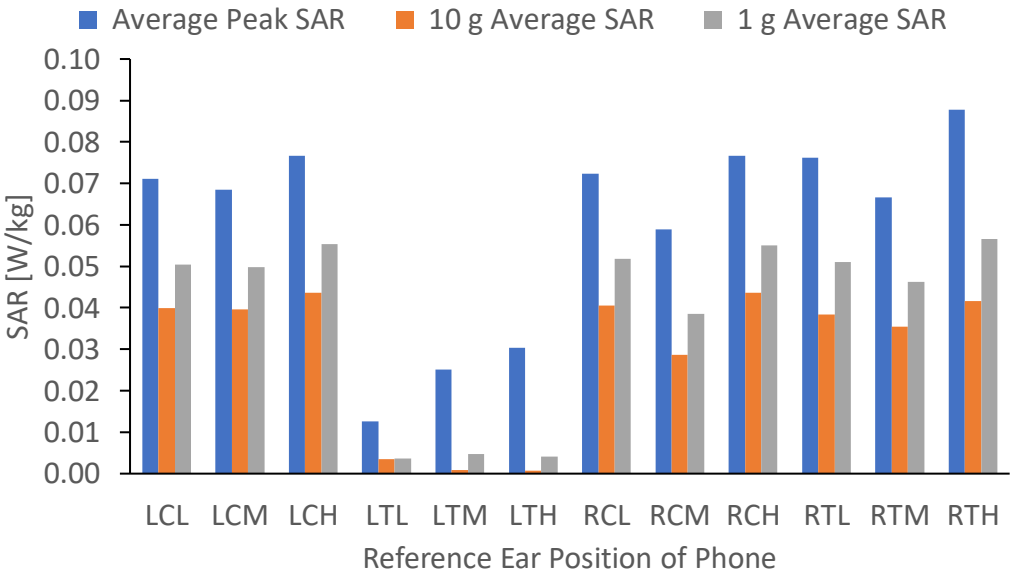

Figure 22: SAR levels of Approved Phone at 3.0 cm from Phantom Head at different Reference Ear Positions.

Reduction in approved phone SAR with distance

It is expected that an increase in the distance of the phone from the phantom head should result in a change in SAR levels. The quantum of these SAR changes over the distances are shown in Figures 23, 25, and 27, whiles the nature of the changes is described in Figures 24, 26 and 28 for 10 g SAR, 1 g SAR and Peak SAR respectively.

There was regular predictable reduction in SAR quantities of average 10 g SAR, average 1 g SAR and average peak SAR in almost all cases (Figures 23, 24, 25, 26, 27 and 28) when distance of phone from phantom head is increased confirming the inverse power relation between SAR and distance. There were exceptions at two situations, all at cheek positions, involving average 10 g SAR at right-cheek-low (RCL) reference position when the phone moved from 0.0 cm to 1.0 cm, and also at left-cheek-middle (LCM) reference position when the phone distance is increased from 1.0 cm to 2.0 cm (Figure 23 and 24).

The SAR reduction trends of decay nature or inverse power relation with distance as presented in Figures 24, 26, and 28 generally agrees with the computed SAR trends of Sole et al. (2013) at different power levels but over the distance of 10 cm m to 100 cm. It also agrees with results of Musiige et al. (2012), Krstić, et al. (2011), and Morega et al. (2015). A model developed by Khalatbari et al. (2006) also produced a relation where the local SAR reduced inversely proportional to the power of the distance but not a square power. There is also similar correlation with the work of Morega et a1. (2010). They analysed measured and numerical simulated head SAR of mobile phones at a working

frequency of 1747.4 MHz. They reported a maximum measured 10 g SAR and 1 g SAR of 0.580 W/kg and 1.023 W/kg respectively for cheek position, and 0.404 W/kg and 0.693 W/kg respectively for tilt positions with a relative error of ±10 %. These compared with the maximum values of the approved phone but not with those of the unapproved phone as presented in Figure 50. The derived SAR-distance relation as depicted from Morega et al. was also non-linear (exponential decay or inverse power) in nature with their SAR-distance graphs producing similar trends to those presented here.

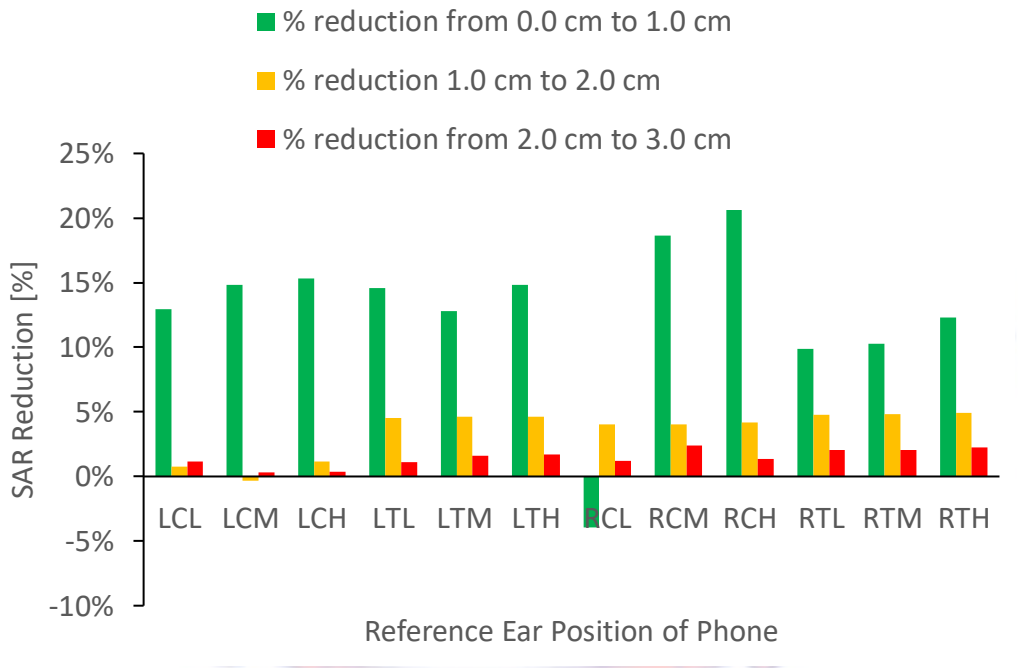

Figure 23: Percentage Reduction of Approved Phone's Average 10 g SAR resulting from changes in Phone Distance at different Reference Ear Positions.

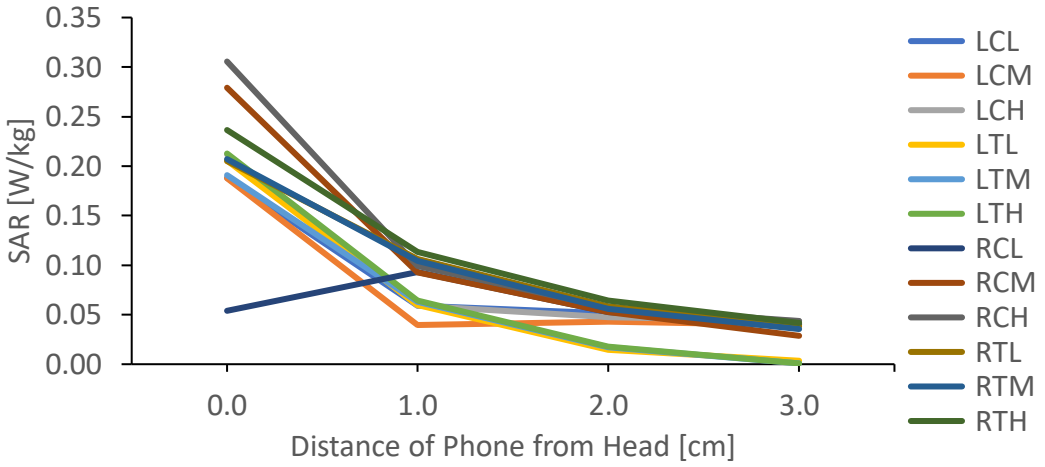

Figure 24: Reduction Trends of Approved Phone's Average 10 g SAR resulting from changes in Phone Distance at different Reference Ear Positions.

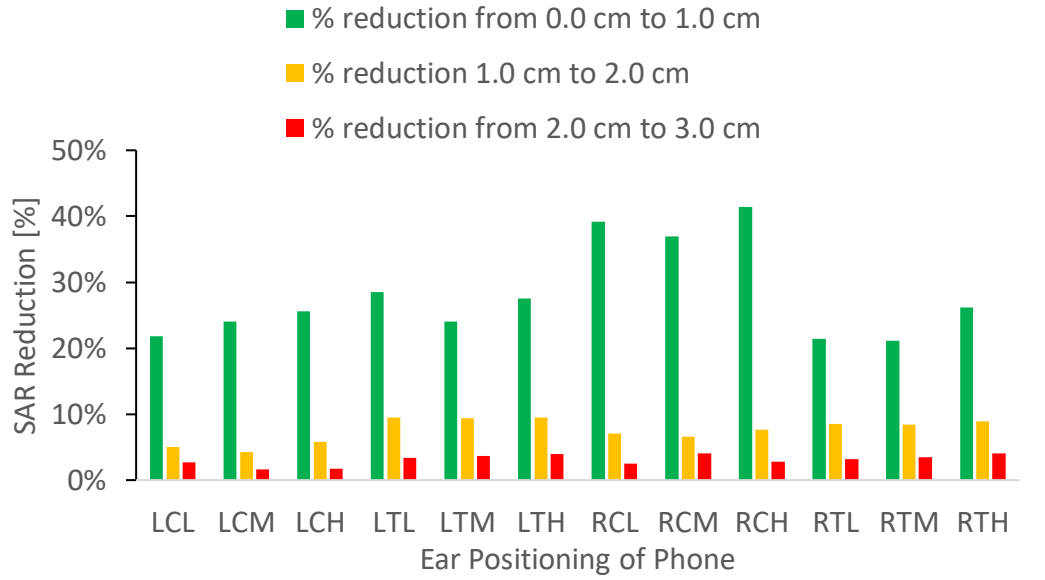

Figure 25: Percentage Reduction of Approved Phone's Average 1 g SAR resulting from changes in Phone Distance at different Reference Ear Positions.

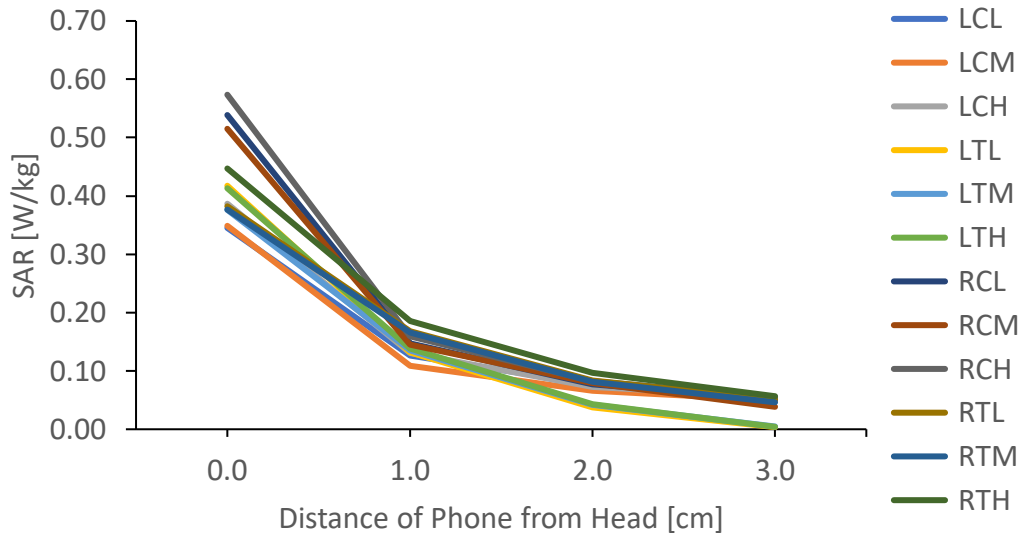

Figure 26: Reduction Trends of Approved Phone's average 1 g SAR resulting from changes in Phone Distance at different Reference Ear Positions.

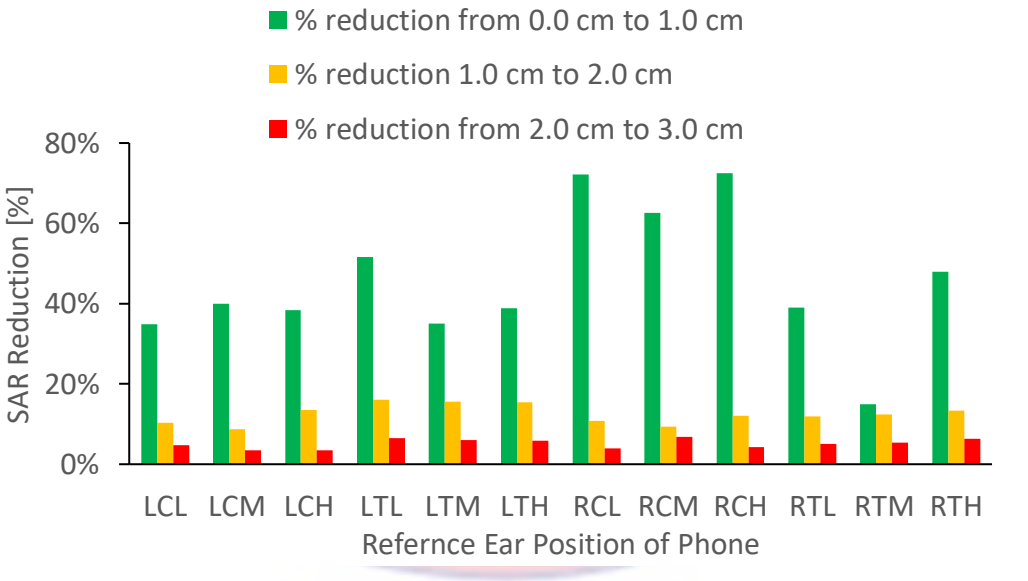

Figure 27: Percentage Reduction of Approved Phone's Average Peak SAR resulting from changes in Phone Distance at different Reference Ear Positions.

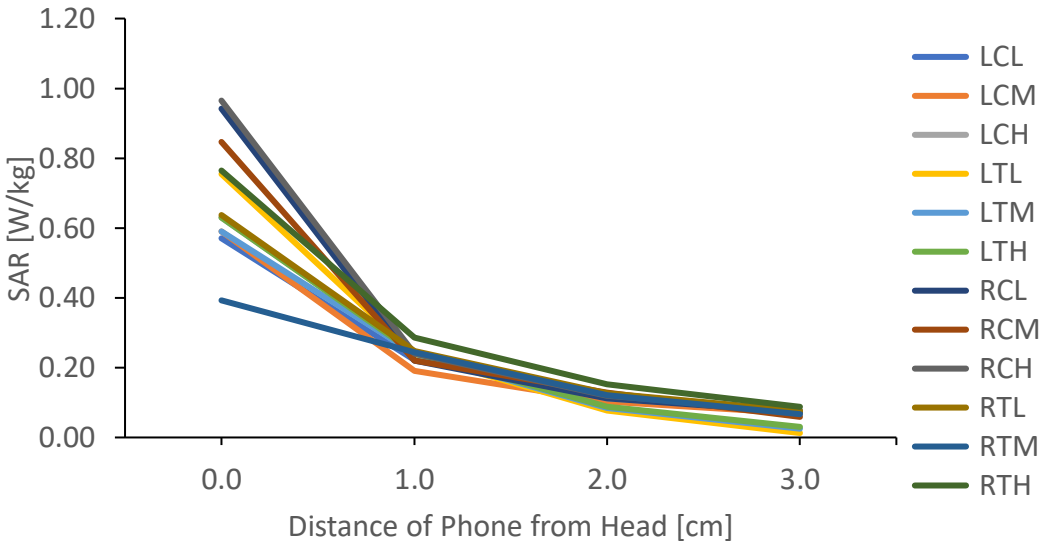

Figure 28: Reduction Trend of Approved Phone's Average Peak SAR resulting from changes in Phone Distance at different Reference Ear Positions.

Comparing nature of approved phone's SAR at all distances

Figures 29, 30 and 31 compares the trend levels of approved phone SAR values over the distances.

A close look at the nature of the average 10 g SAR values of the approved phone over the reference positions show general regular similarities in the trends at 1.0 cm, 2.0 cm, and 3.0 cm with SAR levels raising from the left to the right ear and shown in Figure 29. The levels at 0.0 cm at all positions are relatively higher and follows in that other except right-cheek-low (RCL) position. The trend of 0.0 cm deviates from all others. This situation is not different with the average 1 g SAR (Figures 30 and 31) and the average peak SAR (Figures 37 and 38). However, that of the unapproved phone as displayed in Figures 42, 43 and 44 shows an irregular trend with little similarities between the trends of different distances.

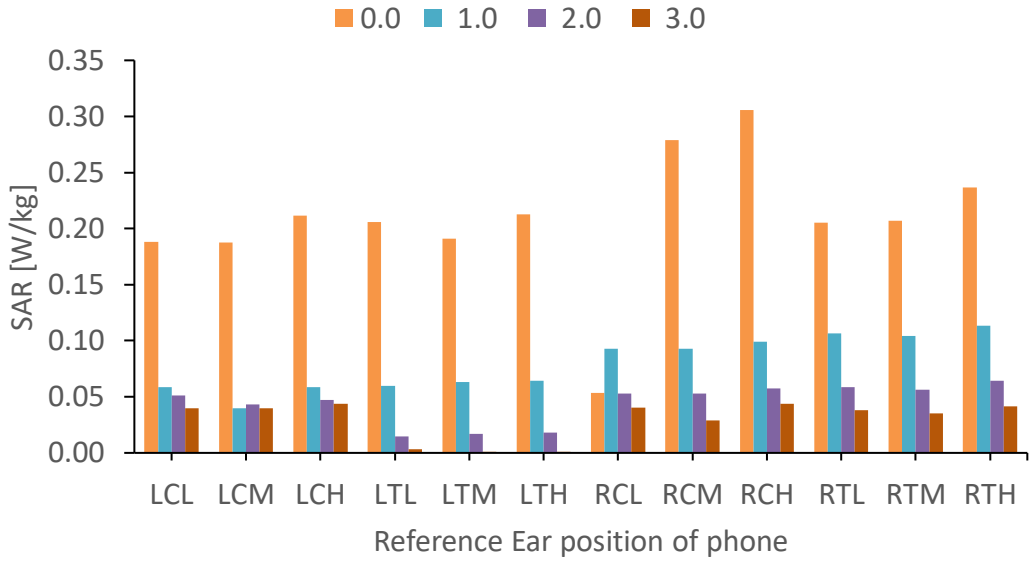

Figure 29: SAR Trends of Approved Phone's Average 10 g SAR for the distance (cm) points at different Reference Ear Positions.

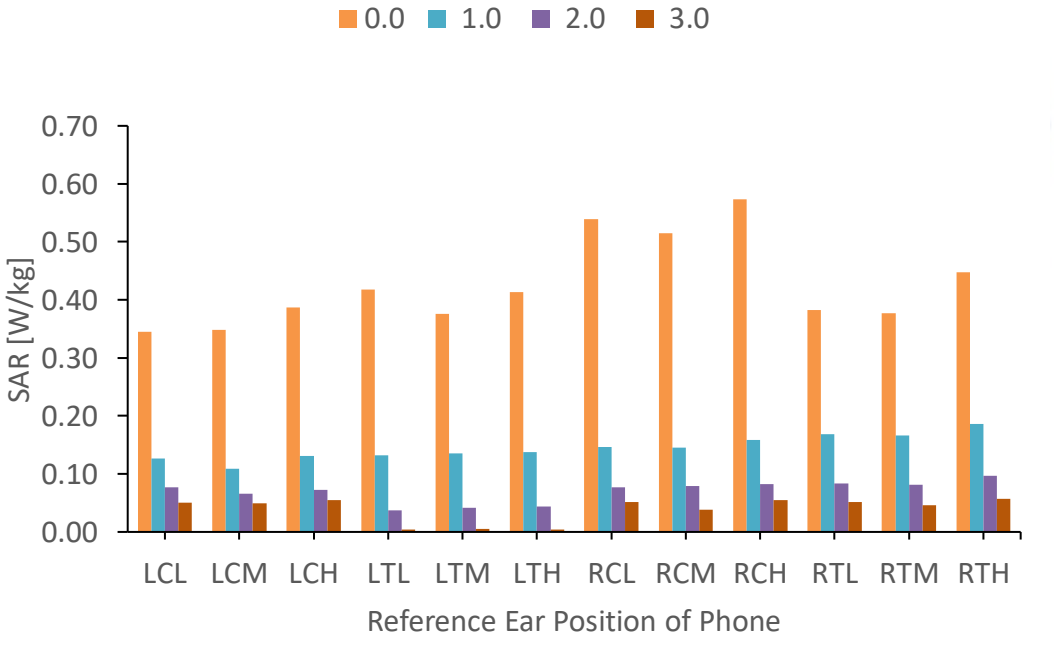

Figure 30: SAR Trends of Approved Phone's Average 1 g SAR for the distance (cm) points at different Reference Ear Positions.

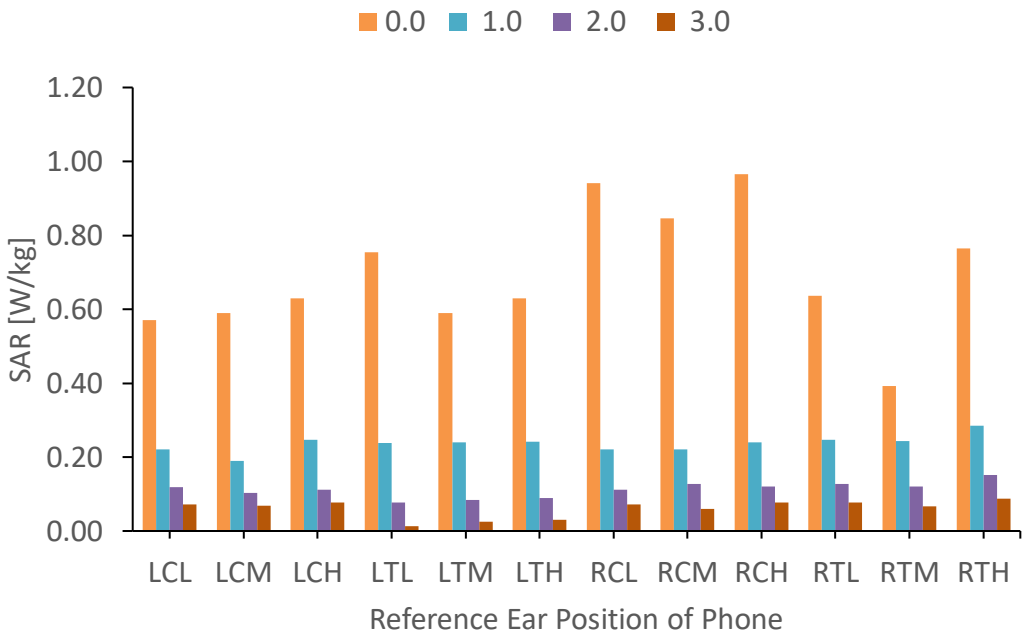

Figure 31: SAR trends of Approved Phone's Average Peak SAR for the distance (cm) points at different Reference Ear Positions.

Results of Regulator Unapproved GSM Phone

SAR measurement results of the unapproved GSM phone are presented in this section.

Nature of unapproved phone SAR values at individual distances

The levels of the SAR quantities at each of the distances for the unapproved phone are presented in Figures 32, 33, 34 and 35. For the unapproved phone, the maximum of both 10 g and 1 g SAR at 0.0 cm occurred at the right-cheek-middle (RCM) band reference position as shown in Figure 32. The trends of the SAR levels over the reference phone positions are similar.

At 1.0 cm, the SAR levels drops when phone is moved the right ear as shown in Figure 33. This is also happened at the 2.0 cm (Figure 34), but in this

case, the high SAR values were recorded on the left-tilt positions. The cheek positions for both left and right ears had increased SAR values for 3.0 cm, shown in Figure 35.

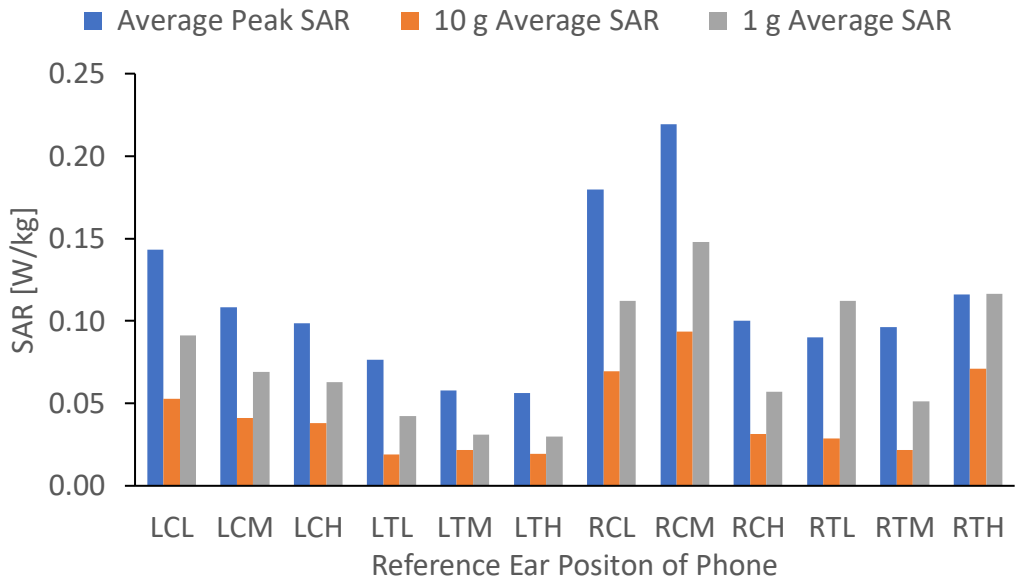

Figure 32: SAR levels of Unapproved Phone at 0.0 cm from Phantom Head at different Reference Ear Positions.

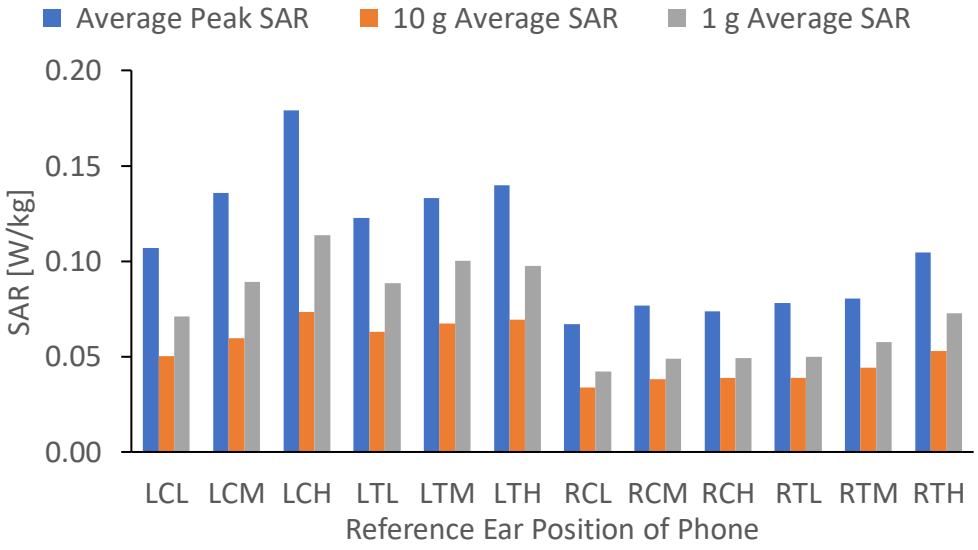

Figure 33: SAR levels of Unapproved Phone at 1.0 cm from Phantom Head at different Reference Ear Positions.

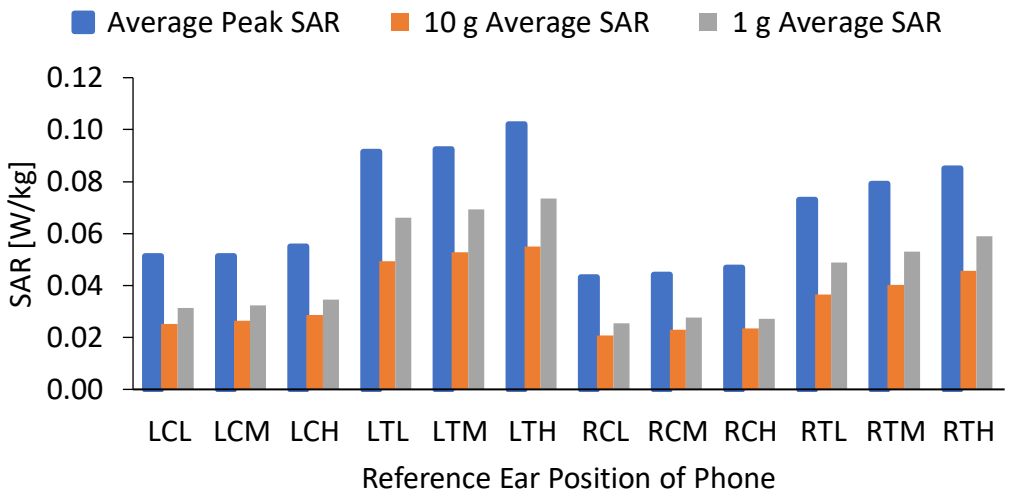

Figure 34: SAR levels of Unapproved Phone at 2.0 cm from Phantom Head at different Reference Ear Positions.

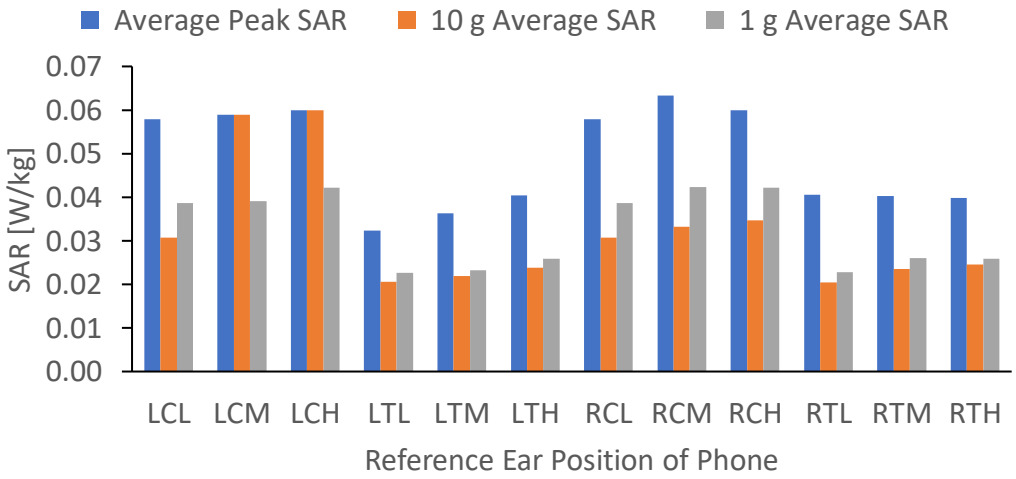

Figure 35: SAR levels of Unapproved Phone at 3.0 cm from Phantom Head at different Reference Ear Positions.

Reduction in unapproved phone SAR with distance

A graphic representation of the values of the change in SAR as the unapproved phone is moved away from the phantom head are depicted in Figures

36, 38, and 40. The nature of the changes when compared with other distances are also shown in Figures 37, 39 and 41.

A critical view of the quantum of reduction in SAR levels as distance from the phantom head increases reveals a clear distinction in the behaviour of the two GSM phones. In sharp contrast to that of the approved phone, the reductions of the unapproved are very irregular as seen in Figures 36, 37, 38, 39, 40 and 41. From these figures, it is observed that, there are SAR increases instead of reduction as distance is increased. There are SAR increases at all cheek positions on both right and left ears. These deviations occur with all SAR quantities and at all levels of distance increase. These results are at variance with those obtained by Musiige et al. (2012), Krstić, et al. (2011), and Morega et al. (2015) in which case SAR decreased at every increase in distance.

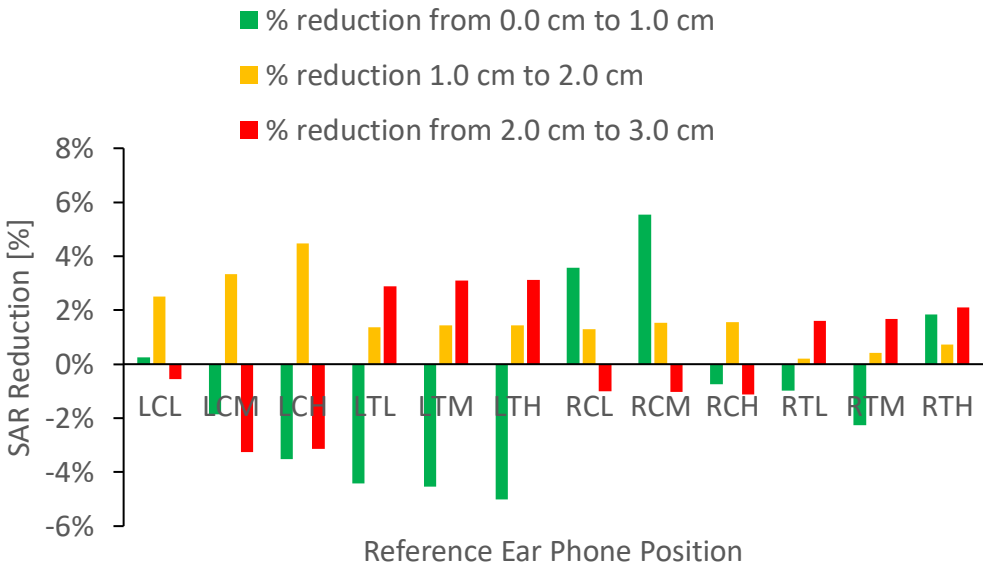

Figure 36: Percentage Reduction of Unapproved Phone's Average 10 g SAR resulting from changes in Phone Distance at different Reference Ear Positions.

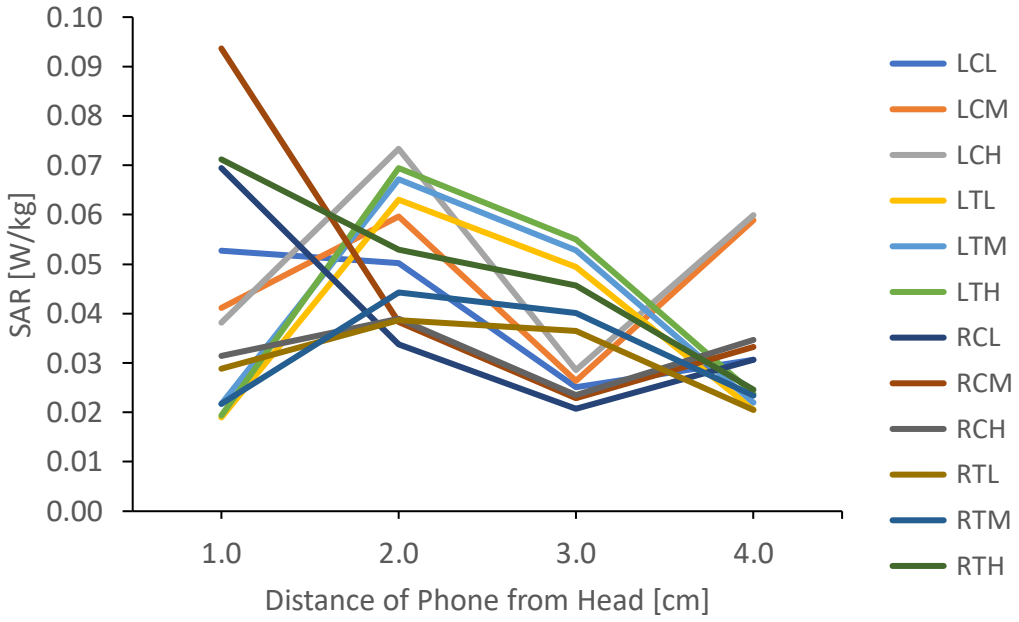

Figure 37: Reduction Trends of Unapproved Phone's Average 10 g SAR resulting from changes in Phone Distance at different Reference Ear Positions.

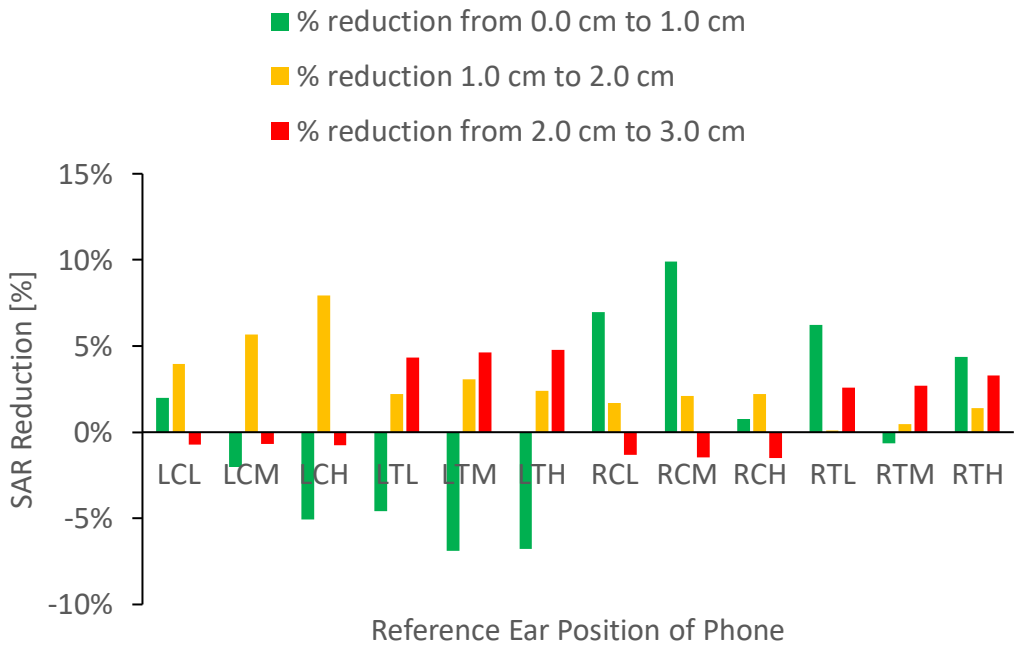

Figure 38: Percentage Reduction of Unapproved Phone's Average 1 g SAR resulting from changes in Phone Distance at different Reference Ear Positions.

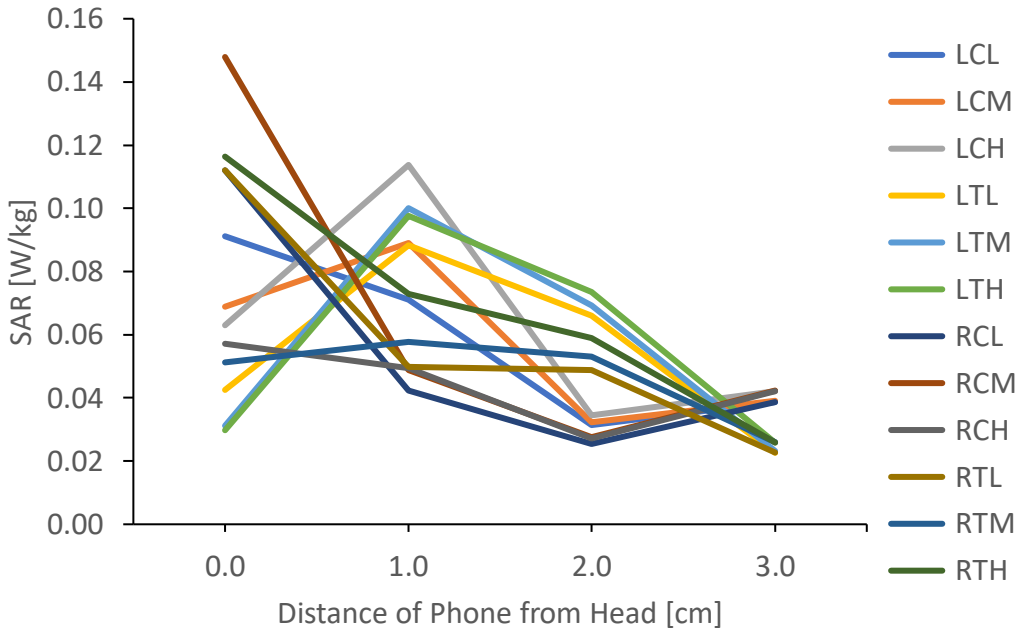

Figure 39: Reduction Trends of Unapproved Phone's Average 1g SAR resulting from changes in Phone Distance at different Reference Ear Positions.

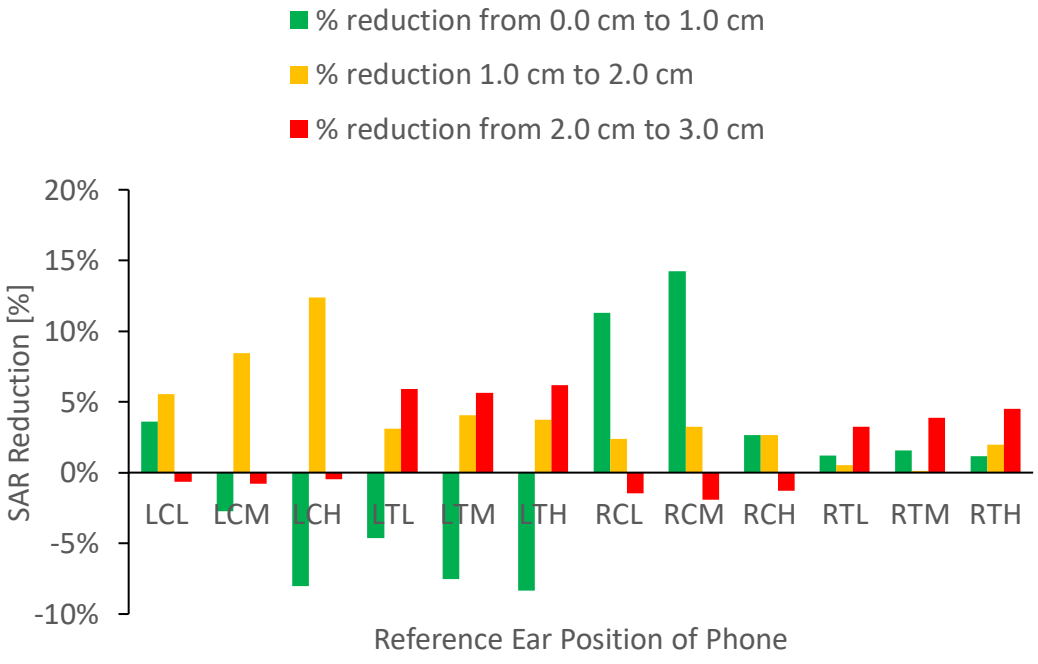

Figure 40: Percentage Reduction of Unapproved Phone's Average Peak SAR resulting from changes in Phone Distance at different Reference Ear Positions.

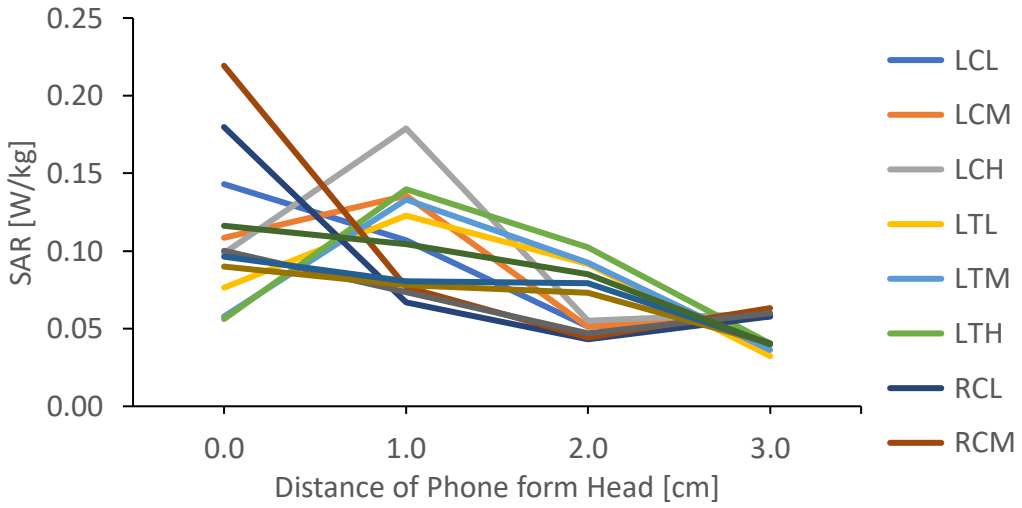

Figure 41: Reduction Trends of Unapproved Phone's Average Peak SAR resulting from changes in Phone Distance at different Reference Ear Positions.

Comparing nature of unapproved phone's SAR at all distances

This stage describes the nature of unapproved phone SAR considering all the four distance positions as presented in Figures 42, 43 and 44.

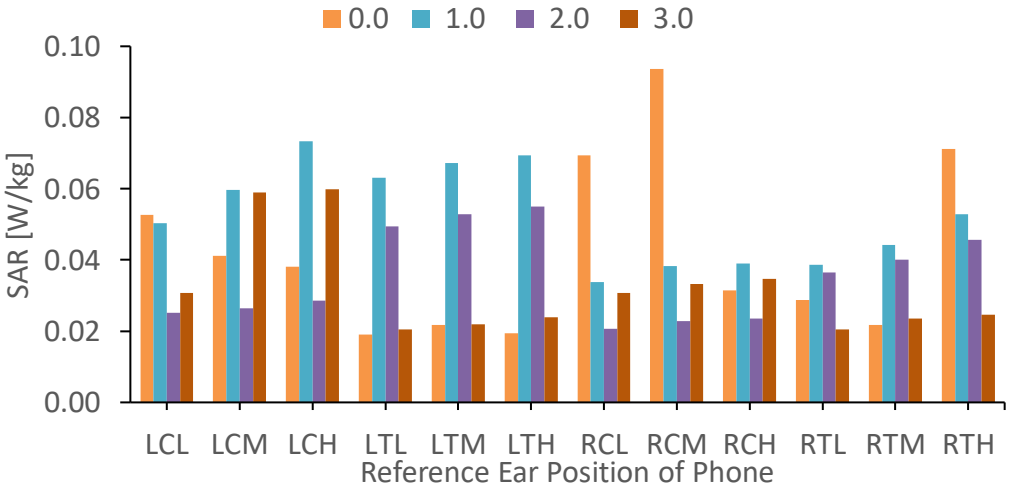

Figure 42: SAR trends of Unapproved Phone's Average 10 g SAR for the distance (cm) points at different Reference Ear Positions.

It is obvious the irregular nature of the SAR values making them difficult to predict. The SAR values of the left ear are more irregular compared to that of the right ear as observed from Figures 42, 43 and 44.

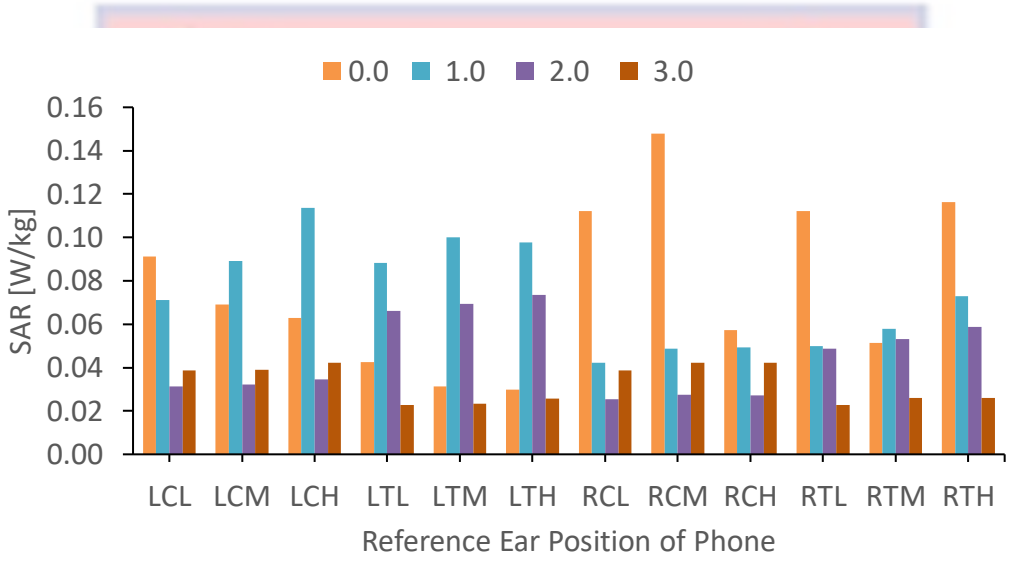

Figure 43: SAR trends of Approved Phone's average 1 g SAR for the distance (cm) points at different Reference Ear Positions.

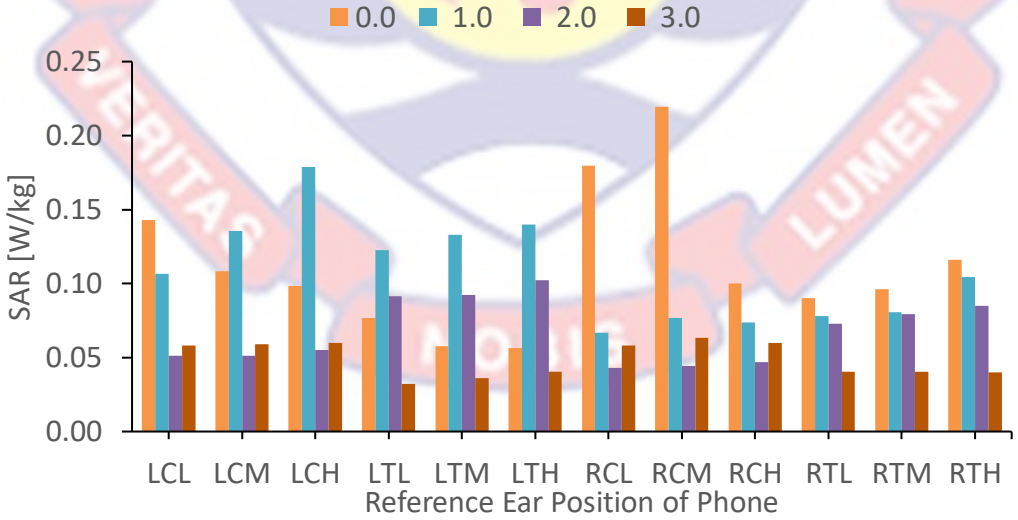

Figure 44: SAR trends of Approved Phone's Average Peak SAR for the distance (cm) points at different Reference Ear Positions.

Comparison of SAR Results of Approved and Unapproved Phones

A comparison of the SAR values of the approved and unapproved phones at four measurement distances are made in this segment as done in Figures 45, 46, 47 and 48. Table 6 compares the average SAR reduction with increase distance. Figures 63 and 64 compares average and maximum SAR values.

A critical assessment of Figure 45, which compares the SAR levels at 0.0 cm, shows that both SAR level tends across the various reference positions of the two phones rise at the right-cheek positions. The approved phones levels are higher in all cases except at the right-cheek-low (RCL) reference position where the 10 g SAR of the approved dips lower than all SAR quantities of the unapproved.

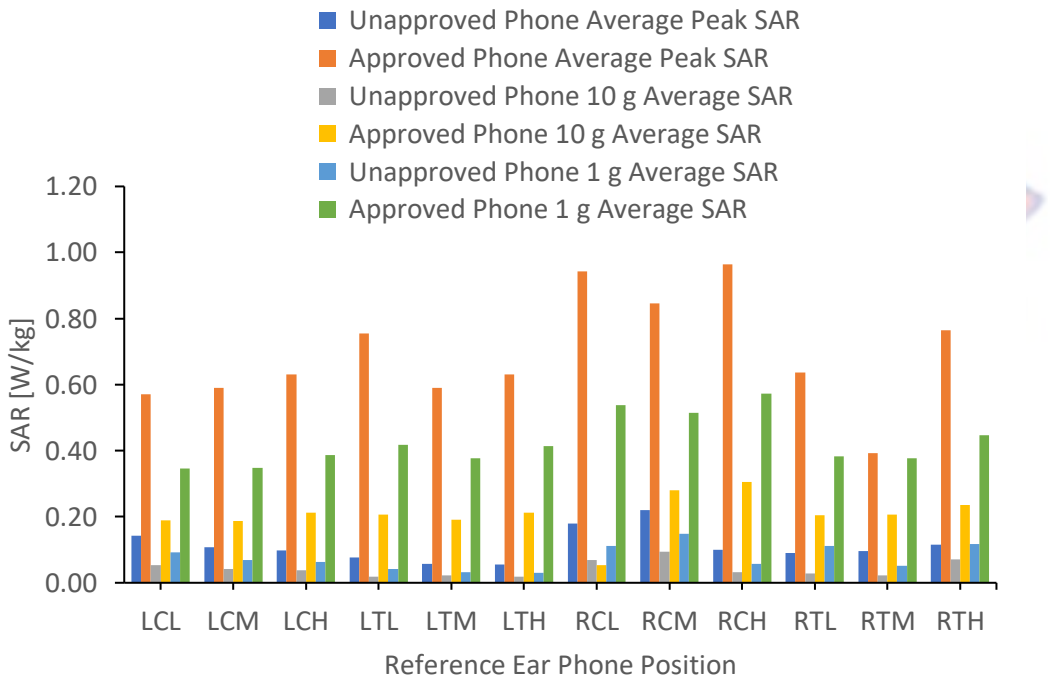

Figure 45: Comparing SAR trends of Approved Phone & Unapproved Phone average SAR at 0.0 cm from Phantom Head at different Reference Ear Positions.

Figure 46 shows increased SAR levels from the left to the right ear reference positions for the approved phone whiles the opposite is the case for the unapproved phone overlapping on the left ear. This happened at 1.0 cm.

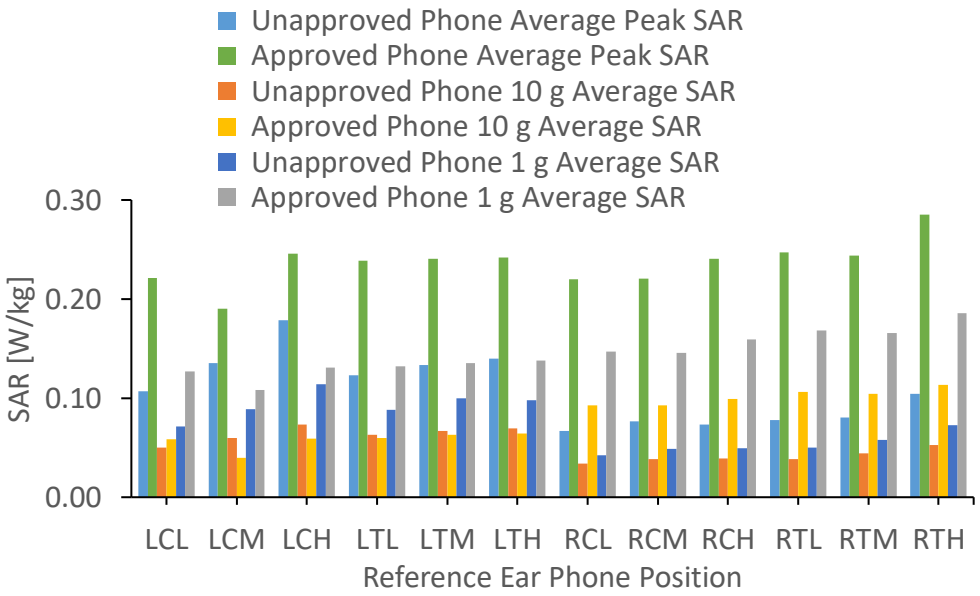

Figure 46: Comparing Average SAR Tends of Approved Phone & Unapproved Phone at 1.0 cm from Phantom Head at different Reference Ear Positions.

At 2.0 cm, there is an alternating SAR levels behaviour of the approved and unapproved phones when the phone orientation is switched from tilt to cheek and vice versa as shown in Figure 47. The levels of the unapproved phone rise and fall as you move from cheek to tilt phone position with the maximum occurring on the left-tilt position whiles that of the approved phone falls on the right-tilt position at 2.0 cm.

It is instructive to note that, in both cases, the higher levels occurred at the tilt position. However, at 3.0 cm, the trends of the SAR levels of the two phones appear similar across the reference phone positions as demonstrated in Figure 48.

The trends of the average 10 g SAR, average 1 g SAR and average peak SAR appear similar over the reference phone positions as demonstrated in Figure 48 with both phones having lower levels at the left-tilt position.

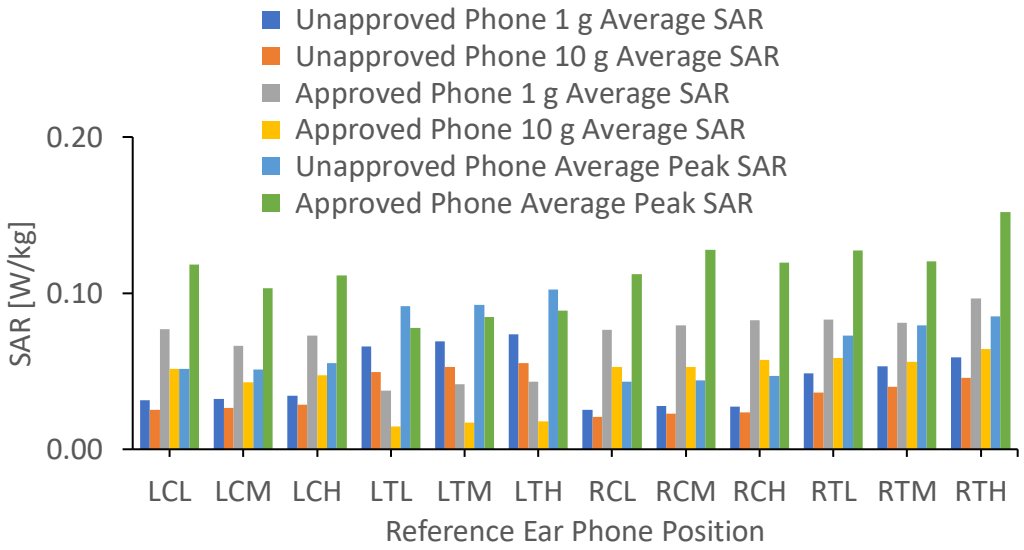

Figure 47: Comparing Average SAR Trends of Approved Phone & Unapproved Phone at 2.0 cm from Phantom Head at different Reference Ear Positions.

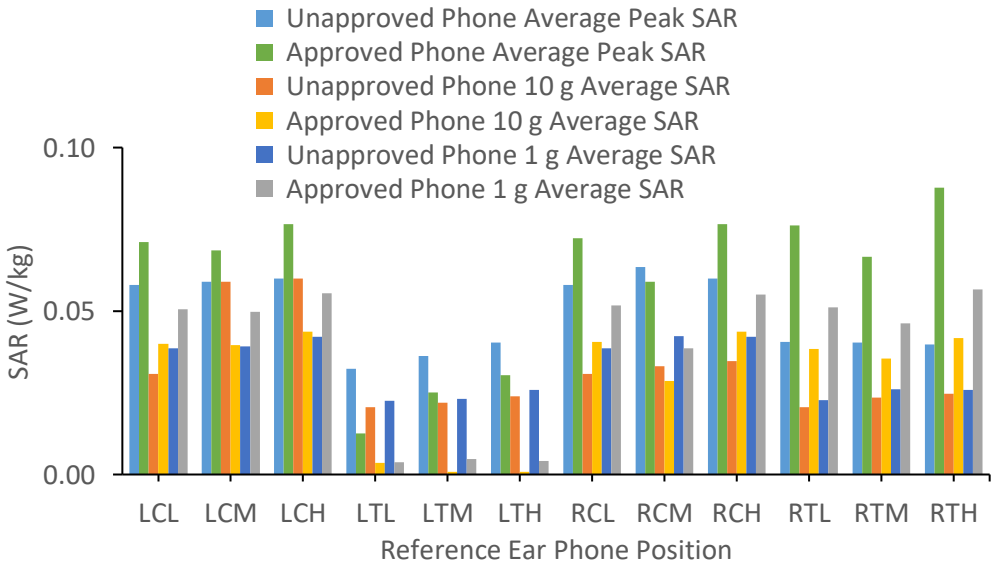

Figure 48: Comparing Average SAR of Approved Phone & Unapproved Phone at 3.0 cm from Phantom Head at different Reference Ear Positions.

Figures 49 and 50 provides the maximum and averages SAR values measured. The reference phone positions that recorded the maximum values are also presented. Note that all maximum SAR values for both approved and unapproved phones occurred at the cheek position as shown in Figure 49. This agrees with results of Morega et al. (2015). They also recorded higher SAR values at cheek position relatively to the tilt position even though their averages of 0.580 W/kg for 10 g W/kg and 1.023 for 1 g are 14 % and 3 % respectively higher than those recorded in this research work. Whiles the approved phone recorded its maximum values on the right ear that of the unapproved was vice versa as seen in Figure 50. This may be due to the relative different position of the phone antenna when the phone is on the left and compared to right ear.

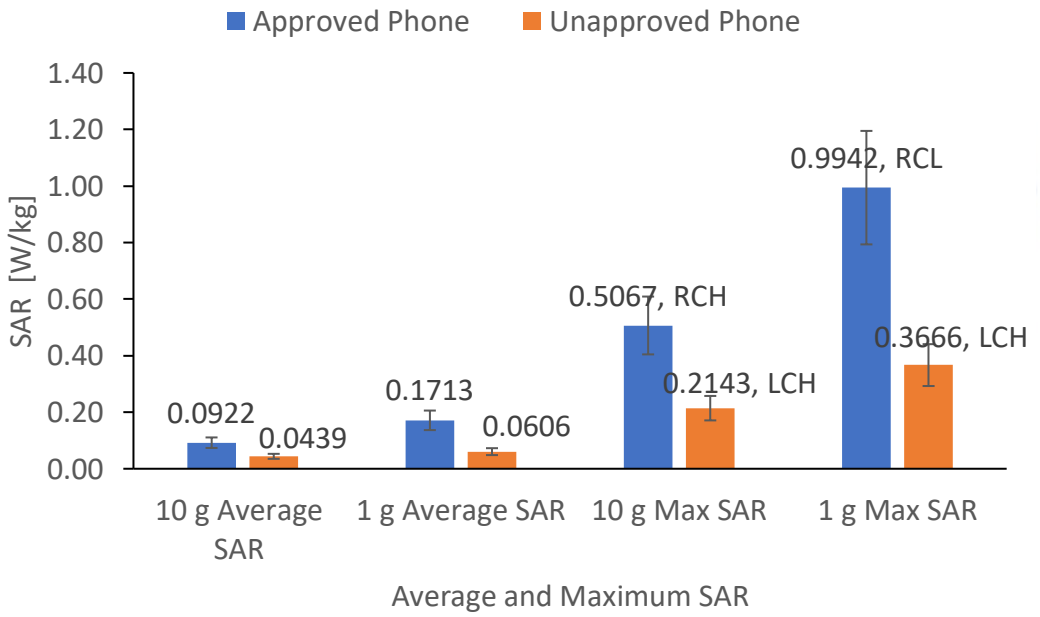

Figure 49: Average and Maximum 10 g and 1g SAR values measured for Approved and Unapproved Phones, and the Reference Positions the Maximum Values occurred.

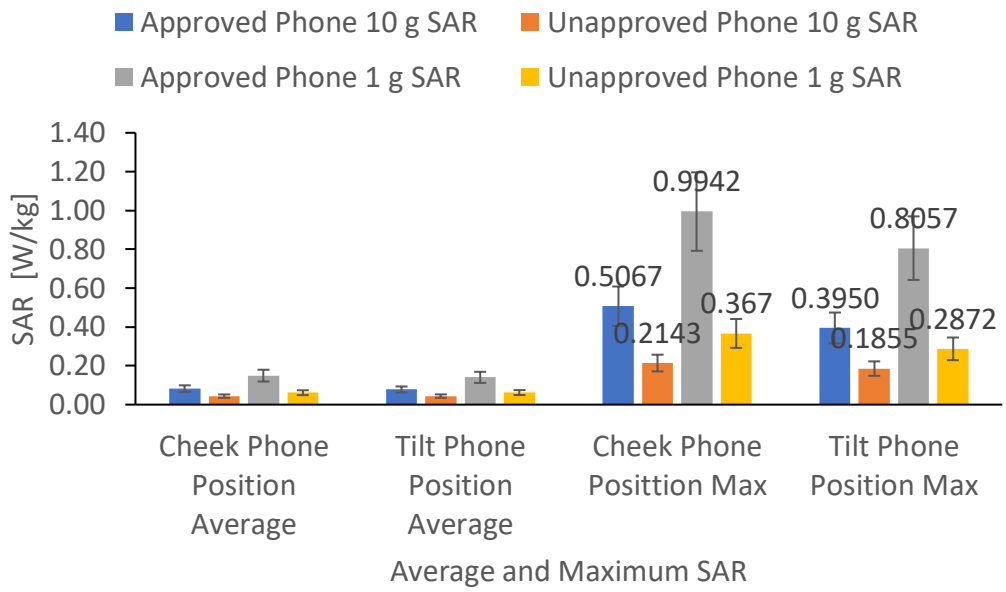

Figure 50: Average and Maximum 10 g and 1 g SAR values measured at Cheek and Tilt Position and the Reference Positions the Maximum Values occurred.

The maximum 10 g SAR was 75 % lower than the ICNIRP basic restriction (or 25 % of ICNIRP), whiles the maximum 1 g SAR was about 62 % below FCC limit of 1.6 W/kg. These are respectively, 14 % and 3 % lower than those recorded in Morga et al. (2015) but 98 % higher than 0.256 W/kg (10 g SAR) of Mahfouz et al (2012).

Table 6 presents the summary of the reductions in SAR. The averaging gave regular reduction numbers for the approved phone whiles it provides undulating values for the unapproved phone and in some cases an increase in SAR instead of a decrease indicated by the negative values. To emphasize, unlike the SAR reduction of the approved phone, the reduction nature of the unapproved phone does not agree with similar works like Morega et al. (2015), Musiige et al. (2012), and Krstić, et al. (2011).

Table 6: Comparison of Percentage Average SAR Reduction

	Average SAR percentage reduction from 0.0 cm to 1.0 cm	Averaged SAR percentage reduction from 1.0 cm to 2.0 cm	Average SAR percentage reduction from 2.0 cm to 3.0 cm
Approved average 10 g SAR	53.19 %	42.31 %	41.97 %
Unapproved average 10 g SAR	-71.48%	31.46 %	-7.57%
Approved average 1 g SAR	65.00 %	51.86 %	49.46 %
Unapproved average 1 g SAR	-35.00 %	35.64 %	10.89 %
Approved average peak SAR	64.00 %	52.47 %	48.08 %
Unapproved average peak SAR	-19.00 %	33.92 %	15.90 %

(Source: Research data)

Comparison of SAR values of the right and left ears

A comparison of the average and maximum SAR measurements of the left and right ears were made. They are presented in Figures 51, 52 and 53.

A comparison of SAR of the right and left ears is made by taking averages of the SAR quantities across all distances. These averages and maximum values are presented in Figures 51, 52, and 53. These figures enforces the observation that, the SAR values of the approved phone been relatively higher than that of the unapproved. Also, the figures clearly show the approved phone recording relatively higher average SAR values on the right ear compared to the left ear

whiles the case is vice versa with the unapproved phone. The maximum values always occur with the right ear in all quantities for both approved and unapproved phones. And the average on the right ear is also higher than the left ear. With this observation, it supports the use of the phone on the left ear to reduce exposure.

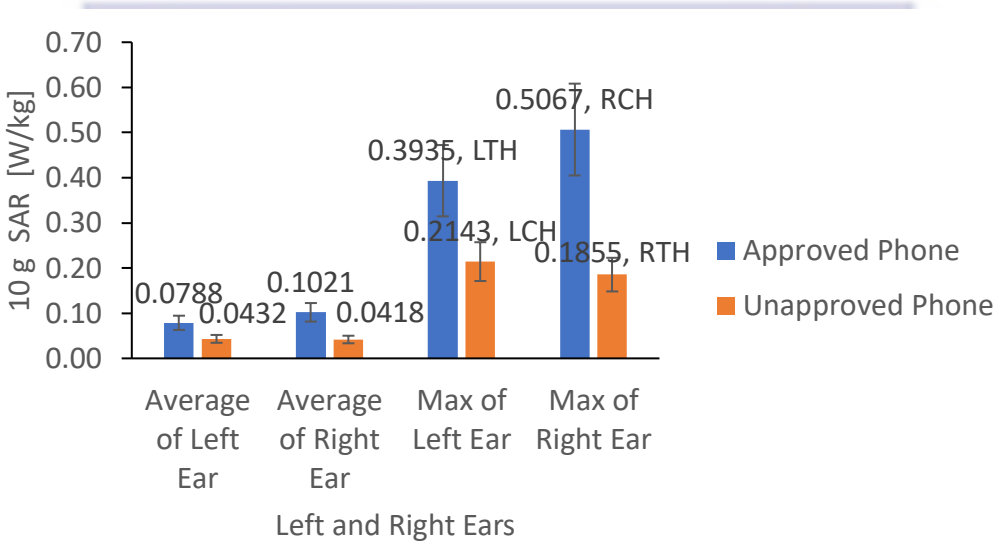

Figure 51: Average and Maximum 10 g SAR of Left and Right Ears and the Reference Positions the Maximum Values occurred.

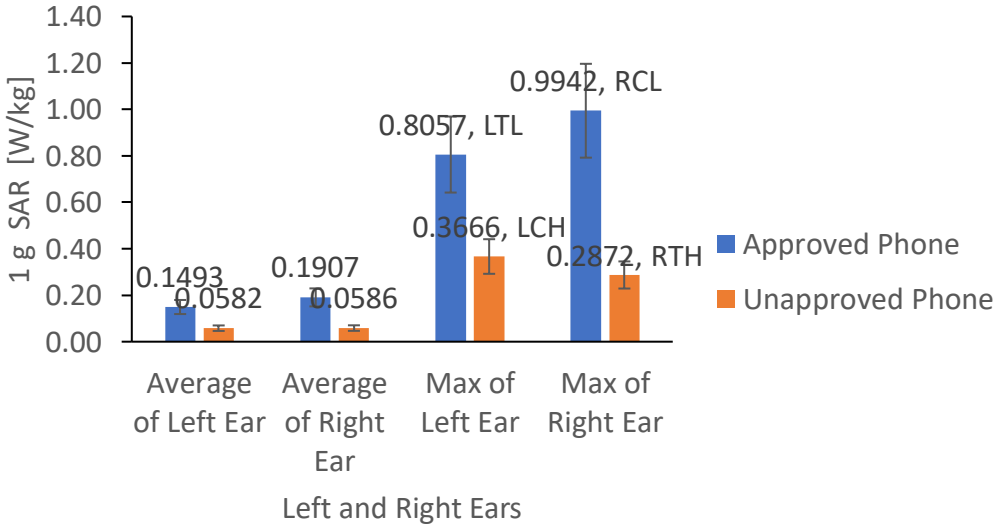

Figure 52: Average and Maximum 1 g SAR of Left and Right Ears and the Reference Positions the Maximum Values occurred.

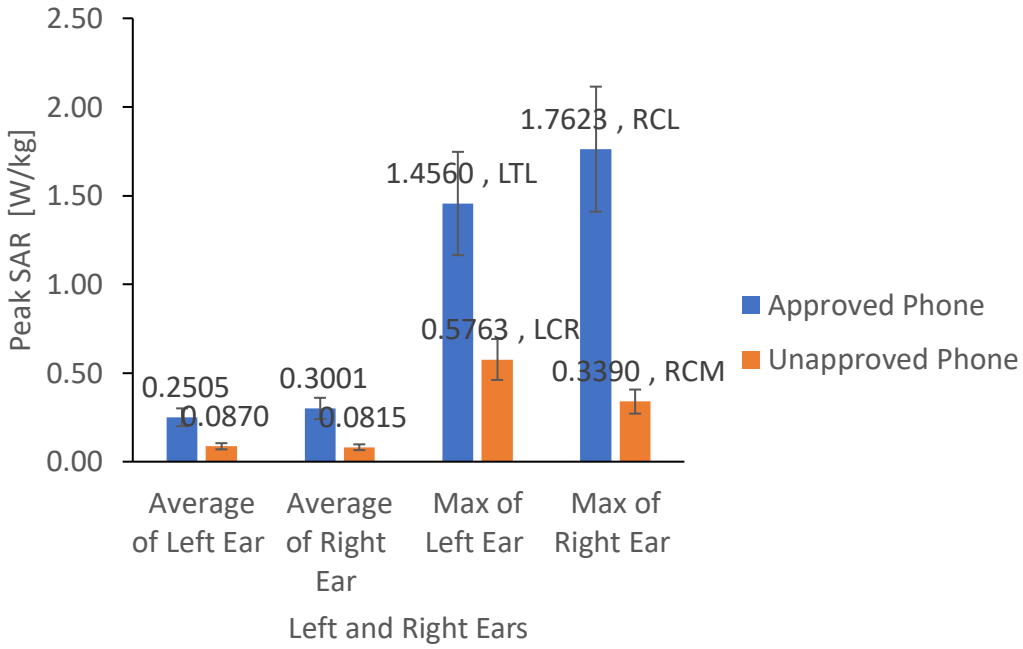

Figure 53: Average and Maximum Peak SAR of Left and Right Ears and the Reference Positions the Maximum Values occurred.

In order to provide a general overview of the results, the maximum (max), minimum (min) and average (ave) SAR values at each of the four measured distances of the approved phone (APP) and unapproved phone (UAP) are presented in Table 7. All the 10 g and 1 g SAR values have related uncertainty of 20.06 % and 20.23 % respectively.

Table 7 provides a broad overview of the results at the individual distances which sees the maximum SAR values of the unapproved phone occurring at 1.0 cm rather than at 0.0 cm as is expected and happened with the approved phone. The Table brings out a critical behaviour of the SAR values at the different distances. Whereas the approved phone has SAR levels of the left ear been lower

than that of the right ear at all distances and for both 10 g and 1 g SAR that of the unapproved phone only agrees with this only at 0.0 cm. Also, it is not always the case that the maximum 1 g SAR and 10 g SAR occur at the same reference phone position. The maximum 10 g SAR of the approved phone occurred at the right-cheek-high (RCH) reference position while its 1 g SAR counterpart happened at right-cheek-low (RCL) reference position. The maximum for the unapproved phone of the 10 g and 1 g SAR all occurred at the same right-cheek-middle (RCM) reference position. Both phones recorded their maximum SAR values at the right ear and with cheek positions. These maximum 10 g SAR values of the approved phone even though lower than the ICNIRP limits was 170 % higher than the FDTD 0.256 W/kg GSM 1800 results of Mahfouz et al (2012).

Table 7: Summary of SAR Measurement Results

	At 0.0 cm		At 1.0 cm		At 2.0 cm		At 3.0 cm	
	10 g	*1 g*	*10 g*	*1 g*	*10 g*	*1 g*	*10 g*	*1 g*
APP max (W/kg)	0.5067	0.9942	0.1142	0.1882	0.0708	0.1099	0.0448	0.0570
APP ave (W/kg)	0.2070	0.4267	0.0861	0.1479	0.0453	0.0710	0.0303	0.0396
APP min (W/kg)	0.0266	0.0294	0.0487	0.1043	0.0116	0.0320	0.0001	0.0003
UAP max (W/kg)	0.1855	0.2872	0.2143	0.3666	0.0560	0.0753	0.0763	0.0532
UAP ave (W/kg)	0.0546	0.0892	0.0534	0.0747	0.0356	0.0457	0.0319	0.0327

Table 7 continue

	At 0.0 cm		At 1.0 cm		At 2.0 cm		At 3.0 cm	
	10 g	*1 g*	*10 g*	*1 g*	*10 g*	*1 g*	*10 g*	*1 g*
UAP min (W/kg)	0.0111	0.0209	0.0196	0.0203	0.0205	0.0253	0.0187	0.0203
APP left ear max (W/kg)	0.3935	0.8057	0.0654	0.1391	0.0651	0.0927	0.0448	0.0561
APP left ear ave (W/kg)	0.1995	0.3813	0.0585	0.1269	0.0338	0.0586	0.0232	0.0303
APP left ear min (W/kg)	0.0266	0.0294	0.0487	0.1043	0.0116	0.0320	0.0001	0.0003
APP right ear max (W/kg)	0.5067	0.9942	0.1142	0.1882	0.0708	0.1099	0.0440	0.0570
APP right ear ave (W/kg)	0.2145	0.4722	0.0994	0.1580	0.0563	0.0827	0.0381	0.0499
APP right ear min (W/kg)	0.0431	0.0586	0.0831	0.1291	0.0702	0.0702	0.0220	0.0270
UAP left ear max (W/kg)	0.0561	0.1005	0.2143	0.3666	0.0560	0.0753	0.0763	0.3666
UAP left ear ave (W/kg)	0.0329	0.0557	0.0646	0.0939	0.0396	0.0512	0.0360	0.0319

Table 7 continue

	At 0.0 cm		At 1.0 cm		At 2.0 cm		At 3.0 cm	
	10 g	*1 g*	*10 g*	*1 g*	*10 g*	*1 g*	*10 g*	*1 g*
UAP left ear min (W/kg)	0.0111	0.0295	0.0215	0.0230	0.0206	0.0254	0.0199	0.0208
UAP right ear max (W/kg)	0.1855	0.2872	0.0697	0.1002	0.0461	0.0615	0.0410	0.0532
UAP right ear ave (W/kg)	0.0679	0.1096	0.0398	0.0512	0.0316	0.0401	0.0281	0.0334
UAP right ear min (W/kg)	0.0186	0.0209	0.0196	0.0203	0.0205	0.0253	0.0187	0.0203

(Source: Research data)

Comparison of results with high earn phone (HEP) at 0.0 cm

The SAR values of the approved and unapproved were compared to that of a high earned phone at 0.0 cm only, as depicted in Figures 54, 55 and 66.

From Figures 54, 55 and 56, it is observed that the measured SAR quantities of the HEP generally agrees with that of the unapproved phone over the reference phone positions but relatively lower than the SAR values of the approved phone. High earn phones are of highest quality and conform to international standards of production, safety and health. However, it is interesting

to observe SAR levels from a regulatory approved phone not just relatively higher, but on the average, over 400 % higher than that of the HEP.

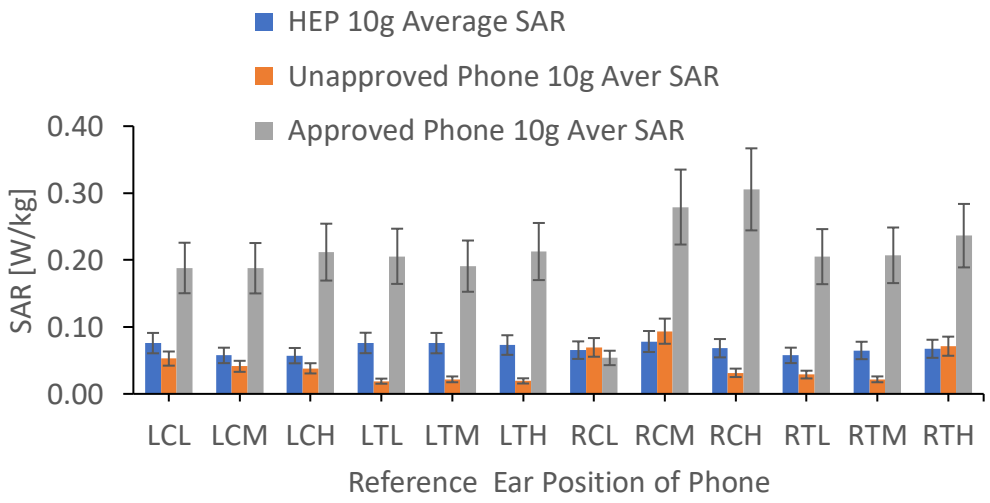

Figure 54: Comparison of Average 10 g SAR of Approved and Unapproved Phones with that of High Earn Phones at 0.0 cm from Phantom Head at different Reference Ear Positions.

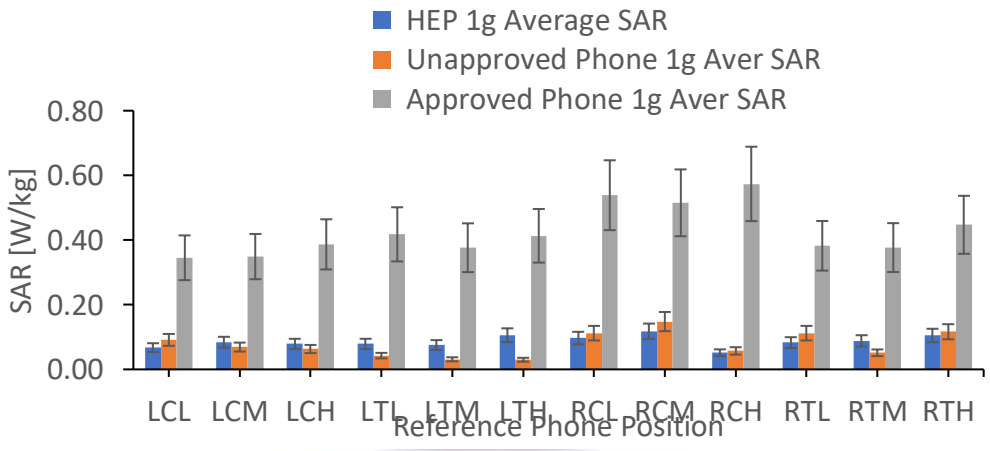

Figure 55: Comparison of Average 1 g SAR of Approved and Unapproved Phones with that of High Earn Phones at 0.0 cm from Phantom Head at different Reference Ear Positions.

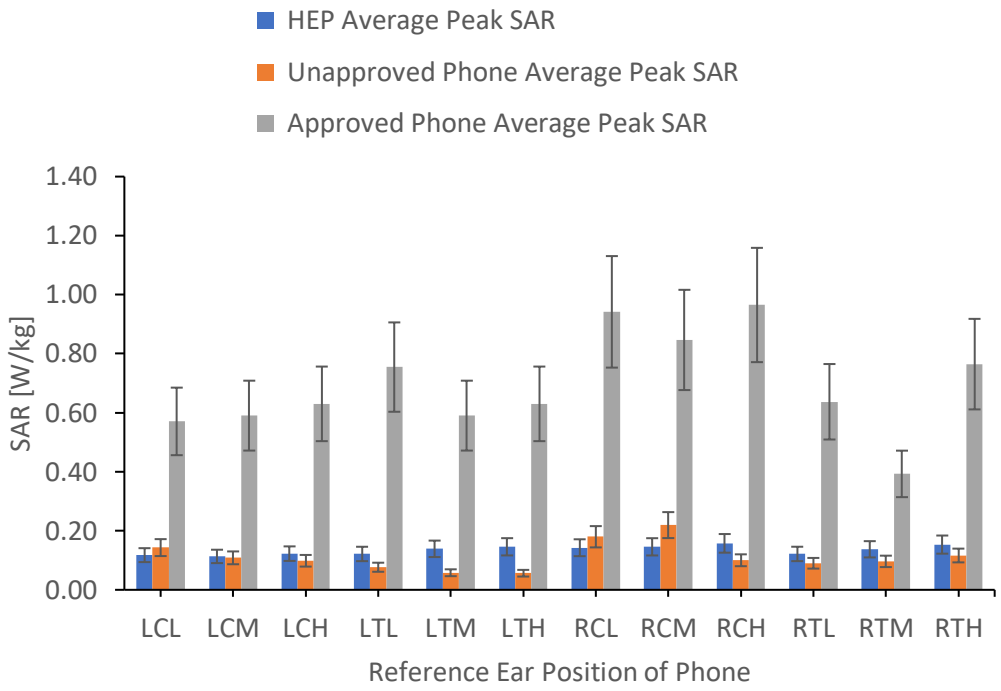

Figure 56: Comparison of Average Peak SAR of Approved and Unapproved Phones with that of High Earn Phones at 0.0 cm from Phantom Head at different Reference Ear Positions.

Statistical Summary of Measurement Results

The statistical summary of the entire SAR measurements of the approved and unapproved phones are presented in Table 8 where N/A means not available.

An analysis of the statistical summary presented in Table 8 reveals further details of the data. The means and medians of the approved phone exceeds that of its counterpart unapproved phone in all measurement quantities and also produced higher data ranges, standard deviations and sample variance. Interestingly, the approved phone gave the most minimum values likewise maximum values of the two phones as shown in Table 8. SAR values from both phones are positively skewed, however, the tails of the distribution of the unapproved phone are

relatively thicker as described by their kurtosis of Table 8. The relative higher spread or dispersion of the approved phone data shows with its higher variance and standard deviation. However, the inconsistency with the data of the unapproved phone is emphasised by its lack of modal values.

Table 8: Statistical Summary of SAR Results

	Approved Phone			Unapproved Phone		
Statistic	10 g SAR	1 g SAR	Peak SAR	10 g SAR	1 g SAR	Peak SAR
Mean	0.09217	0.17138	0.23249	0.04389	0.06055	0.08970
Standard Error	0.00767	0.01638	0.02794	0.00249	0.00411	0.00568
Median	0.05687	0.08348	0.12129	0.03570	0.04611	0.06936
Mode	0.06129	0.09136	0.14123	#N/A	#N/A	#N/A
Standard Deviation	0.09232	0.19726	0.33649	0.03171	0.05227	0.07230
Sample Variance	0.00852	0.03891	0.11323	0.00101	0.00273	0.00523
Kurtosis	8.19868	8.09043	9.17325	8.58681	10.61382	15.21515
Skewness	2.89375	2.95736	3.12664	2.50780	2.79442	3.20369
Range	0.50659	0.99388	1.76049	0.20313	0.34633	0.55401
Minimum	0.00013	0.00033	0.00182	0.01113	0.02032	0.02225
Maximum	0.50672	0.99422	1.76231	0.21426	0.36665	0.57625

(Source: Research data)

A one tailed independent T-test of the SAR quantities of the approved and unapproved phones show there is statistically significant difference between their 10 g SAR (P-value = 9.20676E-06), their 1 g SAR (P-vale = 1.26061E-06) and their Peak SAR (P-value = 7.77388E-07). The low P-values are an indication of the high confidence that if the experiment is repeated, the same results will be arrived at. The single factor unrelated analysis of variance (ANOVA) between the SAR quantities of the two phones shows a statistically significant difference between their means. An alpha level of 0.05 was used for all statistical tests.

Mathematical Model to Predict SAR

The relations between the quantities measured were analysed with the help of Microsoft Excel, GraphPad Prism and RStudio programming. Figure 71 and 72 provides an RStudio matrix relation plot of the distance in cm represented by *ds*, the Peak SAR represented by *P*, 10 g SAR represented by *ten*, and 1 g SAR represented by *one*, all SAR in W/kg for approved and unapproved phone. The plot also predicted their graphical relations as well as the coefficient of correlation (R^2) values for each pair of quantities. An x-y reading of any two quantities will give the corresponding graphical relation or the R^2 value. The R^2 values for all quantity in relation to distance are negatives depicting the decreasing relation with distance. 1 g SAR produced the highest of R^2 with a value of -0.60.

Comparatively, from Figures 71 and 72, the approved phone had relatively higher R^2 values with the independent quantity (distance) accounting or explaining on the average 60 % of its SAR results whiles it is 40% for the unapproved phone. Other factors like the type of phone, type of antenna, source

geometry, and anatomical properties could be accounting for the remaining unexplained SAR results. The R^2 values between the dependent quantities (10 g, 1 g, Peak SAR) are near one, showing a very strong correlation which is supported by theory.

The relations between the dependent quantities are linear as demonstrated by their corresponding graphs. However, the relation of distance and the dependent quantities are all non-linear as shown with their corresponding graphical representations in the same Figures 57 and 58. Further analysis of the non-linear nature of these relations by using RStudio programming language to predict the relations as provided Figures 59, 60, 61, 62, 63, and 64.

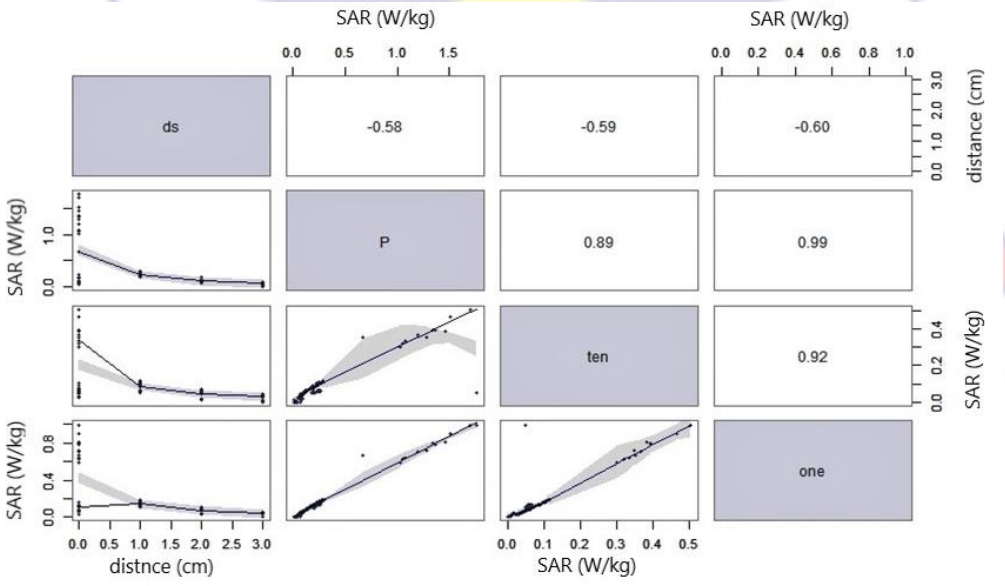

Figure 57: R-programming Matrix Plot of distance with 10 g, 1 g and Peak SAR of Approved Phone showing Graphical Relations and corresponding R^2 values.

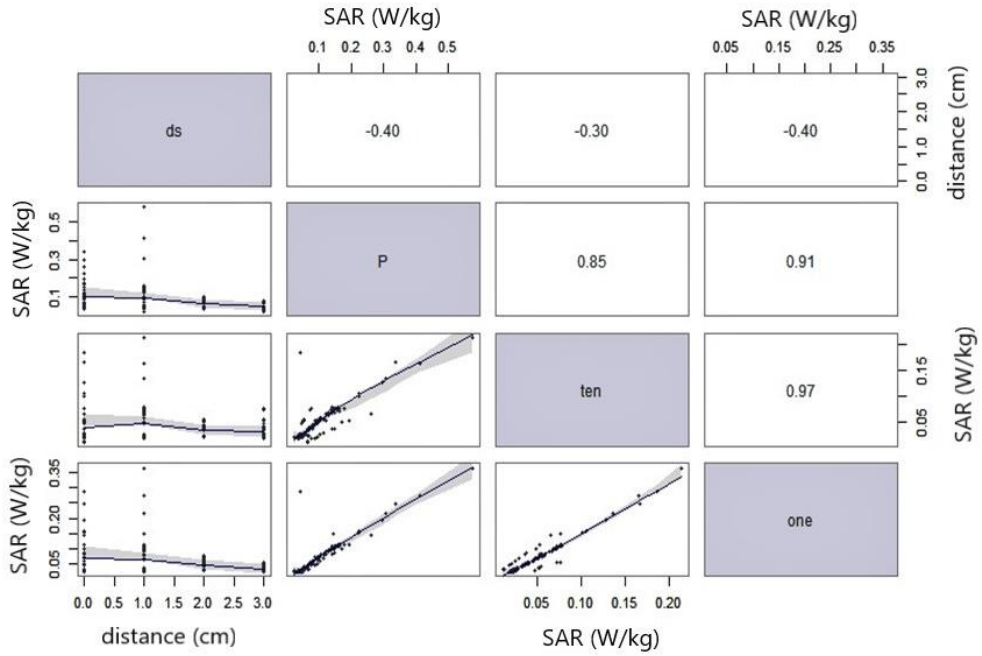

Figure 58: R-programming Matrix Plot of distance with 10 g, 1 g and Peak SAR of Unapproved Phone showing Graphical Relations and corresponding R^2 values

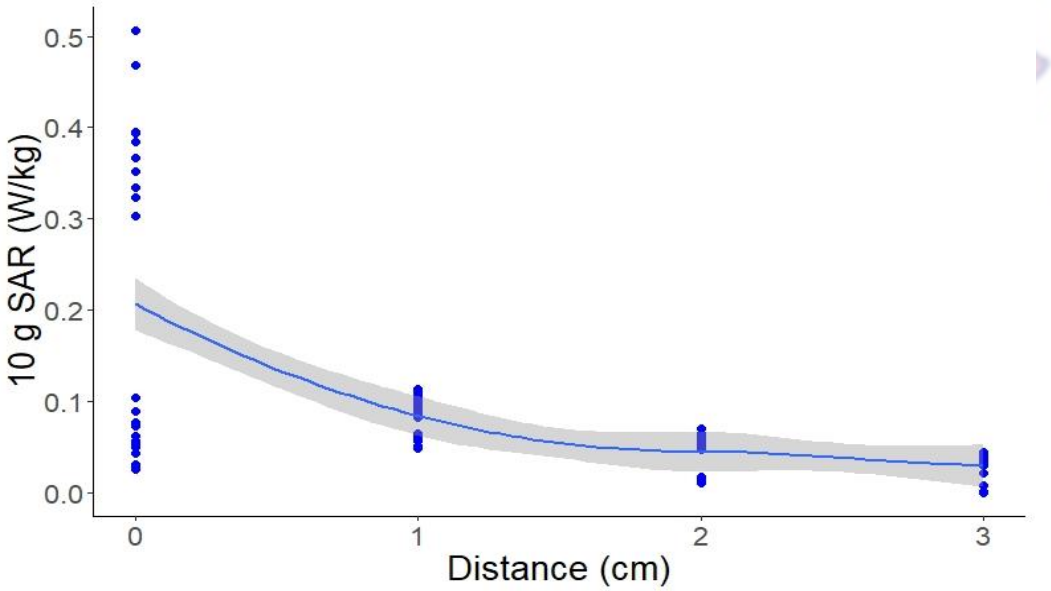

Figure 59: R-programming Fitting Plot of 10 g SAR (ten) and distance (ds) for Approved phone

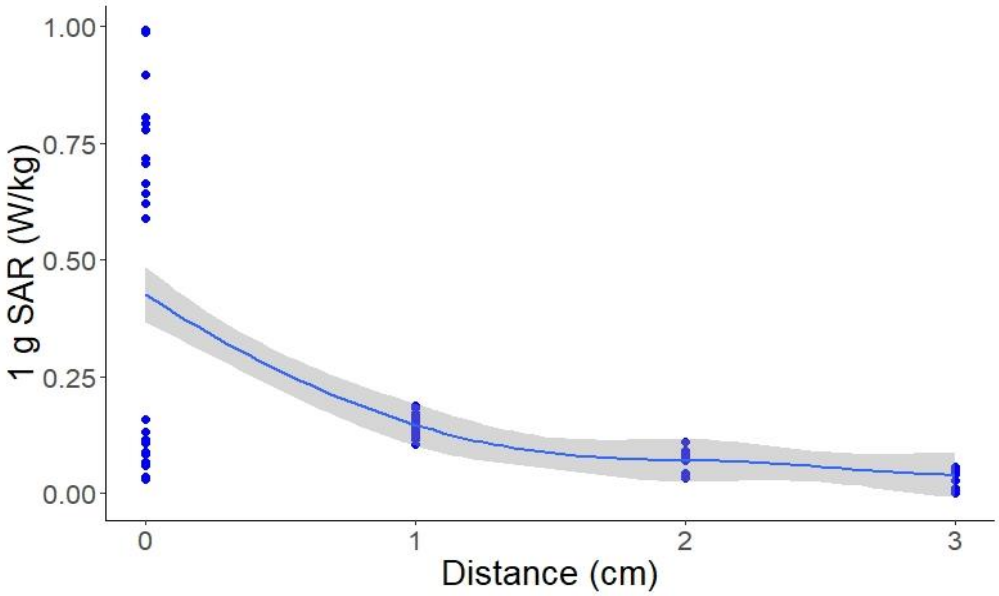

Figure 60: R-programming Fitting Plot of 1 g SAR (one) and distance (ds) for Approved phone

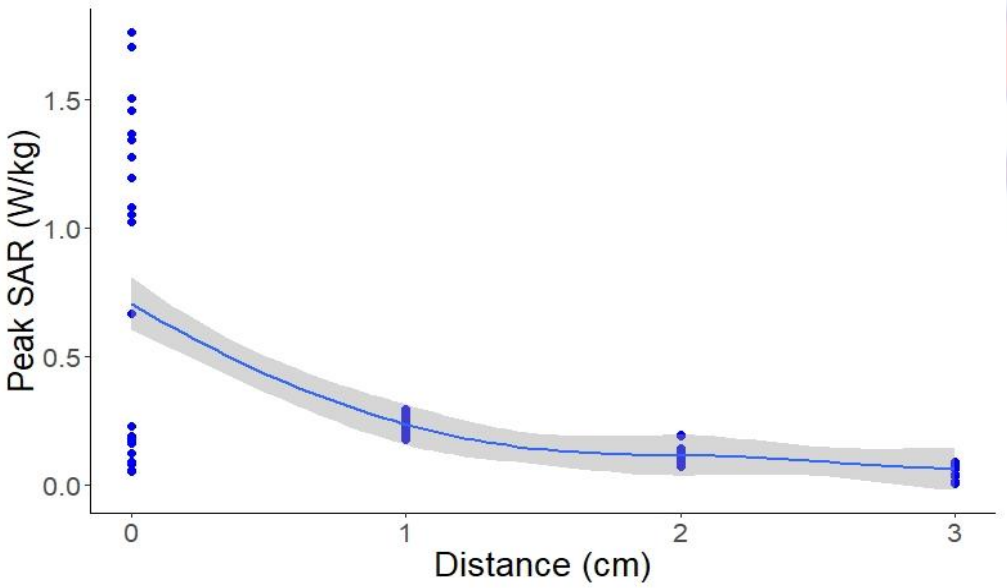

Figure 61: R-programming Fitting Plot of Peak SAR (P) and distance (ds) for Approved phone

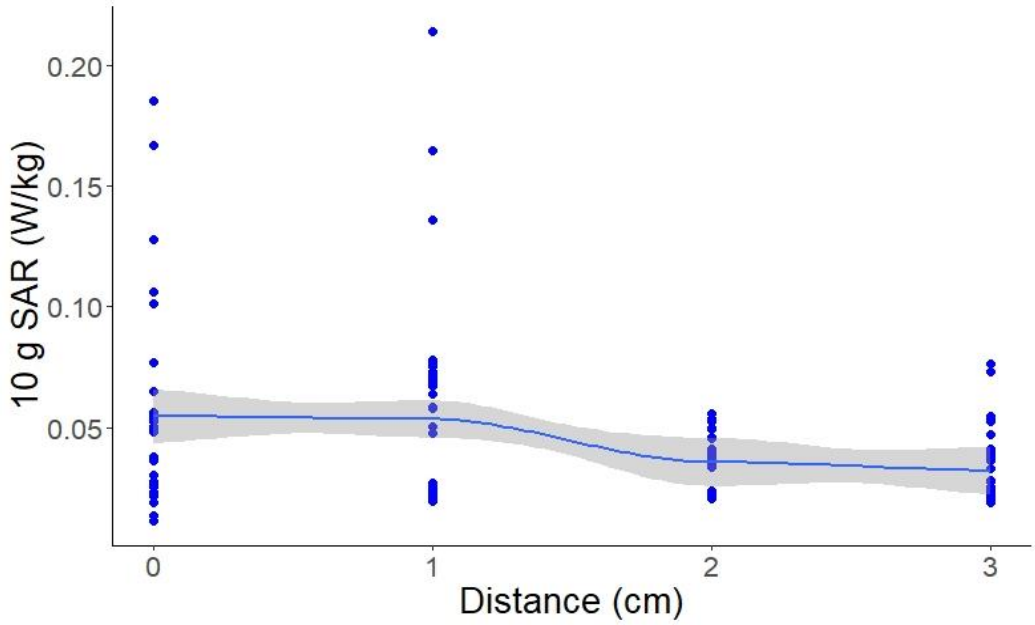

Figure 62: R-programming Fitting Plot of 10 g SAR (ten) and distance (ds) for Unapproved phone

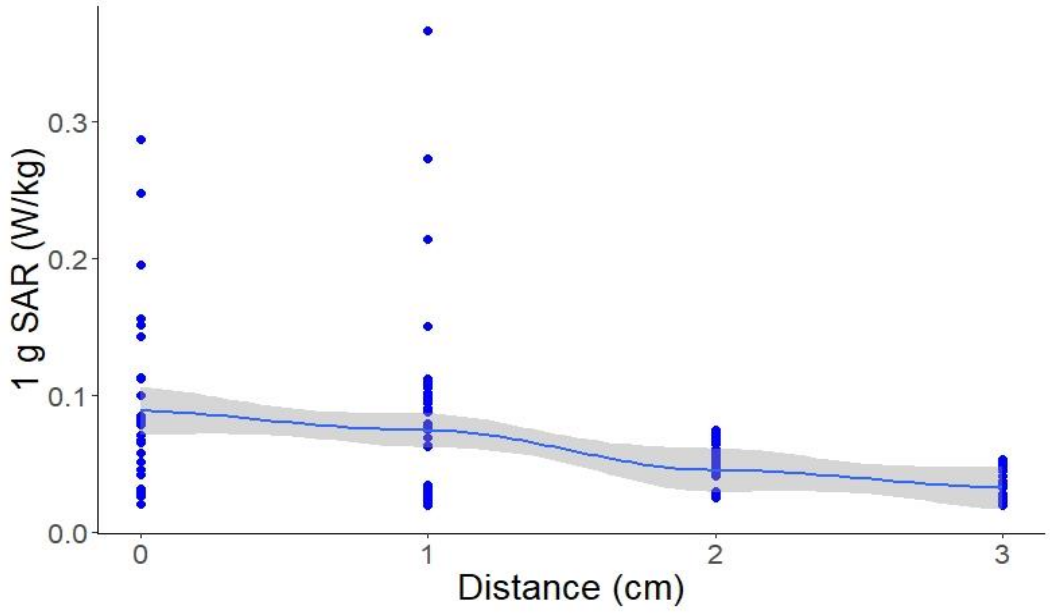

Figure 63: R-programming Fitting Plot of 1 g SAR (one) and distance (ds) for Unapproved phone.

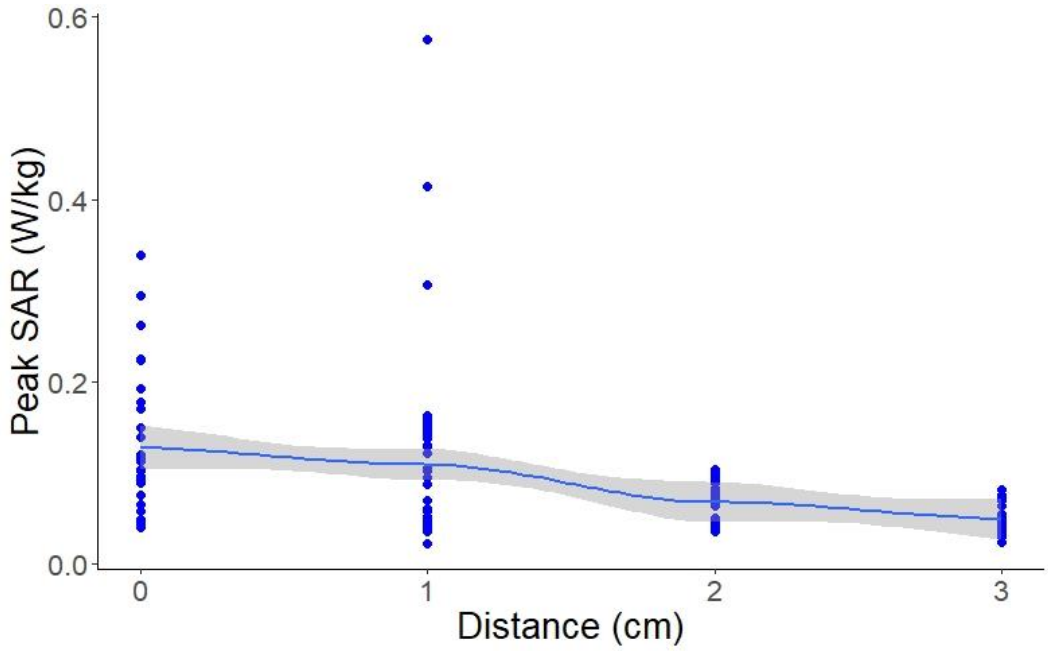

Figure 64: R-programming Fitting Plot of Peak SAR (P) and distance (ds) for Unapproved phone.

What is quite obvious from Figures 59 to 64 is the difference between the nature of the graphs for the approved phone and the unapproved phone. Even though both phones produced a decaying curve, the approved phone produced a smoother decaying curve conforming better to theory. A one phase exponential model better fitted the SAR trends of the approved phone at almost all reference phone positions. The case of the unapproved phone was a exponential decay model all phone positions. The exceptions were the Left ear, Cheek orientation, Middle frequency channel (LCM) and the of Right ear, Cheek orientation, Low frequency channel (RCL) reference positions of the approved phone which produced polynomials of order two. All the fitting models are given in Appendix F and G.

What we should remember here is that, these particular reference positions already gave irregular SAR values during the measurements. The common factor with these three positions is that they all occurred at cheek position.

The general form of the one phase exponential model and the exponential decay model are given in Equations 50 and 51 respectively on pages 94 and 95. The plateau is P_l which is the SAR value at infinite distance, and K is rate constant in m^{-1}. Y_0 is the intercept and d_{head} is the distance from the head or closeness of the mobile phone to the head.

Equations 50 and 51 clearly indicate that, the relation of SAR and distance of the phone from the ear up to 3.0 cm is non-linear, disagreeing with the linear relation proposed by Musiige et al. (2012). The relation also confirms the decreasing nature of the SAR with distance as an inverse power, agreeing with theory. The one phase exponential decay and the exponential decay predictive fitting models derived, agrees with the results of Krstić et al. (2011), Sole et al. (2013), and Morega et al. (2015).

The one phase exponential and exponential decay models relating SAR and distance for each of the 12 different reference phone positions for the approved phone and unapproved phone, and for all the three depended quantities were derived. They are presented in Appendix F and Appendix G. The one phase exponential model has an average coefficient of regression value of 0.96 and 0.99 for 10 g and 1 g SAR respectively for the approved phone, and 0.72 and 0.85 for 10 g and 1 g respectively for the unapproved phone.

Mobile phone SAR calculator application

The predictive models of all the 24 different reference phone positions were used to build a 10 g SAR calculator application, using MATLAB programming. Boolean logic was employed in the coding and looped for all the various reference position for both approved and unapproved phones. The codes are presented in Appendix E.

The interface of the SAR calculator application is shown in Figure 79. The SAR calculator application not only give 10g local head SAR and its uncertainty, but it also provides a graph of predicted SAR for a distance range. The application has a reliability range of 0.0 cm to 3.0 cm.

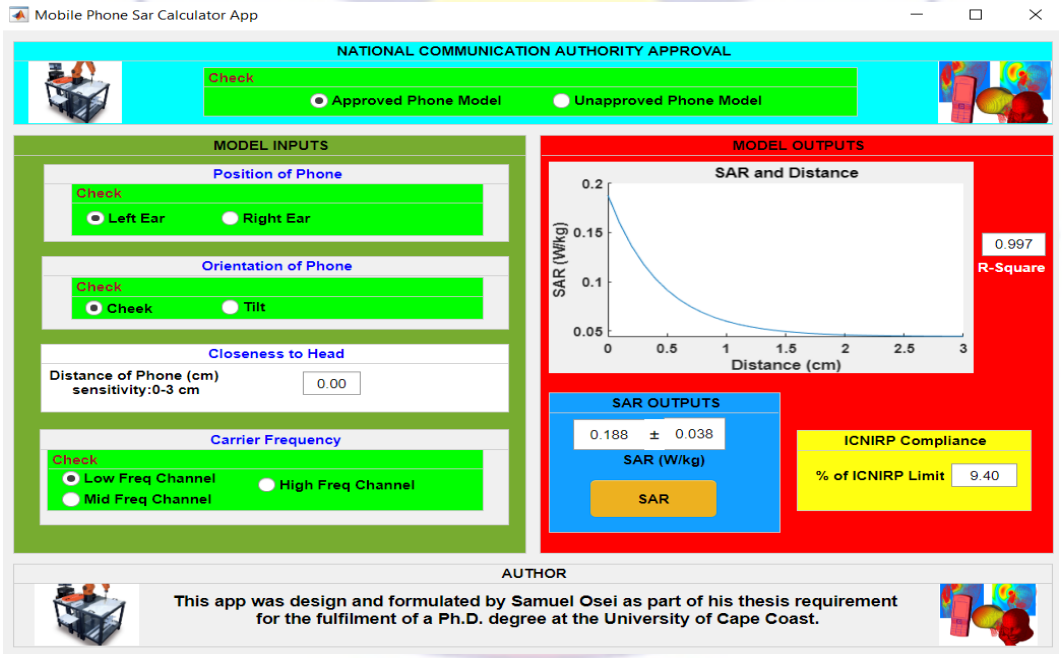

Figure 65: MATLAB Application designed to estimate SAR.

The user selects either he/she is using an NCA approved phone or not. The user then selects which ear the phone is used and also whether the phone is used

at the cheek or tilt position. The distance to the head for which the SAR is been estimated is inputted which should be from 0.0 cm to 3.0 cm, after which the user then selects the operating frequency been used. Clicking on SAR causes the application to calculate not only the SAR at the selected parameters giving the uncertainty, but it also produces a graph SAR against distance, and also provides the percentage ICNIRP limit and the coefficient of determination value.

The application provides an interactive, friendly, inexpensive, easy to assess, and simple to use SAR estimator for mobile phones used in Ghana. It reduces the dependency on expensive SAR measurements and tend to help solve the problem of users not been able to get an idea about the SAR values of their mobile phones.

There are however limitations to this application which include the small number of phones used in the research. Non-consideration of other influencing factors like type of phone antenna and position of antenna in the phone is also a limitation.

Chapter Summary

The measured 10 g SAR and 1 g SAR of both the approved and unapproved phones did not exceed the ICNIRP basic restriction of 2 W/kg and the FCC limit of 1.6 W/kg. SAR levels of the approved phone are generally statistically higher than that of the unapproved phone. However, the SAR levels of the approved phone are consistent and more predictable than that of the unapproved phone. It is not always the case that 1 g SAR exceeds its

corresponding 10 g SAR, there are exceptions. 10 g SAR in some instances exceeds both 1 g SAR and peak SAR.

Phone position configuration affected the SAR levels. The left ear phone position produced relative lower SAR levels compared to the right ear. The cheek phone positions also recorded relative higher SAR values compared to the tilt phone position. SAR levels of the approved phone were relatively higher than that of a high earn phone, even though the levels of the unapproved phone and high earn phone do compare.

With the exception of 0.0 cm position, the approved phone SAR trends for all the quantities over the reference phone position were similar. The SAR level trends of the unapproved phone is different at all distances.

SAR decreased over the distance 0.0 cm to 3.0 cm. This agrees with the works of Musiige et al. (2012), Krstić, et al. (2011), Sole et al (2013) and Morega et al. (2015). The nature of the decreasing SAR with increase in distance of the approved phone were regular and predictable, whiles that of the unapproved produced irregular and less predictable results. In some cases, increase in distance rather resulted in an increase in SAR.

The 10 g SAR, 1 g SAR and Peak SAR have strong linear correlations with each other. A one phase exponential model for the approved phone and an exponential decay model for the unapproved were derived for as distance-SAR relations. They had average coefficient of correlations of 95 % for the exponential model and 70 % for the exponential decay model.

This means, a one phase exponential model better predicts SAR of the approved phone whiles an exponential decay model also better predicts SAR levels of the unapproved phone. An easy-to-use SAR calculator application has been developed to predict 10 g head SAR for the distance 0.0 cm to 3.0 cm at different phone position configurations.

CHAPTER FIVE

SUMMARY, CONCLUSIONS AND RECOMMENDATIONS

Summary

The International Telecommunications Union reveals that, mobile cellular subscriptions per inhabitants in Ghana surpasses the Africa, Europe and United States. Recent figures from the national regulator, the National Communications Authority, indicates that there are over 41 million mobile voice subscribers surpassing or national population of 31 million. The number of subscribers also keeps growing rapidly. This is the result of the 1995 Government of Ghana telecommunications policy for accelerated development. The effect of this rapid growth of the telecommunication industry in Ghana has created of a booming market for mobile phones, resulting in the influx into the country of all manner of mobile phone handsets without much consideration for the RF safety aspect of these mobile phones. Most RF research work in Ghana has concentrated on telecommunication base stations even though typical exposures from mobile phones far exceed those from base station. Understanding the levels of mobile phone RF exposure and the factors that influence the exposure has become very important for a country like Ghana with a high usage of mobile phones.

This research investigated the SAR levels from a regulatory approved phone as opposed to an unapproved phone deploying the IEC 62209-1 (2016) protocol in a standard state of the art SAR laboratory to measure 10 g SAR, 1 g SAR and Peak SAR by varying the phone distance from 0.0 cm to 3.0 cm over 12 different phone position configurations.

The SAR values of the approved phone are statistically higher relative to the unapproved phone with the highest P-value of 9.20676E-06. Even though SAR values of the approved phone had higher variability relative to those of the unapproved phone, the SAR levels of the approved phone were more regular. At an instant, 10 g SAR exceeded 1 g and Peak SAR.

With the exception of 0.0 cm, the SAR level trends over the reference phone positions for the approved phone at all the distance are similar for all three dependent quantities whiles that of the unapproved phone shows no similarities.

It is clear from the results that, phone position configuration relative to the ear affects the SAR values for both phones agreeing with Bread et al. (2006) and Morega et al. (2015). The cheek phone position produced higher SAR values relative to the tilt phone position. Again, the right ear produced relative higher SAR values compared to the left ear for both approved and unapproved phones. The SAR levels of high earn phones were similar to that of the unapproved phone, but were relatively lower than that of the approved phone.

All SAR values (10 g SAR, 1 g SAR and Peak SAR) did not exceed the ICNIRP limit or even the most restrictive FCC limit. The highest measured 10 g SAR which occurred for the approved phone at 0.0 cm was 0.5067 ± 0.0106 W/kg, which is 25 % of the ICNIRP limit of 2 W/kg averaged over 10 g of mass, while the highest 1 g SAR measured was 0.9942 ± 0.1994 W/kg which represent 38 % of the FCC limit 1.6 W/kg averaged over 1 g of mass. The maximum values compared favourably with results of Morega et al. (2010). Interestingly, the highest values for the unapproved phone occurred at 1.0 cm instead of 0.0 cm

with values of 0.2143 ± 0.0429 W/kg for 10 g SAR and 0.3666 ± 0.0745 W/kg for 1 g SAR.

The SAR levels decreased with increased distance over the interval 0.0 cm to 3.0 cm agreeing with theory and also with works done by Musiige et al. (2012), Krstić, et al. (2011), Sole et al (2013) and Morega et al. (2015). The reduction in the approved was regular and predictable unlike the irregular and inconsistent reductions in the unapproved phone.

The nature of the relation between SAR and distance were derived to be an exponential decay and a one phase exponential predictive models for the unapproved and approved phones respectively. The average correlation coefficient of SAR predictive models was 0.95 for the approved phone and 0.70 for the unapproved phone. Results of Musiige et al. (2012), Krstić, et al. (2011), Sole et al (2013) and Morega et al. (2015) correlates the exponential decay relation. The models were developed into a MATLAB application that predicts SAR as a function of distance considering phone position.

Conclusions

This research investigated how distance affects SAR levels of GSM mobile phones. The work measured SAR from regulatory approved and unapproved GSM mobile phone handsets used in Ghana. An exponential decay model was derived predicting SAR as a function of distance and phone positioning, and developed into an inexpensive and easy to use SAR calculator application providing an alternative to the expensive and complex laboratory SAR measurements. Levels of 10 g SAR and 1 g SAR did not exceed ICNIRP or FCC

limits. The highest SAR value measured was 62 % of the limit. In some instances of the unapproved phone, increase in distance rather resulted in increase in SAR.

Also, the maximum SAR values of the unapproved phone occurred at 1.0 cm distance instead of 0.0 cm as predicted by theory. Phone characteristics, and antenna quality could have accounted for this. Surprisingly, the SAR levels of the approved phone rather recorded statistically significant higher SAR levels. The SAR levels of the unapproved phone at 0.0 cm were similar also High Earn Phones. This could be attributed to differences in phone type and other factors affecting SAR such as antenna characteristics and position of antenna that were not considered in the research. The work showed that, using the mobile phone on the left ear produced lower user SAR relative to the right ear.

The study was hugely impacted by availability and assess to the NCA SAR laboratory. But the objectives of the research were achieved. This work has ventured into less researched area in Ghana. The study has added to base line data, providing critical data and information to regulators, relevant institutions and government agencies. The work will also help shape regulations and guide policies in the telecommunication industry. Hopefully, the results of this work will awaken the necessary attention required for RF safety in the mobile communication industry.

It is exciting to mention that as a result of research, the national regulator, NCA, has already launched further studies on RF safety of mobile phone handsets in the Ghanaian market. The SAR calculator application produced, if further developed and enhanced will go a long way to enable users of mobile phones

check and have an idea about the SAR levels of phones which will guide their usage and advise their purchase.

Recommendations

The difficulties in this study encountered with access to laboratories has brought to the fore the need for government institutions and academia to collaborate further in the field of research and development, so as to attract the needed private sector investment and help bridge the gap between research and development on one side, and technology and commercialization on the other side.

This will also help remove some of the preventable barriers for researchers alike. Here are some recommendations to some institutions and mobile phone users.

National communication authority

1. Expand and complete the ongoing research on testing samples of untested/unapproved phones in the market which was precipitated by this research results.
2. Provide easy access to database on approved mobile phones for users and educate on how to verify the NCA approval status of phones.
3. Take advantage of this baseline data to initiate engagements with relevant organizations to discuss strengthening the regulatory regime.
4. Engage stakeholders to reduce untested/unapproved phones on the market.

5. Explore computational and analytical methods like the predictive application developed to estimate SAR and reduce the dependency on expensive time involving actual measurements.

Ghana Atomic Energy Commission

1. Continue with public education on RF safety equipped with this research data.
2. Assist and encourage further research on this subject to improve on the predictive models.

GSM mobile phone users

1. This work supports the use of loud speaker and handsfree to keep phone away from head.
2. The results of the work encourage the increase use of the left ear for calls relative to the right ear to reduce user SAR.
3. Check the NCA approval status of mobile phones before purchasing them.

Suggestions for Further Studies

The work can be considered as completion of stage one of a larger project. There are a number of further studies that can be done to improve the work as enumerated.

a. Investigate other factors that influence SAR that include:
    i. Characteristics of phone and phone antenna.
    ii. The body anatomy and how RF radiation interact.

b. Improve on the predictive models by considering other influencing factors and expanding samples size.

c. Pursue computationally and analytically estimate SAR by the FDTD method involving Pennes' bio-heat model.

d. Consider exposure with multi transmitters of the GSM mobile phone.

REFERENCES

Agarwal, A., Singh, A., Hamada, A., & Kesari, K. (2011). Cell Phones and Male Infertility: A review of Resent Innovations in Technology and Consequences. *International Braz J Urol*, *37* (4), 432-454.

Aly, A. A., & Piket-May, M. (2014). FDTD computations for SAR induced in human head due to exposure to EMF form mobile phone. *Advance Computing An International Journal*, *5*(6), 1-12.

Amoako, J. K., Fletcher, J. J. & Darko, E. O. (2009). Measurement and analysis of radiofrequency radiations from some mobile phone base stations in Ghana. *Radiation Protection Dosimetry, 135*(4), 256-260. Retrieved from http://rpd.oxfordjournals.org/content/135/4/256/F1.expansion.html

Australian Radiation Protection and Nuclear Safety Agency (2002). *Maximum exposure levels to radio frequency fields—3 kHz to 300 GHz (Radiation Protection Series Publication No. 3), 2002*. Canberra, Australia: Author.

Ayinmode, O. B., & Farai, I. P. (2013). Measurement and Method in Radiofrequency Exposure Assessments. *The Pacific Journal of Science and Technology*, *14*(2), 110-118.

Azah, C. K., Amoako, J. K., & Fletcher, J. J. (2013). Levels of Electric Field Strength within the immediate vicinity of FM Radio Stations in Accra, Ghana. *Radiation Protection Dosimetry*, *156*(4). 395-400.

Azah, C. K., Amoako, J. K., & Sam., F. (2019). Spatial Distribution of Electric Field Strength at a Teaching Hospital Premises due to Transmissions between between 87.5 MHz and 2.6 GHz. *Radiation Protection Dosimetry, 183*(3). 348-354.

Bansal, R. (2002). "COMAR [IEEE Committee on Man Radiation]". *IEEE Antennas and Propagation Magazine, 44*(2). 104-105.

BC Center for Disease Control (2016). *2016 Review: Radiofrequency and Health.* Vancouver, Canada: National Collaborating Center for Environmental Health.

Bread, B. B., Kainz, W., Onishi, T. & Iyama, T. (2006). Comparisons of Computed Mobile Phone Induced SAR in the SAM Phantom to that in Anatomically Correct Models of the Human Head. *IEEE Transactions on Electromagnetic Compatibility, 48*(2), 397-407.

Cember, H. & Johnson, T.E. (2009). *Health Physics* (4th ed.). New York, USA: The McGraw-Hill Companies Inc.

Chakraborty, A. (2013). A Study on Third Generation Mobile Technology (3G) and Comparison among all Generations of Mobile Communication. *International Journal of Innovative Technology & Adaptive Management, 1*(2), 22-29.

Das, S. K. (2010). *Mobile Handset Design*. Singapore, Singapore: John Wiley and Sons (Asia).

Deatanyah, P., Abavare. E. K. K., Menyeh, A., & Amoako, J. K. (2018). Public Exposure to Multiple RF Sources in Ghana. *Radiation Protection Dosimetry, 181*(4), 403-411.

Deatanyah, P., Amoako, J. K., Abavare. E. K. K., & Menyeh, A., (2018). Analysis of Electric Field Strength and Power around Selected Mobile Base Stations. *Radiation Protection Dosimetry, 179*(4), 383-390.

Deatanyah, P., Amoako, J. K., Fletcher, J. J., Adjei, D. N., Dwapanyin, G. O. & Amoatey, E. (2012). Assessment of radiofrequency radiation within the vicinity of some GSM base stations in Ghana. *Radiation Protection Dosimetry*, *151*(2), 218-223.

Erdreich, L. S., Kerkhove, V. D. M., Scarfford, G. Carolyn., Barraj L., McNeely, M., Shum, M., Sheppard, R. A., & Kelsh, M. (2007). Factors that Influence the Radiofrequency Power Output of GSM Mobile Phones. *Radiation Research*, *168*. 253-261.

European Commission (2015). *SCENIHR opinion on Potential health effects of exposure to electromagnetic fields*. Luxembourg City, Luxembourg: European Commission.

Expert Group on Health Effects of Electromagnetic Fields (2005). *Health Effects of Electromagnetic Fields*. Dublin, Ireland: Department of communications, Marine and Natural Resources.

Federal Communications Commission (1997a). *Evaluating Compliance with FCC Guidelines for Human Exposure to Radiofrequency Electromagnetic Fields. Additional Information for Radio and Television Broadcast Stations: Supplement A (Edition 97-01) to OET Bulletin 65 (Edition 97-01)*. Washington, DC: FCC.

Federal Communications Commission (1997b). *Evaluating Compliance with FCC Guidelines for Human Exposure to Radiofrequency Electromagnetic Fields: Additional Information for Amateur Radio Stations: Supplement B (Edition 97-01) to OET Bulletin 65 (Edition 97-01)*. Washington, D.C: FCC.

Federal Communications Commission (1999). *Questions and Answers about Biological Effects and Potential Hazards of Radiofrequency Electromagnetic Fields. OET Bulletin 56 (Fourth Edition).* Washington, DC: FCC.

Federal Communications Commission (2001). *Evaluating Compliance with FCC Guidelines for Human Exposure to Radiofrequency Electromagnetic Fields: Additional Information for Evaluating Compliance of Mobile and Portable Devices with FCC Limits for Human Exposure to Radiofrequency Emissions: Supplement C (Edition 97-01) to OET Bulletin 65 (Edition 97-01)*. Washington, D.C: FCC.

Fleisch, D. (2008). *A student's guide to Maxwell's equations*. NY, USA: Cambridge University press.

Fruse, C., Christensen, D. A., & Durney, C. H. (2009). *Basic Introduction to Bioelectromagnetics* (2nd ed.). New York, USA: Tarlor & Francis Group.

Ghana Statistical Service (2021). *Ghana 2021 Population and Housing Census, 2021*. Accra, Ghana: Author.

Giancoli, C. D. (2009). *Physics for scientists & engineers with morden Physics* (4th ed.). NJ, USA: Pearson Educational International.

Habash, R. W. Y., Brodsky, L. M., Leiss, W., Krewski D. & Repacholi, M. (2003). Health Risks of Electromagnetic Fields. Part 1: Evalueation and Assessment of Electric and Magnetic fields. *Critical Reviews™ in Biomedical Engineering*, *31*(3), 114–180.

Health Canada (1999). *Limits of Human Exposure to Radiofrequency Electromagnetic Fields in the Frequency Range from 3 kHz to 300 GHz, Safety Code 6*. Ottawa, Canada: Health Canada.

Health Council of the Netherlands (1998). Radiofrequency electromagnetic fields (300 Hz–300 GHz). Amsterdam, Netherlands: Health Council of the Netherlands.

Hillert, L., Ahlibom, A., Neasham, D., Feychting, M., Jarup, L., Navin, Navin, R., & Elliott, P. (2000). Call-related factors influencing output power from mobile phones. *Journal of Exposure Science and Environmental Epidemiology*. *16*, 507-514.

Industry Canada (2005). *Guidelines for the Measurement of Radio Frequency Fields at Frequencies from 3kHz to 300GHz*. Ottawa, Canada: Industry Canada.

Institute of Electrical and Electronics Engineers (2013). *Determining the Peak Spatial-Average Absorption Rate (SAR) in the Human Body from Wireless Communication Devices, 30 MHz to 6 GHz – Part 1: General Requirements for using the Finite-Difference Time-Domain (FDTD) method for SAR calculations.* IEEE std 1528. New York, USA: IEEE.

Institute of Electrical and Electronics Engineers (2013). *Recommended Practice for Determining the Peak Spatial-Average Specific Absorption Rate (SAR) in the Homan Head from Wireless Communications Devices: Measurement Techniques.* IEEE std 1528. New York, USA: IEEE.

International Agency for Research on Cancer (2011). *IARC Classifies Radiofrequency Electromagnetic Fields as possibly Carcinogenic to Humans*. Lyon, France: IARC

International Agency for Research on Cancer (2013). *Non-Ionizing Radiation, Part 2: Radiofrequency Electromagnetic Eields*. Lyon, France: IARC.

International Commission on Non-Ionizing Radiation Protection (1998). Guidelines for Limiting Exposure to Time-varying Electric, Magnetic and Electromagnetic fields (up to 300 GHz). *Health Physics, 74*(4), 494-522.

International Commission on Non-Ionizing Radiation Protection (2020). Guidelines for Limiting Exposure Electromagnetic fields (100 kHz to 300 GHz). *Health Physics, 118*(5), 483-524.

International Commission on Non-Ionizing Radiation Protection (2009). *Exposure to High Frequency Electromagnetic fields, Biological Effects and Health Consequences (100 kHz – 300 GHz)*. *Health Physics, 74*, 494-522.

International Electrotechnical Commission (2010). *Human exposure to radio frequency fields from hand-held and body-mounted wireless communication devices – Human models, instrumentation, and procedures – Part 2: Procedure to determine the specific absorption rate (SAR) for wireless communication devices used in close proximity to the human body (frequency range of 30 MHz to 6 GHz* IEC 62209-2. Geneva, Switzerland: IEC.

International Electrotechnical Commission (2016). *Measurement procedure for the assessment of specific absorption rate of human exposure to radio frequency fields from hand-held and body-mounted wireless communication devices – Part 1: Devices used next to the ear (Frequency range of 300 MHz to 6 GHz)*. IEC 62209-1. Geneva, Switzerland: IEC.

International Electrotechnical Commission (2017). *Determining the peak spatial-average specific absorption rate (SAR) in the human body from wireless communications devices, 30 MHz to 6 GHz – Part 1: General*

requirements for using the finite-difference time-domain (FDTD) method for SAR calculations. IEC 62704-1. Geneva, Switzerland: IEC.

International Electrotechnical Commission (2017). *Specific absorption rate (SAR) measurement procedure for long term evolution (LTE) devices*. IEC PAS 63083. Geneva, Switzerland: IEC.

International Telecommunication Union (2020). Individual using the Internet by gender. Retrieved from https://www.itu.int/net4/ITU-D/icteye/#/topics/1002

International Telecommunication Union (2020). Mobile Cellular Subscription Per 100 Inhabitants. Retrieved from https://www.itu.int/net4/ITU-D/icteye/#/topics/1002

International Telecommunication Union (2020). Mobile Cellular Subscription Per 100 Inhabitants. Retrieved from https://www.itu.int/net4/ITU-D/icteye/#/topics/1002

International Telecommunications Union (2008). *Guidance to Measurement and Numerical Prediction of Electromagnetic Fields for Compliance with Human Exposure Limits for Telecommunication Installations, Series K: Protection against Interference, Recommendation K.61*. Geneva, Switzerland: ITU.

International Telecommunications Union (2008). *Guidance to Measurement and Numerical Prediction of Electromagnetic Fields for Compliance with*

Human Exposure Limits for Telecommunication Installations, Series K: Protection against Interference, Recommendation K.61. Geneva, Switzerland: ITU.

International Telecommunications Union (2012). *Guidance for Assessment, Evaluation and Monitoring of Human Exposure to Radio Frequency Electromagnetic Fields, Series K: Protection against Interference, Recommendation K.91*. Geneva, Switzerland: ITU.

Jain, S. V., Jain, S., Krrup, L., & Gawade, A. (2014). Overview on Generations of Network: 1G,2G,3G,4G,5G. *International Journal of Computer Technology & Applications, 5* (5),1789-1794.

Khalatbari, S., Sardari, D., Mirzaee, A. A. & Sadafi, A. H. (2006). *Calculating SAR in Two Models of the Human Head Exposed to Mobile Phones Radiations at 900 and 1800MHz.* Paper presented at the Progress in Electromagnetic Research Symposium, Cambridge, USA, 62-29 March, 2006.

Khan, S. & Ahmad, N. (2015). The Reduction of Specific Absorption Rate at different Frequencies. *Journal of Engineering and Applied Sciences, 32*(2). 71-57. Retrieved form https://www.researchgate.net/publication/296332560

Khan, S. & Kaur, J. (2019). *Electric field and specific absorption rate (SAR) analysis in multilayered skin tissue exposed to 5G mobile communication*

frequencies. Paper presented at AIP Conference 2142, 110028, Bahal. Retrieved from https://www.researchgate.net/publication/335507361

Krstić, D., Zigar, D., Petković, D., & Sokolović, D. (2011). Calculation of Absorbed Electromagnetic Energy in Human Head Radiated by Mobile Phones. *International Journal for Emerging Science, 1*(4), 5265-534.

Kumar, A., Suman, & Renu (2013). Comparison of 3G Wireless Networks and 4G Wireless Networks. *International Journal of Electronics and Communication Engineering*. *6*(1). 1-8.

Lönn, S. Forssén, Vecchia, P. Ahlbom, A. & Feychting (2004). Output power levels form mobile phones in different geographical areas; implications for exposure assessment. *Occupational Environmental Medicine, 61*, 769-772.

Mahfouz, Z., Gati, A., Lautru, D., Wiart, J., & Hanna, F. V. (2012). SAR assessment and analysis of cumulative body exposure to multi transmitters from a mobile phone. *IEEE Tropical*, 77-80.

Microwave Vision Group (2018). ComoSsar Twin Configuration. Retrieved from https://www.mvg-world.com/en

Microwave Vision Group (2018). Oopensar SW. Retrieved from https:// www.mvg-world.com/en

Microwave Vision Group (2018). Positioning System. Retrieved from https://www.mvg-world.com/en

Microwave Vision Group (2018). Probes. Retrieved from https://www.mvg-world.com/en

Microwave Vision Group (2018). SAM Phantom. Retrieved from https://www.mvg-world.com/en

Mild, K. H., Alanko, T., Decat, G., Falsaperia, R., Gryz, K., Hietanen, M., Karpowicz, J., Rossi, P., & Sandstorm, M. (2009). Exposure of Workers to Electromagnetic Fields. A Review of Open Questions on Exposure Assessment Techniques. *Journal of Occupational Safety and Ergonomics. 15*(1), 3–33.

Molecular Expressions Microscopy Primer (2016). *The Nature of Electromagnetic Radiation*. Retrieved from https://micro.magnet.fsu.edu

Morega, M., Marinescu, A., & Morega, M. A. (2010). Mobile phone SAR analysis through experimental and numerical simulation. Proceedings of 12th International *Conference on Optimization of Electrical and Electronic Equipment*, pp. 95-102, doi:10.1109/OTPIM.2010.5510423.

Mouradi, R., Desai, N., Erdemir, A., & Agarwal, A. (2011). The use of FDTD establishing in vitro experimentation conditions representative of liflike cell phone radiation on the spermatozoa. *Health Physices, 102*(1), 54-62.

Musiige, D., Laulagnet, V., & Anton, F. (2012). LTE modem power consumption, SAR and RF signal strength emulation. Retrieved from https://www.researchgate.net/publication/256504152

National Communications Authority (2020). Telecom Subscriptions for January 2020, Retrieved from https://nca.org.gh/media-and-news/news/telecom-subsbscriptions-for-january-2020/

National Communications Authority (2022). Approved Equipment, Retrieved from https://portal.nca.org.gh/search_type_approval.php

Ng, K. (2003). *Non-Ionizing Radiation – Sources, Biological Effects, Emissions and Exposures. Proceedings of the international conference of ICNIRP at UNITEN*. Kuala Lumpur, Malaysia: ICNIRP.

Nguyen, D. U., Brown, S., Chang, A. I., Krycia, J., & Mirotznik, S. M. (2004). Numerical Evaluation of Heating of the Human Head Due to Magnetic Resonance Imaging. *IEEE Transactions on Biomedical Engineering, 51*(8). 1301-1309.

Omondi, G. (2020). The state of mobile in Ghana's tech ecosystem. Retrieved from https://www.gsma.com/mobilefordevelopment/blog/the-state-of-mobile-in-ghanas-tech-ecosystem/

Osei, S., Amoako, J.K., & Fletcher, J.J. (2015). Assessment of Levels of Occupational Exposure to Workers in Radiofrequency Fields of Two Television Stations in Accra, Ghana. *Radiation Protection Dosimetry, 169*(3). 1-8.

Sallomi, H. A. (2012). A Theoretical Approach for SAR Calculation in Human Head Exposed to RF Signa Strength. *Journal of Engineering and*

Development, 64(4). 304-313. Retrieved from https://www.researchgate.net/publication/256504152

Shukla, S., Khare, K. V., Garg, S., & Sharma, P. (2013). Comparative Study of 1G, 2G, 3G and 4G. *Journal of Engineering, Computers & Applied Sciences, 2*(4). 55-63.

Sole, M., Musu, C., Bio, F., Giusto, D., & Popescu, V. (2013). RFID Sensor Network for Workplace Safety Management. *IEEE 18th Conference on Emerging Technologies & Factory Automation (ETFA)*, 1-4, doi:10.1109/ETFA.2013.6648157.

Spiegel, R. (1984). A Review of Numerical Models for Predicting the Energy Deposition and Resultant Thermal Response of Humans Exposed to Electromagnetic Fields. *IEEE Transactions on Microwave Theory and Techniques, 32*(8). 739-746.

Spring, K. R., Inoue´, S., Fiynn, B. O., Sutter, R. T., & Davison, M. W. (Assessed on January 2020). *Electromagnetic Wave Propagation*. Olympus Life Science Solutions, Tokyo. Retrieved form https://www.olympuslife science. com/en/microscoperesource/primer/java/polarizedlight/emwave/

Staelin, D. H. (2011). *Electromagnetics and Applications.* Cambridgeshire, England: Massachusetts Institute of Technology.

Subaar, C., Amoako, J. K., Owusu, A., Fletcher, J. J., & Suubaar, J. (2017). Numerical studies of radiofrequency of the electromagnetic radiation

power absorption in paediatrics undergoing brain magnetic resonance imaging. *Journal of Radiation Research and Applied Sciences, 10*(3). 188-193.

Vorst, A. V., Rosen A., & Kotsuka, Y. (2009). *RF/Microwave Interaction with Biological Tissues*. New Jersey, Canada: John Wiley & Sons Inc.

Wassapan, T. & Rattanadecho, P. (2012). Numerical Analysis of Specific Absorption Rate and Heat Transfer in Human Head Subjected to Mobile Phone Radiation: Effects of User Age and Radiated Power. *Journal of Heat Transfer, 134*(12), 1-10.

Wassapan, T., Srisawatdhisukul, S., & Rattanadecho, P. (2011). Numerical Analysis of Specific Absorption Rate and Heat Transfer in the Human Body Exposed to Leakage Electromagnetic Field at 915 MHz and 2450 MHz. *International Journal of Heat and Mass Transfer, 133*(1). 51-101

Wassapan, T., Srisawatdhisukul, S., & Rattanadecho, P. (2012). Specific absorption rate and temperature distributions in human head subjected to mobile phone radiation at different frequencies. *International Journal of Heat and Mass Transfer, 55*, 347-359.

World Health Organisation (2014). *Electromagnetic fields and public health: Mobile Phones, Fact sheet N°193*. Geneva, Switzerland: WHO.

World Health Organisation (2014). Electromagnetic fields and public health: mobile phones, Fact sheet N°193, Reviewed October (2014).

Young, D. H., & Freeman, A. R. (1996). *University Physics* (9th ed.). Reading, Massachusetts: Addison-Wesley

APPENDICES

APPENDIX A

BASIC SAR RESTRICTIONS FOR 1800 MHz

	Organization	Local Head SAR (W/kg)	Whole Body SAR (W/kg)
Public	ICNIRP	2	0.08
	FCC	1.6	0.08
	ITU	2	0.08
	IEEE	2	0.08
Worker	ICNIRP	10	0.4
	FCC	8	0.4
	ITU	10	0.4
	IEEE	10	0.4

APPENDIX B

QUANTITIES USED AND THEIR UNITS

Quantity	Quantity Symbol	Unit	Unit Symbol
Area	A	Square metre	m^{-2}
Charge	Q	Coulombs	C
Conductivity	σ	Siemens per metre	Sm^{-1}
Current	I	Amperes	A
Current density	J	Amperes per square metre	Am^{-2}
Electric field strength	E	Volts per metre	Vm^{-1}
Energy	u	Joules	J
Frequency	f	Hertz	Hz
Gain	G	Decibels	dB
Impedance	Z	Ohms	Ω
Magnetic field strength	H	Ampere per metre	Am^{-1}
Magnetic flux density	B	Tesla	T
Permeability	μ	Siemens per metre	Sm^{-1}
Permittivity	ε	Farad per metre	Fm^{-1}
Power density	S	Watts per square metre	Wkg^{-1}
Relative permeability	μ_r	-	-
Relative permittivity	ε_r	-	-
Specific absorption rate	SAR	Watts per kilogram	Wkg^{-1}
Wavelength	λ	Metres	m

APPENDIX C

MEASURED SAR DATA OF APPROVED PHONE

Position	Channel	Distance	Approved Phone Peak SAR	Approved Phone 10 g SAR	Approved Phone 1 g SAR
LC	Low	0.0	0.090229	0.052992	0.068453
LC	Low	0.0	1.050880	0.323239	0.621881
LC	Middle	0.0	0.158209	0.072842	0.107742
LC	Middle	0.0	1.022173	0.302654	0.589856
LC	High	0.0	0.181780	0.089279	0.131734
LC	High	0.0	1.078218	0.334353	0.641612
LT	Low	0.0	0.053159	0.026648	0.029417
LT	Low	0.0	1.456014	0.384524	0.805689
LT	Middle	0.0	0.057242	0.030434	0.034441
LT	Middle	0.0	1.276786	0.351319	0.717928
LT	High	0.0	0.054239	0.031948	0.033860
LT	High	0.0	1.342686	0.393463	0.792505
RC	Low	0.0	0.121294	0.057599	0.083175
RC	Low	0.0	1.762307	0.049822	0.994215
RC	Middle	0.0	0.187827	0.090241	0.132213
RC	Middle	0.0	1.505295	0.468031	0.897979
RC	High	0.0	0.225524	0.104492	0.158402
RC	High	0.0	1.704456	0.506720	0.988672
RT	Low	0.0	1.192539	0.367044	0.705861
RT	Low	0.0	0.081693	0.043069	0.058590
RT	Middle	0.0	0.665234	0.351687	0.665234
RT	Middle	0.0	0.120221	0.062419	0.088107
RT	High	0.0	1.363544	0.395023	0.778154
RT	High	0.0	0.165768	0.077809	0.115972
LC	Low	1.0	0.242779	0.059141	0.130907
LC	Low	1.0	0.221358	0.059178	0.128105
LC	Low	1.0	0.199359	0.058008	0.121664
LC	Middle	1.0	0.207845	0.051461	0.115840
LC	Middle	1.0	0.185623	0.048691	0.104305
LC	Middle	1.0	0.176376	0.049935	0.105187
LC	High	1.0	0.238171	0.060150	0.132456
LC	High	1.0	0.246144	0.057877	0.128945
LC	High	1.0	0.253565	0.058392	0.131969
LT	Low	1.0	0.248248	0.059859	0.134038
LT	Low	1.0	0.229250	0.059742	0.130158
LT	Middle	1.0	0.243296	0.062723	0.135727
LT	Middle	1.0	0.237586	0.063297	0.135415

Position	Channel	Distance	Approved Phone Peak SAR	Approved Phone 10 g SAR	Approved Phone 1 g SAR
LT	High	1.0	0.229812	0.065387	0.136772
LT	High	1.0	0.254678	0.063357	0.139071
RC	Low	1.0	0.231829	0.098339	0.157149
RC	Low	1.0	0.220473	0.099212	0.154384
RC	Low	1.0	0.251492	0.099161	0.161033
RC	Low	1.0	0.210752	0.086714	0.137432
RC	Low	1.0	0.195504	0.086388	0.132740
RC	Low	1.0	0.210901	0.088434	0.137524
RC	Middle	1.0	0.227591	0.101071	0.156939
RC	Middle	1.0	0.268701	0.101394	0.165530
RC	Middle	1.0	0.231242	0.101131	0.158778
RC	Middle	1.0	0.204398	0.083106	0.129056
RC	Middle	1.0	0.189003	0.084648	0.129450
RC	Middle	1.0	0.203585	0.085279	0.132526
RC	High	1.0	0.252743	0.105301	0.168786
RC	High	1.0	0.251131	0.105038	0.168316
RC	High	1.0	0.261339	0.105843	0.171844
RC	High	1.0	0.234432	0.092857	0.151254
RC	High	1.0	0.223893	0.093194	0.147396
RC	High	1.0	0.220286	0.092921	0.146515
RT	Low	1.0	0.231759	0.105108	0.163298
RT	Low	1.0	0.265242	0.106302	0.171203
RT	Low	1.0	0.243760	0.108121	0.169603
RT	Middle	1.0	0.227913	0.103313	0.160265
RT	Middle	1.0	0.248048	0.105968	0.168630
RT	Middle	1.0	0.255457	0.103782	0.168401
RT	High	1.0	0.295645	0.113253	0.187078
RT	High	1.0	0.285427	0.114240	0.188206
RT	High	1.0	0.274380	0.112801	0.181655
LC	Low	2.0	0.075414	0.014340	0.036297
LC	Low	2.0	0.141225	0.061289	0.091355
LC	Low	2.0	0.116653	0.059803	0.083264
LC	Low	2.0	0.141225	0.061289	0.091355
LC	Low	2.0	0.116653	0.059803	0.083264
LC	Middle	2.0	0.118616	0.058537	0.083478
LC	Middle	2.0	0.120894	0.058753	0.083736
LC	Middle	2.0	0.073141	0.011604	0.031968
LC	High	2.0	0.135865	0.063290	0.092041
LC	High	2.0	0.126847	0.065069	0.092699
LC	High	2.0	0.071701	0.013634	0.034111
LT	Low	2.0	0.079909	0.014315	0.037658

Position	Channel	Distance	Approved Phone Peak SAR	Approved Phone 10 g SAR	Approved Phone 1 g SAR
LT	Low	2.0	0.074325	0.014828	0.036595
LT	Low	2.0	0.079257	0.014847	0.038308
LT	Middle	2.0	0.079803	0.017184	0.041524
LT	Middle	2.0	0.091785	0.017015	0.043074
LT	Middle	2.0	0.082716	0.016797	0.040359
LT	High	2.0	0.094007	0.018313	0.045000
LT	High	2.0	0.094380	0.017513	0.043779
LT	High	2.0	0.077980	0.017984	0.041551
RC	Low	2.0	0.121050	0.052814	0.077462
RC	Low	2.0	0.110876	0.052825	0.076696
RC	Low	2.0	0.104281	0.053015	0.075561
RC	Middle	2.0	0.193471	0.052268	0.090463
RC	Middle	2.0	0.110431	0.054381	0.076518
RC	Middle	2.0	0.105062	0.047524	0.070164
RC	Middle	2.0	0.124438	0.054596	0.081689
RC	Middle	2.0	0.117264	0.052545	0.078054
RC	Middle	2.0	0.115899	0.054546	0.079217
RC	High	2.0	0.125667	0.057674	0.084880
RC	High	2.0	0.114160	0.057216	0.081334
RC	High	2.0	0.119231	0.056871	0.082218
RT	Low	2.0	0.116470	0.056251	0.080130
RT	Low	2.0	0.136422	0.063054	0.088476
RT	Low	2.0	0.128612	0.056498	0.080985
RT	Middle	2.0	0.111951	0.053050	0.076643
RT	Middle	2.0	0.128657	0.061844	0.087979
RT	Middle	2.0	0.120578	0.053395	0.078990
RT	High	2.0	0.135888	0.061757	0.093215
RT	High	2.0	0.187114	0.070829	0.109914
RT	High	2.0	0.132259	0.059629	0.086983
LC	Low	3.0	0.068931	0.039546	0.050650
LC	Low	3.0	0.075279	0.038671	0.048930
LC	Low	3.0	0.076888	0.043266	0.055881
LC	Low	3.0	0.067021	0.039199	0.048432
LC	Low	3.0	0.067021	0.039199	0.048432
LC	Middle	3.0	0.064850	0.039735	0.048866
LC	Middle	3.0	0.073021	0.040064	0.052168
LC	Middle	3.0	0.067635	0.038907	0.048284
LC	High	3.0	0.079559	0.044798	0.056124
LC	High	3.0	0.073557	0.042867	0.054127
LC	High	3.0	0.076888	0.043266	0.055881
LT	Low	3.0	0.001821	0.000242	0.000334

Position	Channel	Distance	Approved Phone Peak SAR	Approved Phone 10 g SAR	Approved Phone 1 g SAR
LT	Low	3.0	0.004182	0.008400	0.002468
LT	Low	3.0	0.031959	0.001823	0.008239
LT	Middle	3.0	0.003689	0.000240	0.000451
LT	Middle	3.0	0.040529	0.001611	0.010627
LT	Middle	3.0	0.031159	0.000664	0.003206
LT	High	3.0	0.071922	0.001520	0.009536
LT	High	3.0	0.003768	0.000671	0.001535
LT	High	3.0	0.015234	0.000131	0.001324
RC	Low	3.0	0.072105	0.039109	0.049790
RC	Low	3.0	0.071955	0.041233	0.052157
RC	Low	3.0	0.072910	0.041406	0.053266
RC	Middle	3.0	0.039885	0.021955	0.027047
RC	Middle	3.0	0.062163	0.030863	0.041205
RC	Middle	3.0	0.074786	0.033198	0.047312
RC	High	3.0	0.076558	0.043833	0.055126
RC	High	3.0	0.075223	0.043067	0.055004
RC	High	3.0	0.078224	0.044032	0.055004
RT	Low	3.0	0.076957	0.038698	0.052605
RT	Low	3.0	0.076788	0.038377	0.050246
RT	Low	3.0	0.074827	0.037850	0.050262
RT	Middle	3.0	0.067499	0.035275	0.045881
RT	Middle	3.0	0.065334	0.035408	0.045489
RT	Middle	3.0	0.067170	0.035759	0.047283
RT	High	3.0	0.087242	0.041374	0.055967
RT	High	3.0	0.088507	0.042016	0.056980
RT	High	3.0	0.087520	0.041639	0.057048

APPENDIX D

MEASURED SAR DATA OF UNAPPROVED PHONE

Position	Channel	Distance	Unapproved Phone Peak SAR	Unapproved Phone 10 g SAR	Unapproved Phone 1 g SAR
LC	Low	0.0	0.169969	0.049298	0.100531
LC	Low	0.0	0.116101	0.056147	0.081784
LC	Middle	0.0	0.112759	0.030131	0.066213
LC	Middle	0.0	0.103858	0.052197	0.071669
LC	High	0.0	0.102132	0.025808	0.058505
LC	High	0.0	0.094745	0.050536	0.067393
LT	Low	0.0	0.076524	0.018975	0.042478
LT	Middle	0.0	0.065026	0.013162	0.032288
LT	Middle	0.0	0.058591	0.026714	0.032463
LT	High	0.0	0.065793	0.011128	0.030066
LT	High	0.0	0.046671	0.027622	0.029472
RC	Low	0.0	0.261749	0.064949	0.142885
RC	Low	0.0	0.045200	0.023025	0.026670
RC	Low	0.0	0.294909	0.127681	0.195223
RC	Low	0.0	0.177912	0.076801	0.113221
RC	Low	0.0	0.119184	0.054806	0.082128
RC	Middle	0.0	0.192504	0.053025	0.112284
RC	Middle	0.0	0.338991	0.167012	0.247676
RC	Middle	0.0	0.225224	0.101137	0.151413
RC	Middle	0.0	0.120328	0.053438	0.080199
RC	High	0.0	0.150342	0.037590	0.085501
RC	High	0.0	0.049894	0.025282	0.028778
RT	Low	0.0	0.140037	0.036292	0.079145
RT	Low	0.0	0.039866	0.021393	0.020867
RT	Middle	0.0	0.096342	0.021730	0.05132
RT	High	0.0	0.088629	0.018649	0.046533
RT	High	0.0	0.041235	0.185517	0.287234
RT	High	0.0	0.223882	0.106225	0.156222
RT	High	0.0	0.093121	0.047847	0.065597
LC	Low	1.0	0.305763	0.135690	0.214155
LC	Low	1.0	0.035198	0.021965	0.024145
LC	Low	1.0	0.040488	0.021545	0.023366
LC	Low	1.0	0.045673	0.021784	0.023000
LC	Middle	1.0	0.414569	0.164625	0.272446
LC	Middle	1.0	0.043706	0.024376	0.028147
LC	Middle	1.0	0.042614	0.025085	0.028526
LC	Middle	1.0	0.041690	0.024501	0.026990

Position	Channel	Distance	Unapproved Phone Peak SAR	Unapproved Phone 10 g SAR	Unapproved Phone 1 g SAR
LC	High	1.0	0.576254	0.214257	0.366647
LC	High	1.0	0.044872	0.026073	0.028144
LC	High	1.0	0.045181	0.026911	0.031394
LC	High	1.0	0.049254	0.026169	0.028765
LT	Low	1.0	0.022249	0.022249	0.026742
LT	Low	1.0	0.146215	0.070591	0.100022
LT	Low	1.0	0.144032	0.071055	0.101861
LT	Low	1.0	0.141370	0.072366	0.101879
LT	Low	1.0	0.138410	0.067953	0.095216
LT	Low	1.0	0.129278	0.068616	0.094548
LT	Low	1.0	0.137820	0.068480	0.097854
LT	Middle	1.0	0.038943	0.024937	0.027359
LT	Middle	1.0	0.155617	0.075325	0.106026
LT	Middle	1.0	0.144757	0.076075	0.150400
LT	Middle	1.0	0.150111	0.076089	0.107421
LT	Middle	1.0	0.162383	0.072091	0.106785
LT	Middle	1.0	0.138787	0.072713	0.100337
LT	Middle	1.0	0.141187	0.072994	0.102044
LT	High	1.0	0.048716	0.026328	0.031738
LT	High	1.0	0.141635	0.078028	0.106982
LT	High	1.0	0.159467	0.078121	0.112517
LT	High	1.0	0.158065	0.076613	0.108286
LT	High	1.0	0.161808	0.076354	0.110028
LT	High	1.0	0.153233	0.075699	0.106599
LT	High	1.0	0.155119	0.074962	0.107150
RC	Low	1.0	0.105066	0.058686	0.076631
RC	Low	1.0	0.070500	0.023271	0.032429
RC	Low	1.0	0.047614	0.022075	0.025666
RC	Low	1.0	0.102986	0.058035	0.074930
RC	Low	1.0	0.037455	0.019554	0.020415
RC	Low	1.0	0.037414	0.020696	0.023691
RC	Middle	1.0	0.131099	0.067043	0.088602
RC	Middle	1.0	0.060886	0.026305	0.035110
RC	Middle	1.0	0.041588	0.023756	0.025080
RC	Middle	1.0	0.139159	0.067895	0.096784
RC	Middle	1.0	0.044597	0.022064	0.020349
RC	Middle	1.0	0.043062	0.022703	0.026474
RC	High	1.0	0.121261	0.067001	0.088067
RC	High	1.0	0.058310	0.026604	0.033938
RC	High	1.0	0.044703	0.024960	0.027480
RC	High	1.0	0.129611	0.068161	0.094696

Position	Channel	Distance	Unapproved Phone Peak SAR	Unapproved Phone 10 g SAR	Unapproved Phone 1 g SAR
RC	High	1.0	0.041663	0.022991	0.023776
RC	High	1.0	0.046035	0.024001	0.028028
RT	Low	1.0	0.094406	0.047510	0.063552
RT	Low	1.0	0.051668	0.020925	0.022740
RT	Low	1.0	0.088270	0.047552	0.063324
RT	Middle	1.0	0.105622	0.058536	0.080156
RT	Middle	1.0	0.040928	0.023823	0.023731
RT	Middle	1.0	0.094867	0.050467	0.069289
RT	High	1.0	0.147485	0.069698	0.100151
RT	High	1.0	0.037690	0.025265	0.027472
RT	High	1.0	0.128508	0.063778	0.090882
LC	Low	2.0	0.069257	0.033970	0.043449
LC	Low	2.0	0.044918	0.020575	0.025353
LC	Low	2.0	0.039842	0.020755	0.025429
LC	Middle	2.0	0.064579	0.033365	0.041704
LC	Middle	2.0	0.048376	0.023127	0.028540
LC	Middle	2.0	0.040709	0.022645	0.026634
LC	High	2.0	0.076257	0.039067	0.050055
LC	High	2.0	0.050575	0.023265	0.027603
LC	High	2.0	0.038499	0.023389	0.025797
LT	Low	2.0	0.090464	0.049792	0.066616
LT	Low	2.0	0.091857	0.049422	0.065092
LT	Low	2.0	0.092136	0.049145	0.066252
LT	Middle	2.0	0.089449	0.053522	0.070051
LT	Middle	2.0	0.095921	0.052645	0.070175
LT	Middle	2.0	0.092079	0.052309	0.067721
LT	High	2.0	0.099757	0.055581	0.073136
LT	High	2.0	0.104602	0.053638	0.072021
LT	High	2.0	0.102042	0.055975	0.075313
RC	Low	2.0	0.039614	0.021058	0.025593
RC	Low	2.0	0.049766	0.020698	0.025442
RC	Low	2.0	0.040070	0.020453	0.025264
RC	Middle	2.0	0.035949	0.022387	0.025656
RC	Middle	2.0	0.051283	0.023351	0.029467
RC	Middle	2.0	0.045469	0.022903	0.027612
RC	High	2.0	0.039754	0.023963	0.026268
RC	High	2.0	0.063905	0.023715	0.029880
RC	High	2.0	0.037245	0.022816	0.025325
RT	Low	2.0	0.079706	0.036992	0.050376
RT	Low	2.0	0.066837	0.035333	0.046689
RT	Low	2.0	0.072456	0.037206	0.049136

Position	Channel	Distance	Unapproved Phone Peak SAR	Unapproved Phone 10 g SAR	Unapproved Phone 1 g SAR
RT	Middle	2.0	0.081283	0.041089	0.054149
RT	Middle	2.0	0.074279	0.039439	0.051323
RT	Middle	2.0	0.082231	0.039800	0.053771
RT	High	2.0	0.082020	0.046051	0.056048
RT	High	2.0	0.083848	0.045225	0.059001
RT	High	2.0	0.088986	0.045753	0.061546
LC	Low	3.0	0.069464	0.036693	0.047747
LC	Low	3.0	0.054591	0.028030	0.035063
LC	Low	3.0	0.049763	0.027399	0.033006
LC	Middle	3.0	0.076255	0.076255	0.051443
LC	Middle	3.0	0.047172	0.0471723	0.028276
LC	Middle	3.0	0.053397	0.0533975	0.037639
LC	High	3.0	0.073117	0.073117	0.051861
LC	High	3.0	0.052250	0.052250	0.036669
LC	High	3.0	0.054417	0.054417	0.038027
LT	Low	3.0	0.038353	0.020912	0.022197
LT	Low	3.0	0.023824	0.019931	0.023824
LT	Low	3.0	0.034827	0.020868	0.021837
LT	Middle	3.0	0.041827	0.022414	0.023856
LT	Middle	3.0	0.036653	0.021509	0.024945
LT	Middle	3.0	0.030317	0.021870	0.020814
LT	High	3.0	0.039063	0.025218	0.028148
LT	High	3.0	0.037525	0.022771	0.024281
LT	High	3.0	0.044558	0.023525	0.025049
RC	Low	3.0	0.064637	0.036062	0.045690
RC	Low	3.0	0.074292	0.037324	0.049804
RC	Low	3.0	0.034890	0.018737	0.020321
RC	Middle	3.0	0.070251	0.038990	0.050555
RC	Middle	3.0	0.082259	0.039615	0.052330
RC	Middle	3.0	0.036544	0.021179	0.024722
RC	Middle	3.0	0.064486	0.032944	0.041558
RC	High	3.0	0.075284	0.041015	0.053219
RC	High	3.0	0.070950	0.040296	0.050502
RC	High	3.0	0.033550	0.022556	0.022835
RT	Low	3.0	0.045698	0.020645	0.023838
RT	Low	3.0	0.043487	0.020392	0.023664
RT	Low	3.0	0.032527	0.020450	0.020673
RT	Middle	3.0	0.039615	0.022738	0.024886
RT	Middle	3.0	0.043580	0.024213	0.028289
RT	Middle	3.0	0.037704	0.023423	0.024791
RT	High	3.0	0.036548	0.024834	0.024624

Position	Channel	Distance	Unapproved Phone Peak SAR	Unapproved Phone 10 g SAR	Unapproved Phone 1 g SAR
RT	High	3.0	0.042406	0.024872	0.026796
RT	High	3.0	0.040468	0.024115	0.026272

APPENDIX E

CODES FOR THE REFERENCE PHONE POSITIONS

Code	Side of Ear	Orientation	Frequency Channel
LCH	Left ear	Cheek position	High channel
LCL	Left ear	Cheek position	Low channel
LCM	Left ear	Cheek position	Middle channel
LTH	Left ear	Tilt position	High channel
LTL	Left ear	Tilt position	Low channel
LTM	Left ear	Tilt position	Middle channel
RCH	Right ear	Cheek position	High channel
RCL	Right ear	Cheek position	Low channel
RCM	Right ear	Cheek position	Middle channel
RTH	Right ear	Tilt position	High channel
RTL	Right ear	Tilt position	Low channel
RTM	Right ear	Tilt position	-
LC	Left ear	Cheek position	-
LT	Left ear	Tilt position	-
RC	Right ear	Cheek position	-
RT	Right ear	Tilt position	-

APPENDIX F

SAR PREDICTIVE MODELS OF APPROVED PHONE

Position	Peak SAR	10 g SAR	1 g SAR
LCH	0.57725EXP(-1.107d)+0.05305	0.167080EXP(-2.459d)+0.04472	0.33449EXP(-1.435d)+0.05211
LCL	0.51273EXP(-1.123d)+0.05737	0.143870EXP(-2.224d)+0.0442	0.2963EXP(-1.298d)+0.0486
LCM	0.52413EXP(-1.42d)+0.06577	$0.1798-0.1527d+0.0362d^2$	0.29829EXP(-1.615d)+0.05041
LTH	0.638758EXP(-0.9361d)-0.008658	0.218661EXP(-1.126d)-0.006061	0.42714EXP(-1.025d)-0.01414
LTL	0.76566EXP(-1.108d)-0.01146	0.208301EXP(-1.212d)-0.002701	0.42967EXP(-1.088d)-0.01517
LTM	0.61545EXP(-0.8479d)-0.02495	0.199283EXP(-1.027d)-0.008383	0.39499EXP(-0.9392d)-0.01879
RCH	0.88621EXP(-1.68d)+0.07849	0.263050EXP(-1.521d)+0.04245	0.51842EXP(-1.587d)+0.05498
RCL	0.86538EXP(-1.773d)+0.07622	$0.05908+0.03077d-0.01291d^2$	0.48661EXP(-1.618d)+0.05189
RCM	0.77564EXP(-1.587d)+0.07016	0.250730EXP(-1.316d)+0.02807	0.47289EXP(-1.475d)+0.04171
RTH	0.69107EXP(-1.158d)+0.07293	0.209020EXP(-0.8809d)+0.02728	0.40768EXP(-1.011d)+0.03912
RTL	0.57806EXP(-1.109d)+0.05874	0.186460EXP(-0.7597d)+0.01874	0.35278EXP(-0.9367d)+0.02952
RTM	0.46575EXP(-0.4175d)-0.07105	0.190210EXP(-0.7815d)+0.01689	0.35351EXP(-0.906d)+0.2309

APPENDIX G

SAR PREDICTIVE MODELS OF UNAPPROVED PHONE

Position	Peak SAR	10 g SAR	1 g SAR
LCH	0.1308EXP(-0.2058d)	0.047EXP(0.0405d)	0.08284EXP(-0.1917d)
LCL	0.1439EXP(-0.3731d)	0.0546EXP(-0.2356d)	0.09237EXP(-0.365d)
LCM	0.1236EXP(-0.2451d)	0.0434EXP(0.0461d)	0.07323EXP(-0.2374d)
LTH	0.09443EXP(-0.07465d)	0.042EXP(-0.0017d)	0.0606EXP(-0.04517d)
LTL	0.1014EXP(-0.1595d)	0.039EXP(-0.0167d)	0.06457EXP(-0.1122d)
LTM	0.0923EXP(-0.09865d)	0.0424EXP(-0.0244d)	0.06196EXP(-0.06917d)
RCH	0.0961EXP(-0.2345d)	0.033EXP(-0.0188d)	0.05549EXP(-0.1682d)
RCL	0.1713EXP(-0.6442d)	0.065EXP(-0.4371d)	0.1065EXP(-0.6332d)
RCM	0.2113EXP(-0.741d)	0.089EXP(-0.5848d)	0.1429EXP(-0.7892d)
RTH	0.1236EXP(-0.2646d)	0.072EXP(-0.2969d)	0.1163EXP(-0.4239d)
RTL	0.09345EXP(-0.2049d)	0.0347EXP(-0.0749d)	0.1079EXP(-0.5278d)
RTM	0.09955EXP(-0.2145d)	0.0.323EXP(0.0025d)	0.05814EXP(-0.1494d)

APPENDIX H

UNCERTAINTY BUDGET OF THE SAR MEASUREMENTS

A	c	d	e= f(d,k)	f	g	h= c*f/e	i= c*g/e	k
Uncertainty Component	Tol (+- %)	Probability Distribution	Div.	C_i (1g)	C_i (10g)	1g U_i (+-%)	10g U_i (+-%)	V_i
Measurement System								
Probe Calibration	5.8	N	1	1	1	5.80	5.80	∞
Axial Isotropy	3.5	R	√3	1	1	2.02	2.02	∞
Hemispherical Isotropy	5.9	R	√3	0	0	0.0	0.0	∞
Boundary Effect	1.0	R	√3	1	1	0.58	0.58	∞
Linearity	4.7	R	√3	1	1	2.71	2.71	∞
System Detection Limits	1.0	R	√3	1	1	0.58	0.58	∞
Modulation response	0.00	N	√3	0	0	0.00	0.00	∞
Readout Electronics	0.50	N	1	1	1	0.50	0.50	∞
Response Time	0.0	R	√3	0	0	0.00	0.00	∞
Integration Time	1.4	R	√3	0	0	0.0	0.0	∞
RF Ambient Conditions - Noise	3.0	R	√3	1	1	1.73	1.73	∞
RF Ambient Conditions – Reflections	3.0	R	√3	1	1	1.73	1.73	∞
Probe Positioner Mechanical Tolerance	1.4	R	√3	1	1	0.81	0.81	∞
Probe Positioning with respect to Phantom Shell	1.40	R	√3	1	1	0.81	0.81	∞

Extrapolation, interpolation and integration Algorithms for Max. SAR Evaluation	2.3	R	√3	1	1	1.33	1.33	∞
Dipole								
Deviation of experimental source from numerical source	5.00	N	1	1	1	5.00	5.00	∞
Input Power and SAR drift measurement	0.50	R	√3	1	1	0.29	0.29	∞
Dipole Axis to Liquid Distance	2.00	R	√3	1	1	1.15	1.15	∞
Phantom and Tissue Parameters								
Phantom Shell Uncertainty - Shape, Thickness and Permittivity	4.00	R	√3	1	1	2.31	2.31	∞
Uncertainty in SAR correction for deviation in permittivity and conductivity	2.00	N	1	1	0.84	2.00	1.68	∞
Liquid Conductivity - Temperature Uncertainty	2.50	R	√3	0.78	0.71	1.13	1.02	∞
Liquid Conductivity Measurement	4.00	N	1	0.78	0.71	3.12	2.84	5
Liquid Permittivity - Temperature Uncertainty	2.50	R	√3	0.23	0.26	0.33	0.38	∞
Liquid Permittivity Measurement	5.00	N	1	0.23	0.26	1.15	1.30	5
Combined Standard Uncertainty		RSS				10.16	10.03	
Expanded Uncertainty (95% Confidence interval)		K				20.32	20.06	

APPENDIX I

MATLAB PROGRAMMING CODES FOR SAR APPLICATION

```
classdef phd5selfdecayavegrowth < matlab.apps.AppBase


% Properties that correspond to app components
properties (Access = public)
MobilePhoneSarCalculatorAppUIFigure matlab.ui.Figure
GridLayout matlab.ui.container.GridLayout
NATIONALCOMMUNICATIONAUTHORITYAPPROVALSTATUSPanel
matlab.ui.container.Panel
Image matlab.ui.control.Image
Image_2 matlab.ui.control.Image
CheckButtonGroup matlab.ui.container.ButtonGroup
ApprovedPhoneModelButton matlab.ui.control.RadioButton
UnapprovedPhoneModelButton matlab.ui.control.RadioButton
MODELINPUTSPanel matlab.ui.container.Panel
PositionofPhonePanel matlab.ui.container.Panel
CheckButtonGroup_2 matlab.ui.container.ButtonGroup
LeftEarButton matlab.ui.control.RadioButton
RightEarButton matlab.ui.control.RadioButton
OrientationofPhonePanel matlab.ui.container.Panel
CheckButtonGroup_3 matlab.ui.container.ButtonGroup
CheekButton matlab.ui.control.RadioButton
TiltButton matlab.ui.control.RadioButton
ClosenesstoHeadPanel matlab.ui.container.Panel
DistanceofPhonecmSensitivity03cmEditFieldLabel
matlab.ui.control.Label
DistanceofPhonecmSensitivity03cmEditField
matlab.ui.control.NumericEditField
CarrierFrequencyPanel matlab.ui.container.Panel
CheckButtonGroup_4 matlab.ui.container.ButtonGroup
LowFreqChannelButton matlab.ui.control.RadioButton
MidFreqChannelButton matlab.ui.control.RadioButton
HighFreqChannelButton matlab.ui.control.RadioButton
MODELOUTPUTSPanel matlab.ui.container.Panel
UIAxes matlab.ui.control.UIAxes
SAROUTPUTSPanel matlab.ui.container.Panel
SARButton matlab.ui.control.Button
SARWkgEditFieldLabel matlab.ui.control.Label
SARWkgEditField matlab.ui.control.NumericEditField
EditField3 matlab.ui.control.NumericEditField
Label matlab.ui.control.Label
ICNIRPCompliancePanel matlab.ui.container.Panel
```

```
ofICNIRPLimitEditFieldLabel matlab.ui.control.Label
ofICNIRPLimitEditField matlab.ui.control.NumericEditField
RSquareEditFieldLabel matlab.ui.control.Label
RSquareEditField matlab.ui.control.NumericEditField
AUTHORPanel matlab.ui.container.Panel
Label_2 matlab.ui.control.Label
Image2 matlab.ui.control.Image
Image3 matlab.ui.control.Image
end


% Callbacks that handle component events
methods (Access = private)


% Button pushed function: SARButton
function SARButtonPushed(app, event)
if app.ApprovedPhoneModelButton.Value
if
(app.LeftEarButton.Value==1)&&(app.CheekButton.Value==1)&&(app.LowFr
eqChannelButton.Value==1)
x=app.DistanceofPhonecmSensitivity03cmEditField.Value;
sar=0.143870.*exp(-2.224.*x)+0.0442;
app.SARWkgEditField.Value=sar;
error = 20.09/100*sar;
app.EditField3.Value=error;
compliance = sar/2*100;
r2=0.9966;
app.RSquareEditField.Value=r2;
app.ofICNIRPLimitEditField.Value=compliance;
x1 = 0:0.1:3;
sar1=0.143870.*exp(-2.224.*x1)+0.0442;
plot(app.UIAxes,x1,sar1);
elseif
(app.LeftEarButton.Value==1)&&(app.CheekButton.Value==1)&&(app.MidFr
eqChannelButton.Value==1)
x=app.DistanceofPhonecmSensitivity03cmEditField.Value;
sar=0.0362.*x^2-0.1527.*x+0.1798;
app.SARWkgEditField.Value=sar;
error = 20.09/100*sar;
app.EditField3.Value=error;
compliance = sar/2*100;
r2=0.9227;
app.RSquareEditField.Value=r2;
app.ofICNIRPLimitEditField.Value=compliance;
x1 = 0:0.1:3;
sar1=0.0362.*x1.^2-0.1527.*x1+0.1798;
plot(app.UIAxes,x1,sar1);
```

```
elseif
(app.LeftEarButton.Value==1)&&(app.CheekButton.Value==1)&&(app.HighF
reqChannelButton.Value==1)
x=app.DistanceofPhonecmSensitivity03cmEditField.Value;
sar=0.167080.*exp(-2.459.*x)+0.04472;
app.SARWkgEditField.Value=sar;
error = 20.09/100*sar;
app.EditField3.Value=error;
compliance = sar/2*100;
r2=0.9998;
app.RSquareEditField.Value=r2;
app.ofICNIRPLimitEditField.Value=compliance;
x1 = 0:0.1:3;
sar1=0.167080.*exp(-2.459.*x1)+0.04472;
plot(app.UIAxes,x1,sar1);
% Left ear and Tilt
;;;;;;;;;;;;;;;;;;;;;;;;;;;;;;;;;;;;;;;;;;;;;;;;;;;;;;;;;;;;;;;;;;;;;;;;
;;;;;;;;
elseif
(app.LeftEarButton.Value==1)&&(app.TiltButton.Value==1)&&(app.LowFre
qChannelButton.Value==1)
x=app.DistanceofPhonecmSensitivity03cmEditField.Value;
sar=0.20830.*exp(-1.212.*x)-0.002701;
app.SARWkgEditField.Value=sar;
error = 20.09/100*sar;
app.EditField3.Value=error;
compliance = sar/2*100;
r2=0.9999;
app.RSquareEditField.Value=r2;
app.ofICNIRPLimitEditField.Value=compliance;
x1 = 0:0.1:3;
sar1=0.20830.*exp(-1.212.*x1)-0.002701;
plot(app.UIAxes,x1,sar1);
elseif
(app.LeftEarButton.Value==1)&&(app.TiltButton.Value==1)&&(app.MidFre
qChannelButton.Value==1)
x=app.DistanceofPhonecmSensitivity03cmEditField.Value;
sar=0.199283.*exp(-1.027.*x)-0.008383;
app.SARWkgEditField.Value=sar;
error = 20.09/100*sar;
app.EditField3.Value=error;
compliance = sar/2*100;
r2=1;
app.RSquareEditField.Value=r2;
app.ofICNIRPLimitEditField.Value=compliance;
x1 = 0:0.1:3;
sar1=0.199283.*exp(-1.027.*x1)-0.008383;
plot(app.UIAxes,x1,sar1);
```

```
elseif
(app.LeftEarButton.Value==1)&&(app.TiltButton.Value==1)&&(app.HighFr
eqChannelButton.Value==1)
x=app.DistanceofPhonecmSensitivity03cmEditField.Value;
sar=0.218861.*exp(-1.126.*x)-0.006061;
app.SARWkgEditField.Value=sar;
error = 20.09/100*sar;
app.EditField3.Value=error;
compliance = sar/2*100;
r2=0.9999;
app.RSquareEditField.Value=r2;
app.ofICNIRPLimitEditField.Value=compliance;
x1 = 0:0.1:3;
sar1=0.218861.*exp(-1.126.*x1)-0.006061;
plot(app.UIAxes,x1,sar1);
% RightEar and Cheek
;;;;;;;;;;;;;;;;;;;;;;;;;;;;;;;;;;;;;;;;;;;;;;;;;;;;;;;;;;;;;;;;;;;;
elseif
(app.RightEarButton.Value==1)&&(app.CheekButton.Value==1)&&(app.LowF
reqChannelButton.Value==1)
x=app.DistanceofPhonecmSensitivity03cmEditField.Value;
sar=-0.01291*x^2+0.03077*x+0.05908;
app.SARWkgEditField.Value=sar;
error = 20.09/100*sar;
app.EditField3.Value=error;
compliance = sar/2*100;
r2=0.6304;
app.RSquareEditField.Value=r2;
app.ofICNIRPLimitEditField.Value=compliance;
x1 = 0:0.1:3;
sar1=-0.01291*x1.^2+0.03077*x1+0.05908;
plot(app.UIAxes,x1,sar1);
elseif
(app.RightEarButton.Value==1)&&(app.CheekButton.Value==1)&&(app.MidF
reqChannelButton.Value==1)
x=app.DistanceofPhonecmSensitivity03cmEditField.Value;
sar=0.25073.*exp(-1.316.*x)+0.02807;
app.SARWkgEditField.Value=sar;
error = 20.09/100*sar;
app.EditField3.Value=error;
compliance = sar/2*100;
r2=0.9983;
app.RSquareEditField.Value=r2;
app.ofICNIRPLimitEditField.Value=compliance;
x1 = 0:0.1:3;
sar1=0.25073.*exp(-1.316.*x1)+0.02807;
plot(app.UIAxes,x1,sar1);
```

```
elseif
(app.RightEarButton.Value==1)&&(app.CheekButton.Value==1)&&(app.High
FreqChannelButton.Value==1)
x=app.DistanceofPhonecmSensitivity03cmEditField.Value;
sar=0.263050.*exp(-1.521.*x)+0.04245;
app.SARWkgEditField.Value=sar;
error = 20.09/100*sar;
app.EditField3.Value=error;
compliance = sar/2*100;
r2=0.9998;
app.RSquareEditField.Value=r2;
app.ofICNIRPLimitEditField.Value=compliance;
x1 = 0:0.1:3;
sar1=0.263050.*exp(-1.521.*x1)+0.04245;
plot(app.UIAxes,x1,sar1);
% Right Ear and Tilt
elseif
(app.RightEarButton.Value==1)&&(app.TiltButton.Value==1)&&(app.LowFr
eqChannelButton.Value==1)
x=app.DistanceofPhonecmSensitivity03cmEditField.Value;
sar=0.186460.*exp(-0.7597.*x)+0.01874;
app.SARWkgEditField.Value=sar;
error = 20.09/100*sar;
app.EditField3.Value=error;
compliance = sar/2*100;
r2=0.9999;
app.RSquareEditField.Value=r2;
app.ofICNIRPLimitEditField.Value=compliance;
x1 = 0:0.1:3;
sar1=0.186460.*exp(-0.7597.*x1)+0.01874;
plot(app.UIAxes,x1,sar1);
elseif
(app.RightEarButton.Value==1)&&(app.TiltButton.Value==1)&&(app.MidFr
eqChannelButton.Value==1)
x=app.DistanceofPhonecmSensitivity03cmEditField.Value;
sar=0.19021.*exp(-0.7815.*x)+0.01689;
app.SARWkgEditField.Value=sar;
error = 20.09/100*sar;
app.EditField3.Value=error;
compliance = sar/2*100;
r2=1;
app.RSquareEditField.Value=r2;
app.ofICNIRPLimitEditField.Value=compliance;
x1 = 0:0.1:3;
sar1=0.19021.*exp(-0.7815.*x1)+0.01689;
plot(app.UIAxes,x1,sar1);
```

```
elseif
(app.RightEarButton.Value==1)&&(app.TiltButton.Value==1)&&(app.HighF
reqChannelButton.Value==1)
x=app.DistanceofPhonecmSensitivity03cmEditField.Value;
sar=0.209020.*exp(-0.8809.*x)+0.02728;
app.SARWkgEditField.Value=sar;
error = 20.09/100*sar;
app.EditField3.Value=error;
compliance = sar/2*100;
r2=0.9999;
app.RSquareEditField.Value=r2;
app.ofICNIRPLimitEditField.Value=compliance;
x1 = 0:0.1:3;
sar1=0.209020.*exp(-0.8809.*x1)+0.02728;
plot(app.UIAxes,x1,sar1);
end
else
app.UnapprovedPhoneModelButton.Value
if
(app.LeftEarButton.Value==1)&&(app.CheekButton.Value==1)&&(app.LowFr
eqChannelButton.Value==1)
x=app.DistanceofPhonecmSensitivity03cmEditField.Value;
sar=0.0546.*exp(-0.2356.*x);
app.SARWkgEditField.Value=sar;
error = 20.09/100*sar;
app.EditField3.Value=error;
compliance = sar/2*100;
r2=0.7408;
app.RSquareEditField.Value=r2;
app.ofICNIRPLimitEditField.Value=compliance;
x1 = 0:0.1:3;
sar1=0.0546.*exp(-0.2356.*x1);
plot(app.UIAxes,x1,sar1);
elseif
(app.LeftEarButton.Value==1)&&(app.CheekButton.Value==1)&&(app.MidFr
eqChannelButton.Value==1)
x=app.DistanceofPhonecmSensitivity03cmEditField.Value;
sar=0.0434.*exp(0.0461.*x);
app.SARWkgEditField.Value=sar;
error = 20.09/100*sar;
app.EditField3.Value=error;
compliance = sar/2*100;
r2=0.02822;
app.RSquareEditField.Value=r2;
app.ofICNIRPLimitEditField.Value=compliance;
x1 = 0:0.1:3;
sar1=0.0434.*exp(0.0461.*x1);
plot(app.UIAxes,x1,sar1);
```

```
elseif
(app.LeftEarButton.Value==1)&&(app.CheekButton.Value==1)&&(app.HighF
reqChannelButton.Value==1)
x=app.DistanceofPhonecmSensitivity03cmEditField.Value;
sar=0.047.*exp(0.0405.*x);
app.SARWkgEditField.Value=sar;
error = 20.09/100*sar;
app.EditField3.Value=error;
compliance = sar/2*100;
r2=0.01667;
app.RSquareEditField.Value=r2;
app.ofICNIRPLimitEditField.Value=compliance;
x1 = 0:0.1:3;
sar1=0.047.*exp(0.0405.*x1);
plot(app.UIAxes,x1,sar1);
% Left ear and Tilt
;;;;;;;;;;;;;;;;;;;;;;;;;;;;;;;;;;;;;;;;;;;;;;;;;;;;;;;;;;;;;;;;;;;;
;;;;;;;;
elseif
(app.LeftEarButton.Value==1)&&(app.TiltButton.Value==1)&&(app.LowFre
qChannelButton.Value==1)
x=app.DistanceofPhonecmSensitivity03cmEditField.Value;
sar=0.039.*exp(-0.0167.*x);
app.SARWkgEditField.Value=sar;
error = 20.09/100*sar;
app.EditField3.Value=error;
compliance = sar/2*100;
r2=0.00197;
app.RSquareEditField.Value=r2;
app.ofICNIRPLimitEditField.Value=compliance;
x1 = 0:0.1:3;
sar1=0.039.*exp(-0.0167.*x1);
plot(app.UIAxes,x1,sar1);
elseif
(app.LeftEarButton.Value==1)&&(app.TiltButton.Value==1)&&(app.MidFre
qChannelButton.Value==1)
x=app.DistanceofPhonecmSensitivity03cmEditField.Value;
sar=0.0424.*exp(-0.0244.*x);
app.SARWkgEditField.Value=sar;
error = 20.09/100*sar;
app.EditField3.Value=error;
compliance = sar/2*100;
r2=0.004387;
app.RSquareEditField.Value=r2;
app.ofICNIRPLimitEditField.Value=compliance;
x1 = 0:0.1:3;
sar1=0.0424.*exp(-0.0244.*x1);
plot(app.UIAxes,x1,sar1);
```

```
elseif
(app.LeftEarButton.Value==1)&&(app.TiltButton.Value==1)&&(app.HighFr
eqChannelButton.Value==1)
x=app.DistanceofPhonecmSensitivity03cmEditField.Value;
sar=0.0434.*exp(-0.0017.*x);
app.SARWkgEditField.Value=sar;
error = 20.09/100*sar;
app.EditField3.Value=error;
compliance = sar/2*100;
r2=0.00002;
app.RSquareEditField.Value=r2;
app.ofICNIRPLimitEditField.Value=compliance;
x1 = 0:0.1:3;
sar1=0.0434.*exp(-0.0017.*x1);
plot(app.UIAxes,x1,sar1);
% RightEar and Cheek
;;;;;;;;;;;;;;;;;;;;;;;;;;;;;;;;;;;;;;;;;;;;;;;;;;;;;;;;;;;;;;;;;;;;
elseif
(app.RightEarButton.Value==1)&&(app.CheekButton.Value==1)&&(app.LowF
reqChannelButton.Value==1)
x=app.DistanceofPhonecmSensitivity03cmEditField.Value;
sar=0.065.*exp(-0.4371.*x);
app.SARWkgEditField.Value=sar;
error = 20.09/100*sar;
app.EditField3.Value=error;
compliance = sar/2*100;
r2=0.7768;
app.RSquareEditField.Value=r2;
app.ofICNIRPLimitEditField.Value=compliance;
x1 = 0:0.1:3;
sar1=0.065.*exp(-0.4371.*x1);
plot(app.UIAxes,x1,sar1);
elseif
(app.RightEarButton.Value==1)&&(app.CheekButton.Value==1)&&(app.MidF
reqChannelButton.Value==1)
x=app.DistanceofPhonecmSensitivity03cmEditField.Value;
sar=0.089.*exp(-0.5848.*x);
app.SARWkgEditField.Value=sar;
error = 20.09/100*sar;
app.EditField3.Value=error;
compliance = sar/2*100;
r2=0.8386;
app.RSquareEditField.Value=r2;
app.ofICNIRPLimitEditField.Value=compliance;
x1 = 0:0.1:3;
sar1=0.089.*exp(-0.5848.*x1);
plot(app.UIAxes,x1,sar1);
```

```
elseif
(app.RightEarButton.Value==1)&&(app.CheekButton.Value==1)&&(app.High
FreqChannelButton.Value==1)
x=app.DistanceofPhonecmSensitivity03cmEditField.Value;
sar=00.033.*exp(-0.0188.*x);
app.SARWkgEditField.Value=sar;
error = 20.09/100*sar;
app.EditField3.Value=error;
compliance = sar/2*100;
r2=0.01319;
app.RSquareEditField.Value=r2;
app.ofICNIRPLimitEditField.Value=compliance;
x1 = 0:0.1:3;
sar1=0.033.*exp(-0.0188.*x1);
plot(app.UIAxes,x1,sar1);
% Right Ear and Tilt
elseif
(app.RightEarButton.Value==1)&&(app.TiltButton.Value==1)&&(app.LowFr
eqChannelButton.Value==1)
x=app.DistanceofPhonecmSensitivity03cmEditField.Value;
sar=0.0347.*exp(-0.0749.*x);
app.SARWkgEditField.Value=sar;
error = 20.09/100*sar;
app.EditField3.Value=error;
compliance = sar/2*100;
r2=0.1553;
app.RSquareEditField.Value=r2;
app.ofICNIRPLimitEditField.Value=compliance;
x1 = 0:0.1:3;
sar1=0.0347.*exp(-0.0749.*x1);
plot(app.UIAxes,x1,sar1);
elseif
(app.RightEarButton.Value==1)&&(app.TiltButton.Value==1)&&(app.MidFr
eqChannelButton.Value==1)
x=app.DistanceofPhonecmSensitivity03cmEditField.Value;
sar=0.0323.*exp(0.0025.*x);
app.SARWkgEditField.Value=sar;
error = 20.09/100*sar;
app.EditField3.Value=error;
compliance = sar/2*100;
r2=0.000106;
app.RSquareEditField.Value=r2;
app.ofICNIRPLimitEditField.Value=compliance;
x1 = 0:0.1:3;
sar1=0.0323.*exp(0.0025.*x1);
plot(app.UIAxes,x1,sar1);
```

```
elseif
(app.RightEarButton.Value==1)&&(app.TiltButton.Value==1)&&(app.HighF
reqChannelButton.Value==1)
x=app.DistanceofPhonecmSensitivity03cmEditField.Value;
sar=0.072.*exp(-0.02969.*x);
app.SARWkgEditField.Value=sar;
error = 20.09/100*sar;
app.EditField3.Value=error;
compliance = sar/2*100;
r2=0.9458;
app.RSquareEditField.Value=r2;
app.ofICNIRPLimitEditField.Value=compliance;
x1 = 0:0.1:3;
sar1=0.072.*exp(-0.02969.*x1);
plot(app.UIAxes,x1,sar1);
end
%%%%%%%%%%%%%%%%%%%%%%%%%%%%%%%%%%%%%%%%%%%%%%%%%%%%%%%%%%%%%%%%%%%%%%%
%%%%%%%%%%%%%%%%%%%%%%%%%%%%%%%%%%%%
end
end


% Callback function
function PlotButtonPushed(app, event)
x1 = 0:0.1:3;
sar1=0.0255.*x1.^2-0.1206.*x1+0.1767;
plot(app.UIAxes,x1,sar1);
end
end


% Component initialization
methods (Access = private)


% Create UIFigure and components
function createComponents(app)


% Create MobilePhoneSarCalculatorAppUIFigure and hide until all
components are created
app.MobilePhoneSarCalculatorAppUIFigure = uifigure('Visible',
'off');
app.MobilePhoneSarCalculatorAppUIFigure.Position = [100 100 839
601];
app.MobilePhoneSarCalculatorAppUIFigure.Name = 'Mobile Phone Sar
Calculator App';
```

```
% Create GridLayout
app.GridLayout =
uigridlayout(app.MobilePhoneSarCalculatorAppUIFigure);
app.GridLayout.ColumnWidth = {'5.42x', '5.42x'};
app.GridLayout.RowHeight = {'0.2x', '1x', '0.2x'};


% Create NATIONALCOMMUNICATIONAUTHORITYAPPROVALSTATUSPanel
app.NATIONALCOMMUNICATIONAUTHORITYAPPROVALSTATUSPanel =
uipanel(app.GridLayout);
app.NATIONALCOMMUNICATIONAUTHORITYAPPROVALSTATUSPanel.TitlePosition
= 'centertop';
app.NATIONALCOMMUNICATIONAUTHORITYAPPROVALSTATUSPanel.Title =
'NATIONAL COMMUNICATION AUTHORITY APPROVAL STATUS';
app.NATIONALCOMMUNICATIONAUTHORITYAPPROVALSTATUSPanel.BackgroundColo
r = [0 1 1];
app.NATIONALCOMMUNICATIONAUTHORITYAPPROVALSTATUSPanel.Layout.Row =
1;
app.NATIONALCOMMUNICATIONAUTHORITYAPPROVALSTATUSPanel.Layout.Column
= [1 2];
app.NATIONALCOMMUNICATIONAUTHORITYAPPROVALSTATUSPanel.FontWeight =
'bold';


% Create Image
app.Image =
uiimage(app.NATIONALCOMMUNICATIONAUTHORITYAPPROVALSTATUSPanel);
app.Image.Position = [-54 0 207 71];
app.Image.ImageSource = 'COMSAR BENCH.png';


% Create Image_2
app.Image_2 =
uiimage(app.NATIONALCOMMUNICATIONAUTHORITYAPPROVALSTATUSPanel);
app.Image_2.Position = [664 -11 219 91];
app.Image_2.ImageSource = 'sar.png';


% Create CheckButtonGroup
app.CheckButtonGroup =
uibuttongroup(app.NATIONALCOMMUNICATIONAUTHORITYAPPROVALSTATUSPanel)
;
app.CheckButtonGroup.ForegroundColor = [0.6353 0.0784 0.1843];
app.CheckButtonGroup.Title = 'Check';
app.CheckButtonGroup.BackgroundColor = [0 1 0];
app.CheckButtonGroup.FontWeight = 'bold';
app.CheckButtonGroup.Position = [150 8 515 47];
```

```
% Create ApprovedPhoneModelButton
app.ApprovedPhoneModelButton = uiradiobutton(app.CheckButtonGroup);
app.ApprovedPhoneModelButton.Tag = 'radbtnApproved';
app.ApprovedPhoneModelButton.Text = 'Approved Phone Model';
app.ApprovedPhoneModelButton.FontWeight = 'bold';
app.ApprovedPhoneModelButton.Position = [84 4 156 22];
app.ApprovedPhoneModelButton.Value = true;


% Create UnapprovedPhoneModelButton
app.UnapprovedPhoneModelButton =
uiradiobutton(app.CheckButtonGroup);
app.UnapprovedPhoneModelButton.Tag = 'radbtnUnapproved';
app.UnapprovedPhoneModelButton.Text = 'Unapproved Phone Model';
app.UnapprovedPhoneModelButton.FontWeight = 'bold';
app.UnapprovedPhoneModelButton.Position = [275 4 170 22];


% Create MODELINPUTSPanel
app.MODELINPUTSPanel = uipanel(app.GridLayout);
app.MODELINPUTSPanel.TitlePosition = 'centertop';
app.MODELINPUTSPanel.Title = 'MODEL INPUTS';
app.MODELINPUTSPanel.BackgroundColor = [0.4667 0.6745 0.1882];
app.MODELINPUTSPanel.Layout.Row = 2;
app.MODELINPUTSPanel.Layout.Column = 1;
app.MODELINPUTSPanel.FontWeight = 'bold';


% Create PositionofPhonePanel
app.PositionofPhonePanel = uipanel(app.MODELINPUTSPanel);
app.PositionofPhonePanel.ForegroundColor = [0 0 1];
app.PositionofPhonePanel.TitlePosition = 'centertop';
app.PositionofPhonePanel.Title = 'Position of Phone';
app.PositionofPhonePanel.FontWeight = 'bold';
app.PositionofPhonePanel.Position = [24 298 367 75];


% Create CheckButtonGroup_2
app.CheckButtonGroup_2 = uibuttongroup(app.PositionofPhonePanel);
app.CheckButtonGroup_2.ForegroundColor = [0.6353 0.0784 0.1843];
app.CheckButtonGroup_2.Title = 'Check';
app.CheckButtonGroup_2.BackgroundColor = [0 1 0];
app.CheckButtonGroup_2.FontWeight = 'bold';
app.CheckButtonGroup_2.Position = [22 6 325 51];


% Create LeftEarButton
app.LeftEarButton = uiradiobutton(app.CheckButtonGroup_2);
app.LeftEarButton.Tag = 'radbtnLeftEar';
```

```
app.LeftEarButton.Text = 'Left Ear';
app.LeftEarButton.FontWeight = 'bold';
app.LeftEarButton.Position = [12 6 67 22];
app.LeftEarButton.Value = true;


% Create RightEarButton
app.RightEarButton = uiradiobutton(app.CheckButtonGroup_2);
app.RightEarButton.Tag = 'radbtnRightEar';
app.RightEarButton.Text = 'Right Ear';
app.RightEarButton.FontWeight = 'bold';
app.RightEarButton.Position = [118 6 75 22];


% Create OrientationofPhonePanel
app.OrientationofPhonePanel = uipanel(app.MODELINPUTSPanel);
app.OrientationofPhonePanel.ForegroundColor = [0 0 1];
app.OrientationofPhonePanel.TitlePosition = 'centertop';
app.OrientationofPhonePanel.Title = 'Orientation of Phone';
app.OrientationofPhonePanel.FontWeight = 'bold';
app.OrientationofPhonePanel.Position = [23 214 368 71];


% Create CheckButtonGroup_3
app.CheckButtonGroup_3 = uibuttongroup(app.OrientationofPhonePanel);
app.CheckButtonGroup_3.ForegroundColor = [0.6353 0.0784 0.1843];
app.CheckButtonGroup_3.Title = 'Check';
app.CheckButtonGroup_3.BackgroundColor = [0 1 0];
app.CheckButtonGroup_3.FontWeight = 'bold';
app.CheckButtonGroup_3.Position = [23 10 325 41];


% Create CheekButton
app.CheekButton = uiradiobutton(app.CheckButtonGroup_3);
app.CheekButton.Tag = 'radbtnCheek';
app.CheekButton.Text = 'Cheek';
app.CheekButton.FontWeight = 'bold';
app.CheekButton.Position = [11 0 58 22];
app.CheekButton.Value = true;


% Create TiltButton
app.TiltButton = uiradiobutton(app.CheckButtonGroup_3);
app.TiltButton.Tag = 'radbtnTilt';
app.TiltButton.Text = 'Tilt';
app.TiltButton.FontWeight = 'bold';
app.TiltButton.Position = [118 1 65 22];
```

```
% Create ClosenesstoHeadPanel
app.ClosenesstoHeadPanel = uipanel(app.MODELINPUTSPanel);
app.ClosenesstoHeadPanel.ForegroundColor = [0 0 1];
app.ClosenesstoHeadPanel.TitlePosition = 'centertop';
app.ClosenesstoHeadPanel.Title = 'Closeness to Head';
app.ClosenesstoHeadPanel.BackgroundColor = [1 1 1];
app.ClosenesstoHeadPanel.FontWeight = 'bold';
app.ClosenesstoHeadPanel.Position = [22 135 369 66];


% Create DistanceofPhonecmSensitivity03cmEditFieldLabel
app.DistanceofPhonecmSensitivity03cmEditFieldLabel =
uilabel(app.ClosenesstoHeadPanel);
app.DistanceofPhonecmSensitivity03cmEditFieldLabel.HorizontalAlignme
nt = 'center';
app.DistanceofPhonecmSensitivity03cmEditFieldLabel.FontWeight =
'bold';
app.DistanceofPhonecmSensitivity03cmEditFieldLabel.Position = [8 5
159 41];
app.DistanceofPhonecmSensitivity03cmEditFieldLabel.Text = {'Distance
of Phone (cm) '; '[Sensitivity:0-3 cm]'};


% Create DistanceofPhonecmSensitivity03cmEditField
app.DistanceofPhonecmSensitivity03cmEditField =
uieditfield(app.ClosenesstoHeadPanel, 'numeric');
app.DistanceofPhonecmSensitivity03cmEditField.ValueDisplayFormat =
'%.2f';
app.DistanceofPhonecmSensitivity03cmEditField.Tag = 'txtDistance';
app.DistanceofPhonecmSensitivity03cmEditField.HorizontalAlignment =
'center';
app.DistanceofPhonecmSensitivity03cmEditField.Position = [218 14 46
22];


% Create CarrierFrequencyPanel
app.CarrierFrequencyPanel = uipanel(app.MODELINPUTSPanel);
app.CarrierFrequencyPanel.ForegroundColor = [0 0 1];
app.CarrierFrequencyPanel.TitlePosition = 'centertop';
app.CarrierFrequencyPanel.Title = 'Carrier Frequency';
app.CarrierFrequencyPanel.FontWeight = 'bold';
app.CarrierFrequencyPanel.Position = [21 27 370 92];


% Create CheckButtonGroup_4
app.CheckButtonGroup_4 = uibuttongroup(app.CarrierFrequencyPanel);
app.CheckButtonGroup_4.ForegroundColor = [0.6353 0.0784 0.1843];
app.CheckButtonGroup_4.Title = 'Check';
app.CheckButtonGroup_4.BackgroundColor = [0 1 0];
```

```
app.CheckButtonGroup_4.FontWeight = 'bold';
app.CheckButtonGroup_4.Position = [6 14 344 59];


% Create LowFreqChannelButton
app.LowFreqChannelButton = uiradiobutton(app.CheckButtonGroup_4);
app.LowFreqChannelButton.Tag = 'radbtnLFC';
app.LowFreqChannelButton.Text = 'Low Freq Channel';
app.LowFreqChannelButton.FontWeight = 'bold';
app.LowFreqChannelButton.Position = [12 20 126 22];
app.LowFreqChannelButton.Value = true;


% Create MidFreqChannelButton
app.MidFreqChannelButton = uiradiobutton(app.CheckButtonGroup_4);
app.MidFreqChannelButton.Tag = 'radbtnMFC';
app.MidFreqChannelButton.Text = 'Mid Freq Channel';
app.MidFreqChannelButton.FontWeight = 'bold';
app.MidFreqChannelButton.Position = [12 0 123 22];


% Create HighFreqChannelButton
app.HighFreqChannelButton = uiradiobutton(app.CheckButtonGroup_4);
app.HighFreqChannelButton.Tag = 'radbtnHFC';
app.HighFreqChannelButton.Text = 'High Freq Channel';
app.HighFreqChannelButton.FontWeight = 'bold';
app.HighFreqChannelButton.Position = [166 14 129 22];


% Create MODELOUTPUTSPanel
app.MODELOUTPUTSPanel = uipanel(app.GridLayout);
app.MODELOUTPUTSPanel.TitlePosition = 'centertop';
app.MODELOUTPUTSPanel.Title = 'MODEL OUTPUTS';
app.MODELOUTPUTSPanel.BackgroundColor = [1 0 0];
app.MODELOUTPUTSPanel.Layout.Row = 2;
app.MODELOUTPUTSPanel.Layout.Column = 2;
app.MODELOUTPUTSPanel.FontWeight = 'bold';


% Create UIAxes
app.UIAxes = uiaxes(app.MODELOUTPUTSPanel);
title(app.UIAxes, 'SAR and Distance')
xlabel(app.UIAxes, 'Distance (cm)')
ylabel(app.UIAxes, 'SAR (W/kg)')
app.UIAxes.FontWeight = 'bold';
app.UIAxes.Position = [7 173 334 202];


% Create SAROUTPUTSPanel
```

```
app.SAROUTPUTSPanel = uipanel(app.MODELOUTPUTSPanel);
app.SAROUTPUTSPanel.TitlePosition = 'centertop';
app.SAROUTPUTSPanel.Title = 'SAR OUTPUTS';
app.SAROUTPUTSPanel.BackgroundColor = [0.0745 0.6235 1];
app.SAROUTPUTSPanel.FontWeight = 'bold';
app.SAROUTPUTSPanel.Position = [7 20 182 134];


% Create SARButton
app.SARButton = uibutton(app.SAROUTPUTSPanel, 'push');
app.SARButton.ButtonPushedFcn = createCallbackFcn(app,
@SARButtonPushed, true);
app.SARButton.Tag = 'pbtnSar';
app.SARButton.BackgroundColor = [0.9294 0.6941 0.1255];
app.SARButton.FontWeight = 'bold';
app.SARButton.Position = [32 14 101 37];
app.SARButton.Text = 'SAR';


% Create SARWkgEditFieldLabel
app.SARWkgEditFieldLabel = uilabel(app.SAROUTPUTSPanel);
app.SARWkgEditFieldLabel.HorizontalAlignment = 'center';
app.SARWkgEditFieldLabel.FontWeight = 'bold';
app.SARWkgEditFieldLabel.Position = [18 54 145 32];
app.SARWkgEditFieldLabel.Text = 'SAR (W/kg)';


% Create SARWkgEditField
app.SARWkgEditField = uieditfield(app.SAROUTPUTSPanel, 'numeric');
app.SARWkgEditField.ValueDisplayFormat = '%.3f';
app.SARWkgEditField.Tag = 'ntxtSar';
app.SARWkgEditField.HorizontalAlignment = 'center';
app.SARWkgEditField.Position = [19 79 57 30];


% Create EditField3
app.EditField3 = uieditfield(app.SAROUTPUTSPanel, 'numeric');
app.EditField3.ValueDisplayFormat = '%.3f';
app.EditField3.Tag = 'ntxtError';
app.EditField3.HorizontalAlignment = 'center';
app.EditField3.Position = [90 79 49 31];


% Create Label
app.Label = uilabel(app.SAROUTPUTSPanel);
app.Label.BackgroundColor = [1 1 1];
app.Label.HorizontalAlignment = 'center';
app.Label.FontSize = 14;
app.Label.Position = [75 79 16 30];
```

```
app.Label.Text = '±';


% Create ICNIRPCompliancePanel
app.ICNIRPCompliancePanel = uipanel(app.MODELOUTPUTSPanel);
app.ICNIRPCompliancePanel.TitlePosition = 'centertop';
app.ICNIRPCompliancePanel.Title = 'ICNIRP Compliance';
app.ICNIRPCompliancePanel.BackgroundColor = [1 1 0.0667];
app.ICNIRPCompliancePanel.FontWeight = 'bold';
app.ICNIRPCompliancePanel.Position = [202 41 185 77];


% Create ofICNIRPLimitEditFieldLabel
app.ofICNIRPLimitEditFieldLabel =
uilabel(app.ICNIRPCompliancePanel);
app.ofICNIRPLimitEditFieldLabel.HorizontalAlignment = 'right';
app.ofICNIRPLimitEditFieldLabel.FontWeight = 'bold';
app.ofICNIRPLimitEditFieldLabel.Position = [10 23 107 22];
app.ofICNIRPLimitEditFieldLabel.Text = '% of ICNIRP Limit';


% Create ofICNIRPLimitEditField
app.ofICNIRPLimitEditField = uieditfield(app.ICNIRPCompliancePanel,
'numeric');
app.ofICNIRPLimitEditField.ValueDisplayFormat = '%.2f';
app.ofICNIRPLimitEditField.Tag = 'ntxtIcnirp';
app.ofICNIRPLimitEditField.HorizontalAlignment = 'center';
app.ofICNIRPLimitEditField.Position = [122 23 52 22];


% Create RSquareEditFieldLabel
app.RSquareEditFieldLabel = uilabel(app.MODELOUTPUTSPanel);
            app.RSquareEditFieldLabel.HorizontalAlignment =
'center';
            app.RSquareEditFieldLabel.FontWeight = 'bold';
            app.RSquareEditFieldLabel.FontColor = [1 1 1];
            app.RSquareEditFieldLabel.Position = [342 263 59 22];
            app.RSquareEditFieldLabel.Text = 'R-Square';


            % Create RSquareEditField
            app.RSquareEditField =
uieditfield(app.MODELOUTPUTSPanel, 'numeric');
            app.RSquareEditField.ValueDisplayFormat = '%.3f';
            app.RSquareEditField.HorizontalAlignment = 'center';
            app.RSquareEditField.Position = [348 285 50 22];


            % Create AUTHORPanel
```

```
            app.AUTHORPanel = uipanel(app.GridLayout);
            app.AUTHORPanel.TitlePosition = 'centertop';
            app.AUTHORPanel.Title = 'AUTHOR';
            app.AUTHORPanel.Layout.Row = 3;
            app.AUTHORPanel.Layout.Column = [1 2];
            app.AUTHORPanel.FontWeight = 'bold';

            % Create Label_2
            app.Label_2 = uilabel(app.AUTHORPanel);
            app.Label_2.HorizontalAlignment = 'center';
            app.Label_2.FontSize = 14;
            app.Label_2.FontWeight = 'bold';
            app.Label_2.Position = [195 21 433 22];
            app.Label_2.Text = 'This application was designed and
formulated by Samuel Osei ';

            % Create Image2
            app.Image2 = uiimage(app.AUTHORPanel);
            app.Image2.Position = [0 0 117 79];
            app.Image2.ImageSource = 'COMSAR BENCH.png';

            % Create Image3
            app.Image3 = uiimage(app.AUTHORPanel);
            app.Image3.Position = [718 0 100 79];
            app.Image3.ImageSource = 'sar.png';

            % Show the figure after all components are created
            app.MobilePhoneSarCalculatorAppUIFigure.Visible = 'on';
        end
    end

    % App creation and deletion
    methods (Access = public)

        % Construct app
        function app = phd5selfdecayavegrowth

            % Create UIFigure and components
            createComponents(app)

            % Register the app with App Designer
```

```
            registerApp(app,
app.MobilePhoneSarCalculatorAppUIFigure)


            if nargout == 0
                clear app
            end
        end


        % Code that executes before app deletion
        function delete(app)


            % Delete UIFigure when app is deleted
            delete(app.MobilePhoneSarCalculatorAppUIFigure)
        end
    end
end
```